PB2001-107414

U.S. Department
of Transportation
**National Highway
Traffic Safety
Administration**

People Saving People
www.nhtsa.dot.gov

DOT HS 809 283

June 2001

Test and Evaluation of the Ford/SAE Air Bag Interaction Arm

Technical Report Documentation Page

1. Report No. DOT HS 809 283	2. Government Accession No.	3. Recipient's Catalog No.
4. Title and Subtitle Test and Evaluation of the Ford/SAE Air Bag Interaction Arm		5. Report Date June 2001 6. Performing Organization Code NRD-21
7. Author(s) Daniel Rhule and Matthew Freyhof		8. Performing Organization Report No.
9. Performing Organization Name and Address National Highway Traffic Safety Administration Vehicle Research and Test Center P.O. Box 37 East Liberty, OH 43319		10. Work Unit No. (TRAIS)n code 11. Contract of Grant No.
12. Sponsoring Agency Name and Address National Highway Traffic Safety Administration 400 Seventh Street, S.W. Washington, DC 20590		13. Type of Report and Period Covered Technical Report 14. Sponsoring Agency Code

15. Supplementary Notes

16. Abstract

This paper summarizes an evaluation program of a newly developed test device - the Ford/SAE Air Bag Interaction Arm. The device has been developed in response to recent findings which indicate that injuries to the upper extremities are more likely to occur in vehicles equipped with air bag restraint systems. The instrumented arm is designed to attach to a small female Hybrid III crash test dummy. It contains instrumentation in both the upper and lower arm segments allowing for the measurement of forces, moments, and accelerations. The arm was subjected to pendulum impacts and static deployment tests using driver and side impact air bag systems.

17. Key Words Air Bag Upper Extremities		18. Distribution Statement Document is available to the public through the National Technical Information Service, Springfield, VA 22161	
19. Security Classif. (of this report) Unclassified	20. Security Classif. (of this page) Unclassified	21. No of Pages	22. Price

Form DOT F1700.7 (8-72) **Reproduction of completed page authorized**

TABLE OF CONTENTS

Page

TABLE OF CONTENTS
(Continued)

LIST OF FIGURES

LIST OF FIGURES
(Continued)

LIST OF FIGURES
(Continued)

LIST OF FIGURES
(Continued)

LIST OF TABLES

1.0 INTRODUCTION

According to a National Highway Traffic Safety Administration (NHTSA) study of 1988 - 94 National Automotive Sampling System (NASS) cases conducted by Conrad Technologies, Inc. [1], the likelihood of injury to the upper extremities is significantly increased in vehicle accidents involving driver's side air bags. In the study, it was determined that drivers who were restrained by 3-point belts and air bags suffered injuries to the upper extremities at a rate four times greater than those drivers who were restrained by 3-point belts alone. The case studies revealed that the majority of upper extremity injuries associated with air bag deployments were to the forearm or hand. In addition, injury data indicated that small females are most frequently injured during these accidents.

1.1 Previous Developments

The Research Arm Injury Device (RAID) was developed by Conrad Technologies Inc. under a contract to NHTSA [1]. The device was intended to evaluate the aggressivity of air bags in a static laboratory setting. Its structure consisted of a 46 cm long aluminum tube with a concentrated mass of 0.5 kg located at one end to simulate the mass of the hand. At the opposite end was a double jointed pivot which allowed rotations in two directions. The RAID contained instrumentation for measuring the bending moment and acceleration experienced by the device. The test protocol called for hanging the device from a pivot in front of the air bag and steering wheel. In their study, it was determined that the two most important contributors to the peak bending response were the orientation of the device relative to the air bag and the offset distance between the device and the air bag.

The Vehicle Research and Test Center also developed an instrumented device for assessing arm injuries due to air bag interaction [2]. The arm of a 50th percentile male Hybrid III dummy was modified to incorporate strain gages and accelerometer mounts. The arm was assembled to the standard crash test dummy and the dummy could then be positioned in a vehicle with the arm placed across the air bag. Integrating the instrumented arm to the dummy provided the potential for assessing the arm's interaction with the occupant and vehicle interior, as well as with the deploying air bag.

1.2 Small Female Instrumented Arm

In order to study the small female injuries further, Ford Motor Company and the Society of Automotive Engineers (SAE) have cooperated in developing an instrumented arm for quantitative analysis. The instrumented arm, known in the industry as the Model J3525 Air Bag Interaction Arm, has been specifically designed for use with air bags and can be assembled to either the Hybrid III 5th percentile small female dummy or the SID-IIs side impact dummy. The instrumented arm contains upper and lower arm segments, each with a removable flesh covering, and molded hands for both the right and left hand. To facilitate data acquisition, the arm is instrumented with a six-channel force/moment load cell in both the upper and lower arm segments; a two-channel moment load cell located at the elbow-end of the upper arm (distal humerus); a rotary potentiometer in the elbow; and mounting provisions for triaxial accelerometer arrays near both the wrist and distal humerus.

The elbow joint is a single degree of freedom joint and allows for flexion/extension. The proximal end of the humerus contains provisions for attaching the device to the shoulder of the small female dummy. The shoulder joint allows for three primary rotations of the shoulder (flexion/extension; abduction/adduction; and rotation about the long axis of the humerus). However, when mounted to the Hybrid III small female, it lacks clavicle/scapula translation, a motion which a human shoulder is capable of achieving. The device is convertible for use as either a right or left arm. A picture of the instrumented arm is shown in Figure 1.

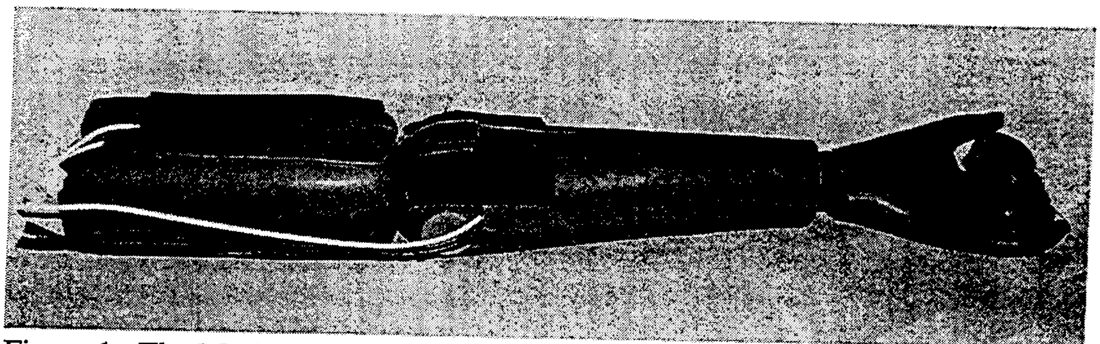

Figure 1. The Model J3525 Air Bag Interaction Arm

2.0 OBJECTIVE

The purpose of this study was to conduct basic research in the area of small female upper extremity injuries induced by air bag deployment and to evaluate the capabilities of the instrumented arm as a research tool. To that end, a calibration testing procedure has been developed and tested in order to evaluate the arm's repeatability. Furthermore, the instrumented arm was subjected to a series of static air bag tests including driver and side impact air bags. Driver air bags were selected to cover a range of aggressivities in order to evaluate the instrumented arm's ability to distinguish air bag characteristics. Along with driver air bags, door-mounted and seat-mounted air bags were selected to analyze the instrumented arm's performance with side impact restraining air bags.

3.0 CALIBRATION PROCEDURE DEVELOPMENT

One feature of the instrumented arm that was evaluated was its ability to provide consistent, repeatable responses to a known input. Prior to VRTC procuring the instrumented arm, there had been no calibration procedure established. Therefore, two calibration test approaches were examined. One approach separated the arm into its upper and lower segments and tested them separately, while the second method utilized the entire arm assembly. The first method is referred to as the component test and the second method is referred to as the assembly test.

In the component test method, the upper and lower segments of the arm are impacted with each segment attached to a rigid fixture. Figures 2 and 3 depict the upper and lower arm segment test set-ups, respectively. The posterior surface of the humerus and the anterior (volar) surface of the forearm were selected for the impact surfaces as these surfaces represent areas of probable impact during a crash.

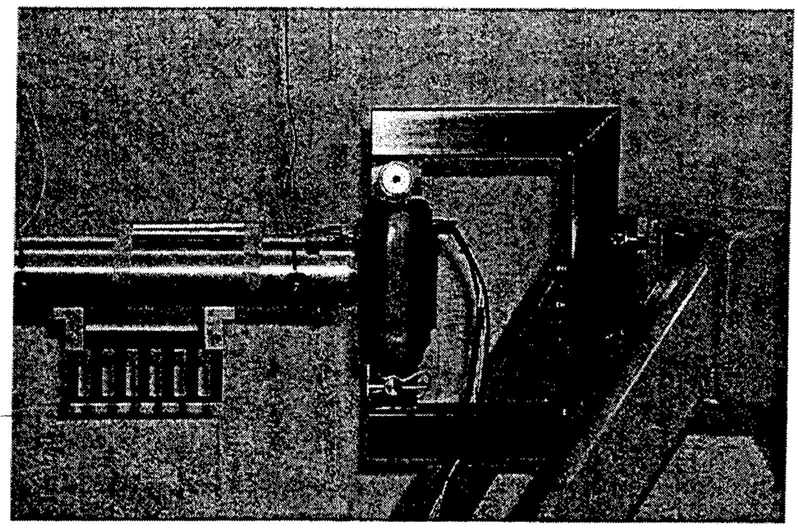

Figure 2. Upper arm segment calibration test set-up.

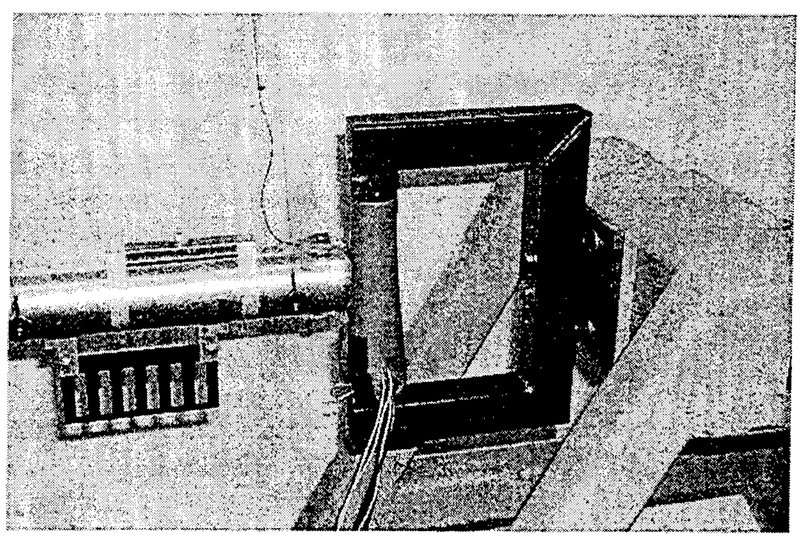

Figure 3. Lower arm segment calibration test set-up.

In the assembly calibration test, the entire arm assembly was mounted to a rigid fixture as shown in Figure 4. The primary reason for considering an assembled calibration test was ease of use; that is, it would be much more efficient in terms of time and simplicity if the arm did not have to be disassembled into its component segments before conducting the calibration test. Two separate tests were designed, one which struck the humerus and one which impacted the forearm. The posterior surfaces of the humerus and forearm were selected as the impact surfaces. The fixture for the dynamic testing allowed the arm to rotate after impact.

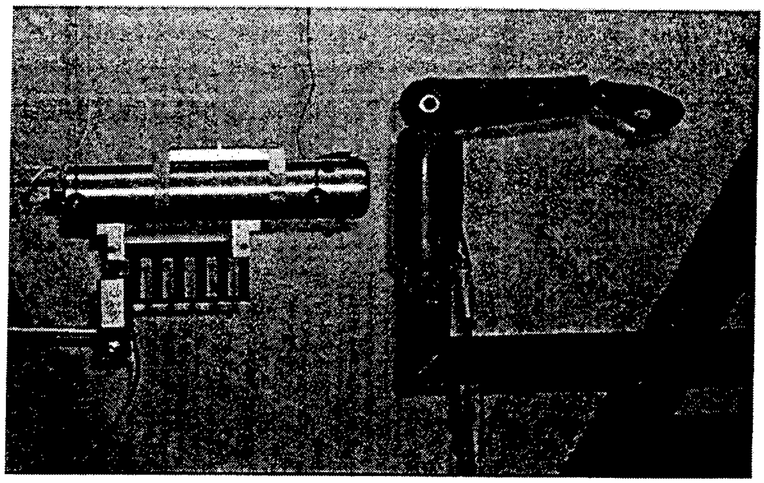

Figure 4. Assembled arm calibration test.

3.1 Literature Review

Before proceeding with development of the calibration tests, a review of the available literature was conducted to collect data regarding the human arm's injury tolerance. For the humerus, two recent studies were examined: a 1996 study conducted by Kirkish, et. al [3], and a 1998 report published by Duma, et. al [4]. In the Kirkish study, unembalmed cadaver arms were subjected to quasi-static three-point bending. The study recommends an Injury Assessment Reference Value (IARV) of 130 Nm for the 5th percentile female arm. The Duma study utilized a dynamic three-point bending test configuration and recommends an IARV of 128 Nm.

Papers by Saul, et. al. [5], Bass, et. al. [6], and Pintar, et. al. [7] were identified for reference to the forearm injury tolerance. The Saul study indicates that an appropriate injury tolerance for both the radius and ulna in the forearm of female subjects would be 70 to 90 Nm. Bass tested cadaveric arms and an initial version of the SAE instrumented arm and determined that there was a 50% risk of radius and ulna fracture at 91 Nm. In the Pintar study, which utilized fresh cadaveric human forearm samples in a dynamic three-point bending test, failure was observed at a load of 1380 N and a bending moment of 66 Nm.

After conducting the literature review, it was apparent that the dynamic three-point bending tests used in Duma's humerus study and in Pintar's forearm study displayed the most similarity to the experimental set-up proposed for calibrating the instrumented arm. Therefore, it was determined that the calibration tests should be designed to achieve loading responses similar to the IARVs reported in the respective studies.

During the literature search for this project, it was discovered that very little upper extremity injury tolerance data exists. It is likely that the IARVs used in this study may need to be updated as the biomechanics community gathers data and knowledge of the human arm's injury tolerance.

3.2 Exploratory Testing

Initial testing was aimed at determining the test parameters which would provide responses approximating the selected IARVs. Essentially, the goal of this testing was to establish the amount of energy input required from the impactor and the location of impact. It was desired to maintain the velocity of the impactor to approximate the speeds used in the Duma and Pintar studies respectively. Given this loose constraint, impactors were selected from the set of standard available impact probes in the VRTC laboratory. Also, it was decided to use the neutral axis of the forearm and humerus load cells respectively as the location of impact (see Appendix A for details of location).

3.2.1. Exploratory Testing - Forearm Segment

Initial testing with a 2.86 kg impactor at approximately 3 m/s provided a bending moment response that was significantly higher than the Pintar recommended IARV. Therefore, a 1.57 kg, 2 inch diameter impactor was selected. Using this impactor while maintaining the speed of impact near the range of the Pintar tests provided a bending moment response that was still high relative to the IARV; however, the resultant loads were well within the range of Pintar's results. Four tests were conducted and the results are contained in Table 1. The target response for this test was 1380 N of resultant load (resultant of X-force and Y-force) measured in the forearm.

Table 1. Forearm Segment Exploratory Tests

Test Number	Impactor Mass (kg)	Impact Velocity (m/s)	Forearm Resultant Load (N)
cal-01	1.57	2.99	n/a*
cal-02	1.57	2.99	1498
cal-03	1.57	2.65	1325
cal-04	1.57	2.44	1186

* modification made to test rig following test cal-01

Following test number cal-01, a large spike in the z-axis force (along the longitudinal axis of the forearm) was observed. The spikes were attributed to the end condition constraints of the test rig which fixed both ends of the forearm to the device. To remedy this artifact, the rig was modified to allow one of the pivots freedom to slide in the vertical direction. As a result, the z-force spike was significantly reduced in the subsequent exploratory tests (see Figure 5). As indicated in Table 1, test number cal-03 provided a combined load closest to the target response. Therefore, the impact speed of 2.65 m/s was selected as the target test parameter.

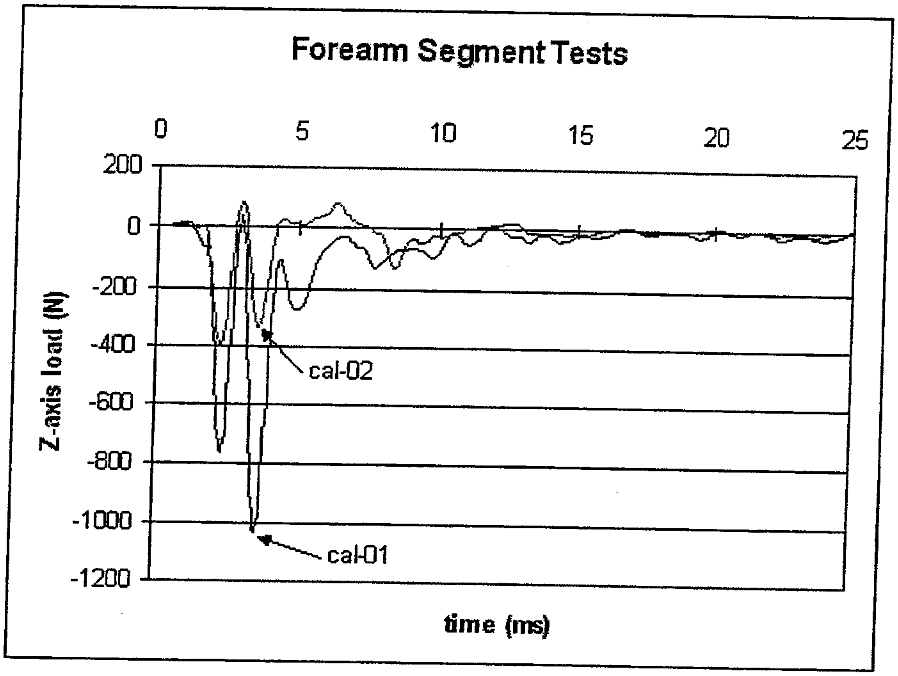

Figure 5. Z-axis Load Response of Forearm in Tests Cal-01 and Cal-02 Demonstrating the Reduction in the Load Spike.

3.2.2. Exploratory Testing - Upper Arm Segment

A 2.86 kg, 100 mm diameter impactor was selected for the upper arm testing. The results of four exploratory tests are contained in Table 2. The target response for this test was 128 Nm of bending moment.

Table 2. Upper Arm Segment Exploratory Tests

Test Number	Impactor Mass (kg)	Impact Velocity (m/s)	Bending Moment (Nm)
cal-05	2.86	2.44	100.9
cal-06	2.86	2.82	145.4
cal-07	2.86	2.99	165.4
cal-08	2.86	2.62	122.8

The target response was best approximated by test number cal-08 and thus an impact velocity of 2.6 m/s was selected for this test.

3.2.3. Exploratory Testing - Assembled Arm - Humerus

The 2.86 kg, 100 mm diameter impactor was preselected for the humerus impact of the assembled arm testing. The impact location was selected to be at the neutral axis of the load cell in the upper arm. The results of four exploratory tests are contained in Table 3. The target response for this test was 128 Nm of bending moment.

Table 3. Assembled Arm - Humerus Exploratory Tests

Test Number	Impactor Mass (kg)	Impact Velocity (m/s)	Bending Moment (Nm)
cal-09	2.86	2.62	52.6
cal-10	2.86	2.99	79.9
cal-11	2.86	3.30	96.1
cal-12	2.86	3.73	109.4

The impact velocity of 3.73 m/s in test number cal-12 provided a response closest to the target response.

3.2.4. Exploratory Testing - Assembled Arm - Forearm

For the forearm impact of the assembled arm test, the 1.57 kg, 50 mm diameter was selected. The impact location was selected to be at the neutral axis of the load cell in the forearm. However, to facilitate ease of test set up the impact surface was the posterior surface of the arm as opposed to the anterior surface which was used in the component test. The results are summarized in Table 4.

Table 4. Assembled Arm - Forearm Exploratory Tests

Test Number	Impactor Mass (kg)	Impact Velocity (m/s)	Forearm Resultant Load (N)
cal-13	1.57	2.65	760.8
cal-14	1.57	3.02	1115.1
cal-15	1.57	3.17	1028.3
cal-16	1.57	2.89	577.3

One important observation can be made from Table 4. Comparing the results of tests cal-14 and cal-15, it is observed that the resultant load for cal-15 was lower than that of cal-14 even though the impact speed of cal-15 was greater. This result demonstrates one of the shortcomings of the assembled arm testing method. The measured responses were greatly influenced by the elbow and shoulder joint torques. Similarly, comparison of tests cal-13 and cal-16 demonstrates the same unexpected trend. Although efforts were made to ensure that the joint torques were set consistently prior to each impact, variation in the response was still evident.

4.0 STATIC AIR BAG TESTING

During the inflation process, an air bag generates a significant amount of energy. As a result, substantial forces can be developed between the deploying air bag and the vehicle occupant, particularly when the occupant is positioned in close proximity to the deploying air bag. In some instances, the occupant's arm may be located on or across the steering wheel rim, or in close proximity to a side impact air bag and thus be at risk to interacting with the deploying restraint systems.

One of the primary objectives in developing an instrumented arm was to study arm injuries caused by deploying air bags. Therefore, static air bag tests were conducted to evaluate the performance of the instrumented arm. An attempt was made to select driver air bags which covered a range of aggressivities in order to evaluate the instrumented arm's capability to distinguish air bag characteristics. Along with driver air bags, door-mounted and seat-mounted air bags were selected to investigate the instrumented arm's performance with side impact air bags.

4.1 Static Driver Air Bag Testing

Driver air bag tests were conducted using a generic fixture. The fixture included an adjustable metal seat and adjustable steering column. The procedures contained in Draft ISO Technical Report 15827 (Rev. April '98) [8] were used as a guideline for dummy positioning, where applicable. Figures 6 and 7 illustrate a typical driver air bag test setup. The steering column was placed at an angle of 20 degrees above the horizontal and the steering wheel was rotated 60 degrees towards the centerline for all tests. As shown in Figure 7, the instrumented arm was placed with the elbow at the 8 o'clock position and the hand at the 2 o'clock position with the fingers wrapped around the steering wheel rim. The net result of the arm positioning was to place the forearm directly across the air bag deployment seam, subjecting the arm to a condition in which it would be most likely to measure maximum loading.

The Draft ISO Technical Report 15827 specifies that the midsagittal plane of the dummy be placed on the centerline of the seat, which is typically coincident with the centerline of the steering wheel. Notice, however, in Figure 7 that the dummy's midsagittal plane is approximately 100 mm inboard of the vertical longitudinal plane of the steering column's centerline. This is due to the limited motion range of the arm. In this particular position, the humerus cannot rotate any further inboard as it is limited by contact with the dummy's chest jacket. As a result, the entire dummy was shifted inboard to achieve the desired positioning of the arm relative to the steering wheel. Furthermore, observe in Figure 6 that the dummy's upper torso is in close proximity to the steering wheel. There are three factors which contribute to this result: 1) the short length of the humerus segment of the arm, 2) the requirement by the draft ISO document that the elbow be placed at the 8 o'clock position on the steering wheel rim, and 3) the inability of the shoulder joint to allow for any translation in the fore/aft direction. While it is clear that this arm orientation represents a high injury risk potential, it is questionable as to whether this represents a realistic driving posture representative of real world drivers.

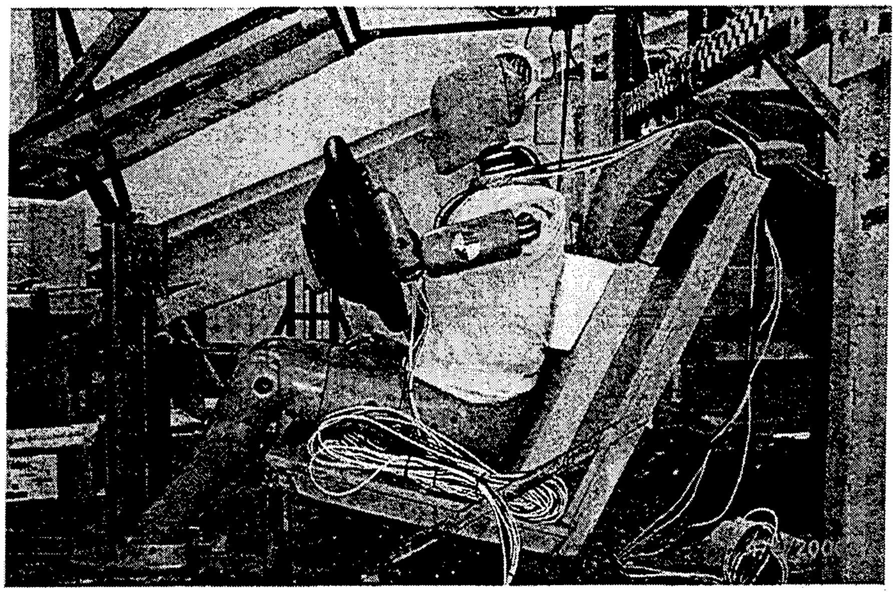

Figure 6. Typical driver air bag test configuration (side view).

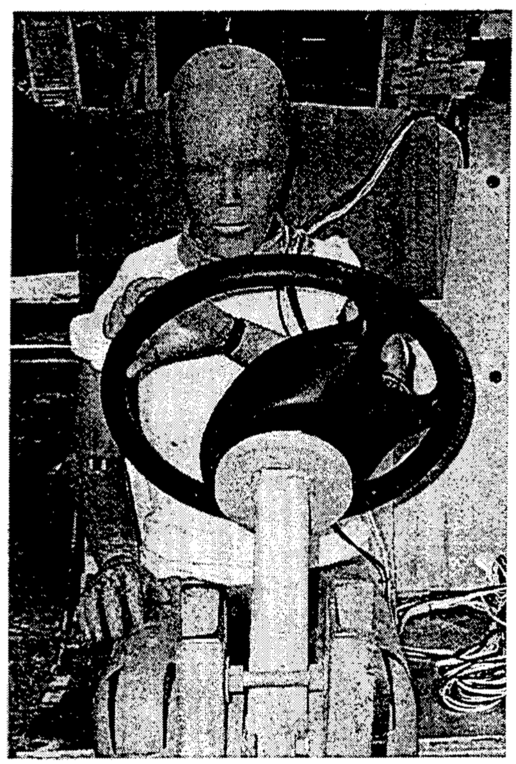

Figure 7. Typical driver air bag test configuration (front view).

Three different driver air bag systems were tested - a '95 Ford Explorer, a de-powered '98 Ford Explorer, and a '99 Dodge Intrepid - with multiple tests of each system being conducted.

4.2 Driver Air Bag Characterization

In order to make a comparison of the driver air bags, tank tests were performed using the inflators from the three different air bag systems tested. Closed tank pressure-versus-time history provides a comparative indication of the aggressiveness of different air bag systems. However, it should be pointed out that tank pressure and onset rate are just two components of the air bag system performance. Other factors also play an important role in determining the performance of the air bag system, such as cushion fold pattern, module materials, presence of tethers, cushion venting, and inflator type (compressed gas versus solid propellant).

Figure 8 contains the closed tank pressure curves for the three different driver air bag systems tested.

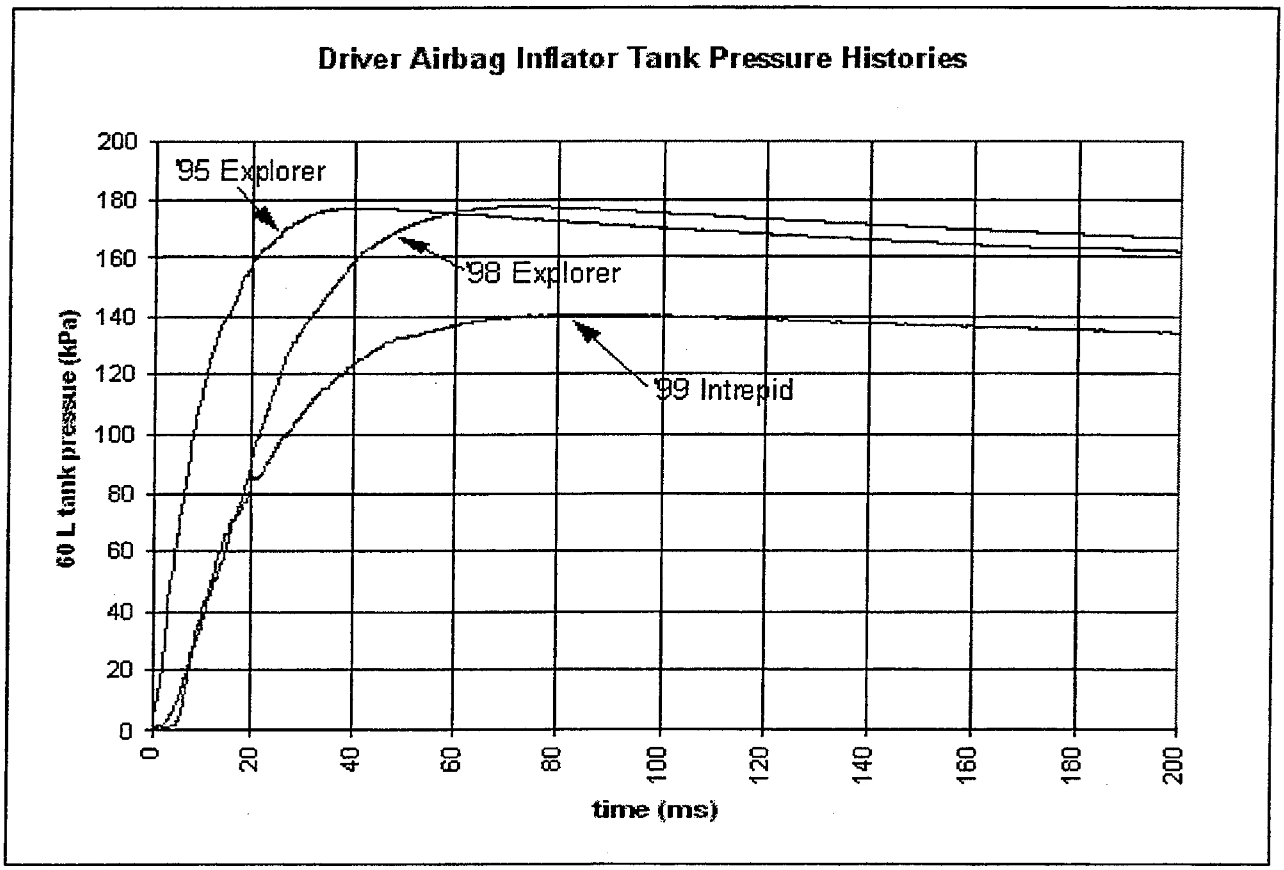

Figure 8. Driver Air Bag Inflator Tank Pressure Traces

The '95 and '98 Explorer inflators each had roughly the same peak pressure, but the '98 version displayed a lower onset rate. The '98 Explorer and the '99 Intrepid each had approximately the same onset rate, but the Intrepid had a lower peak pressure.

4.3 Side Impact Air Bags

Side impact air bag tests were conducted using both a seat-mounted and a door-mounted air bag. The door-mounted system utilized a generic test fixture which allowed for testing to be conducted without actual vehicle doors. For the seat-mounted systems, the actual vehicle seat was available from a separate VRTC research program, and therefore was used in this testing.

The test setup for the door-mounted air bag system is shown in Figures 9 through 11. The air bag was mounted to a rigid steel fixture. The dummy was seated in a generic steel seat with the instrumented arm placed directly in front of the air bag deployment seam. As seen in Figure 11, the instrumented arm was placed approximately 25 mm away from the surface of the air bag.

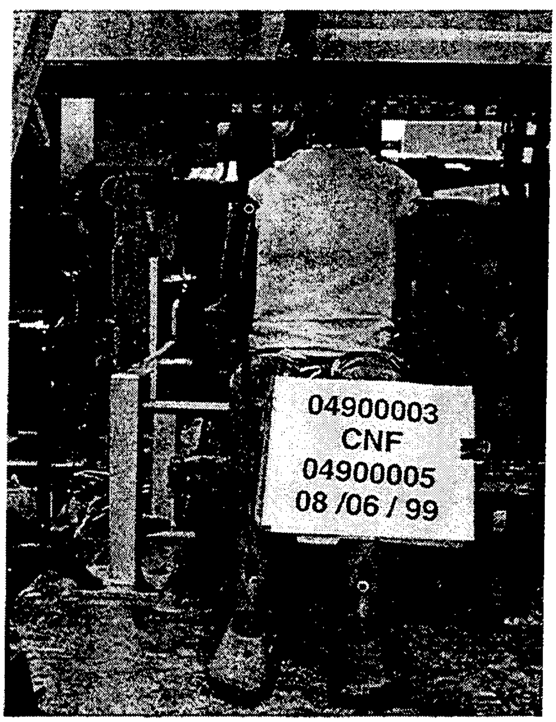

Figure 9. Door mounted air bag test setup (front view).

Figure 10. Door mounted air bag test setup (oblique view).

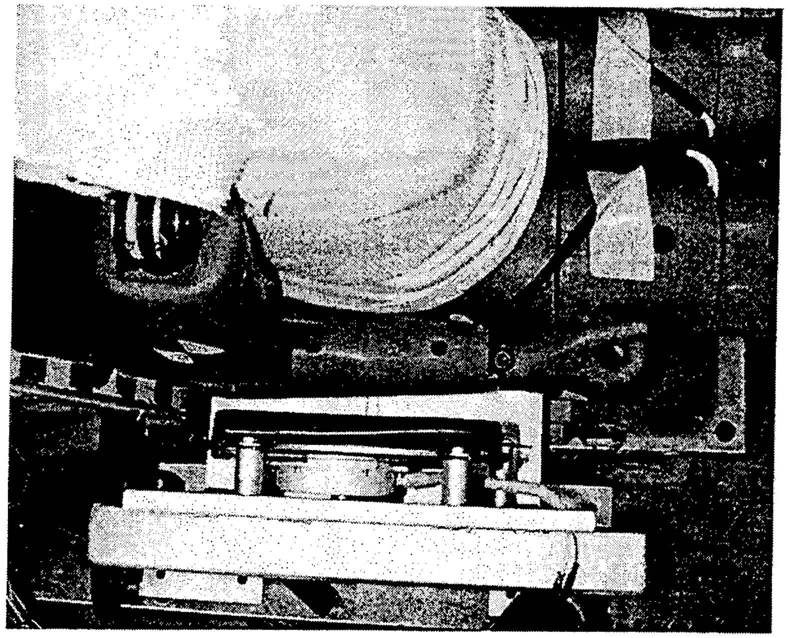

Figure 11. Overhead view of door mounted air bag test setup showing spacing between the instrumented arm and air bag surface.

Only one door-mounted air bag system was selected for testing - the '98 Cadillac DeVille. Three tests were conducted with this system.

The seat-mounted air bag testing was conducted using the seat from the actual vehicle for the system selected - a '98 Chevrolet Venture. The seat was mounted inside a Chevy Venture frame/body which had the doors and windows removed. The dummy was placed in the vehicle seat and the instrumented arm was positioned in close proximity to the air bag.

In the initial test, the dummy was positioned such that the upper arm was horizontal and at shoulder height. The elbow was bent so that the forearm was approximately horizontal and 90 degrees relative to the upper arm. The position was intended to simulate a vehicle occupant with their arm resting on the arm rest or window sill (see Figures 12 and 13). Subsequent testing in this configuration, however, resulted in very little of the deployment energy being transferred to the arm. Upon initiation, the air bag's deployment path was primarily directed out of the vehicle, parallel to the upper arm. Thus, the responses measured by the arm were quite small and well below the level of potential injury risk.

Following the initial test, it was hypothesized that a vehicle door (or door simulator) might assist in directing the air bag towards the front of the vehicle, and thus increase the interaction of the air bag with the arm. Therefore, a clear Lexan door simulator was fabricated and attached to the vehicle door frame. This material was selected so that high speed digital video of the event could continue to be captured without being obscured by an actual door. The door simulator, however, interfered with the positioning of the arm and required a new position to be established.

Figure 12. Initial seat mounted air bag test setup (no vehicle door - side view).

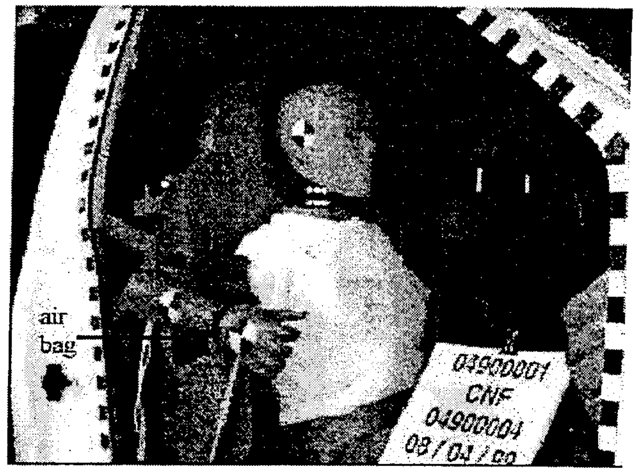

Figure 13. Initial seat mounted air bag test setup (no vehicle door - oblique view).

For the second test, the upper arm was once again placed horizontal at the height of the shoulder, but flexed slightly forward. This allowed the forearm to be placed horizontal and remain inside the door simulator. Figure 14 shows the setup for the second test. Upon conducting the test, the deployment energy again was not efficiently transferred to the upper arm. Dictated by the presence of the door simulator, the placement of the upper arm was too distant from the surface of the deploying air bag and as a result, the instrumented arm again measured very low responses.

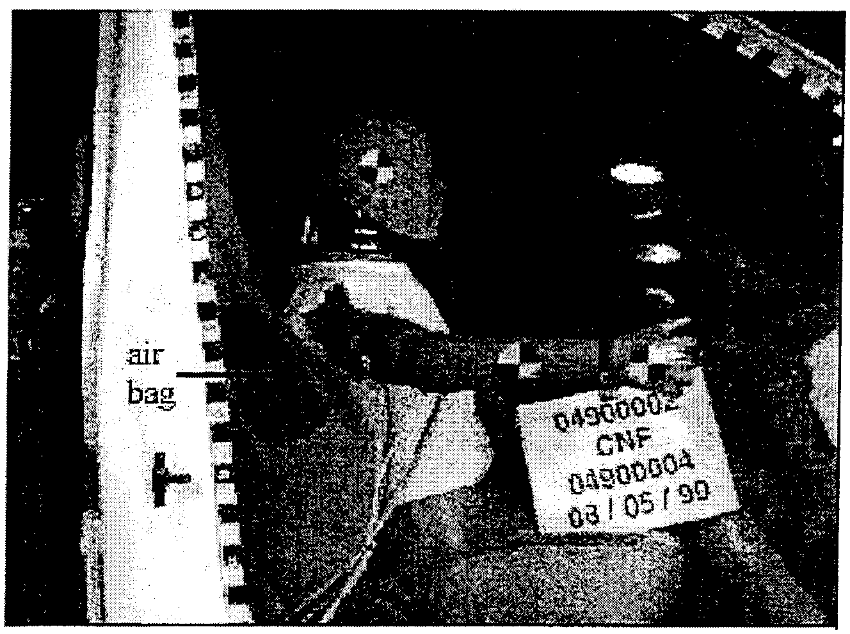

Figure 14. Second seat mounted air bag test setup (with Lexan door simulator).

For the third and final test, the arm was placed with the upper arm vertical and along the upper torso. The elbow was flexed and the forearm was horizontal. The upper arm was located as close as possible to the air bag deployment surface (see Figure 15). Once again, the deployment energy of the air bag was not effectively directed into the upper arm resulting in low measured responses.

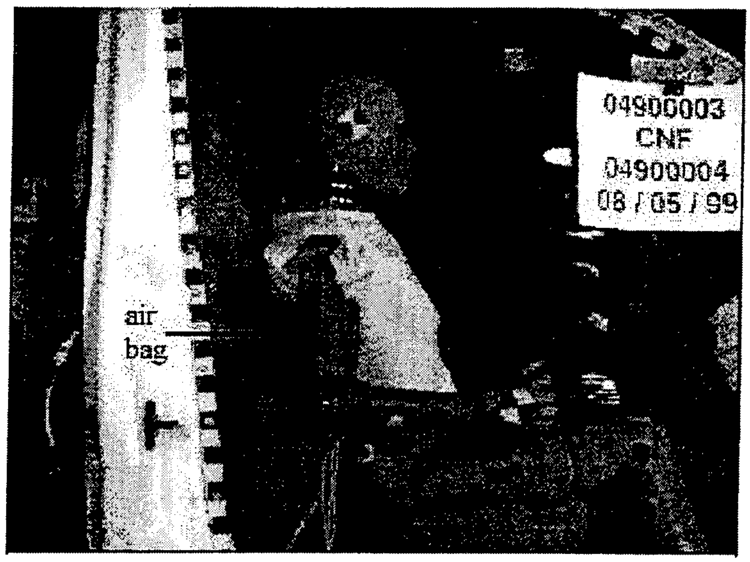

Figure 15. Third seat mounted air bag test setup.

5.0 CALIBRATION RESULTS

5.1 Repeatability

After the calibration test parameters had been established through the exploratory testing (described in Section 3), additional testing was then conducted to determine the repeatability of the responses.

5.1.1 Repeatability Testing - Forearm Segment

Three additional tests were performed and the results are tabulated in Table 5 along with the results from test cal-04. The average combined load for the four tests was 1309 N and the standard deviation was 19.87 N. The resulting coefficient of variation (%CV) was 1.52.

Table 5. Forearm Segment Repeatability Tests

Test Number	Impact Velocity (m/s)	Combined Load (N)
cal-04	2.65	1325
cal-17	2.67	1281
cal-18	2.67	1321
cal-19	2.65	1310
	avg.	1309.25
	std. dev.	19.87
	% CV	1.52

5.1.2 Repeatability Testing - Humerus Segment

Table 6 shows the results for the repeatability testing conducted on the humerus segment. The average bending moment was 128.6 Nm and the standard deviation was 3.95 Nm. The resulting coefficient of variation (%CV) was 3.07.

5.1.3 Repeatability Testing - Assembled Arm - Humerus

The results of the assembled arm - humerus repeatability testing are tabulated in Table 7. The average bending moment was 118.5 Nm and the standard deviation was 7.97 Nm. The coefficient of variation (%CV) was 6.73 which is considered marginal.

Table 6. Humerus Repeatability Tests

Test Number	Impact Velocity (m/s)	Bending Moment (Nm)
cal-08	2.62	122.8
cal-20	2.65	130.6
cal-21	2.65	129.5
cal-22	2.67	131.5
	avg.	128.60
	std. dev.	3.95
	% CV	3.07

Table 7. Assembled Arm Repeatability Tests

Test Number	Impact Velocity (m/s)	Bending Moment (Nm)
cal-12	3.73	109.4
cal-23	3.58	114.2
cal-24	3.58	126.1
cal-25	3.58	124.1
	avg.	118.45
	std. dev.	7.97
	% CV	6.73

One primary reason for the reduced repeatability of the assembled arm was the variability of the shoulder and elbow joint torque settings. Efforts were made to set the joint torques consistently before conducting each test, however, because of the presence of the rubber grommets in each of the joints, it was difficult to insure precise joint torques for each test. As a result, it was determined that the assembled arm test was not suitable for a calibration test. Based on this conclusion, it was decided that forearm repeatability tests for the assembled arm would not be meaningful.

5.2 Post-Air Bag Testing Component Calibrations

Following completion of the air bag testing, the arm was again subjected to the component calibration tests to determine how the arm's responses might change over time and after use. Four tests were conducted with the forearm segment and three tests were conducted with the humerus segments. The results are summarized in Tables 8 and 9.

Table 8. Post Air Bag Testing - Forearm Segment

Test Number	Impact Velocity (m/s)	Combined Load (N)
cal-124	2.65	1570
cal-125	2.67	1595
cal-126	2.67	1587
cal-127	2.67	1590
	avg.	1585.5
	std. dev.	9.39
	% CV	0.59

Table 9. Post Air Bag Testing - Humerus Segment

Test Number	Impact Velocity (m/s)	Bending Moment (Nm)
cal-120	2.65	115.9
cal-121	2.67	119.1
cal-122	2.67	118.5
	avg.	117.8
	std. dev.	1.39
	% CV	1.18

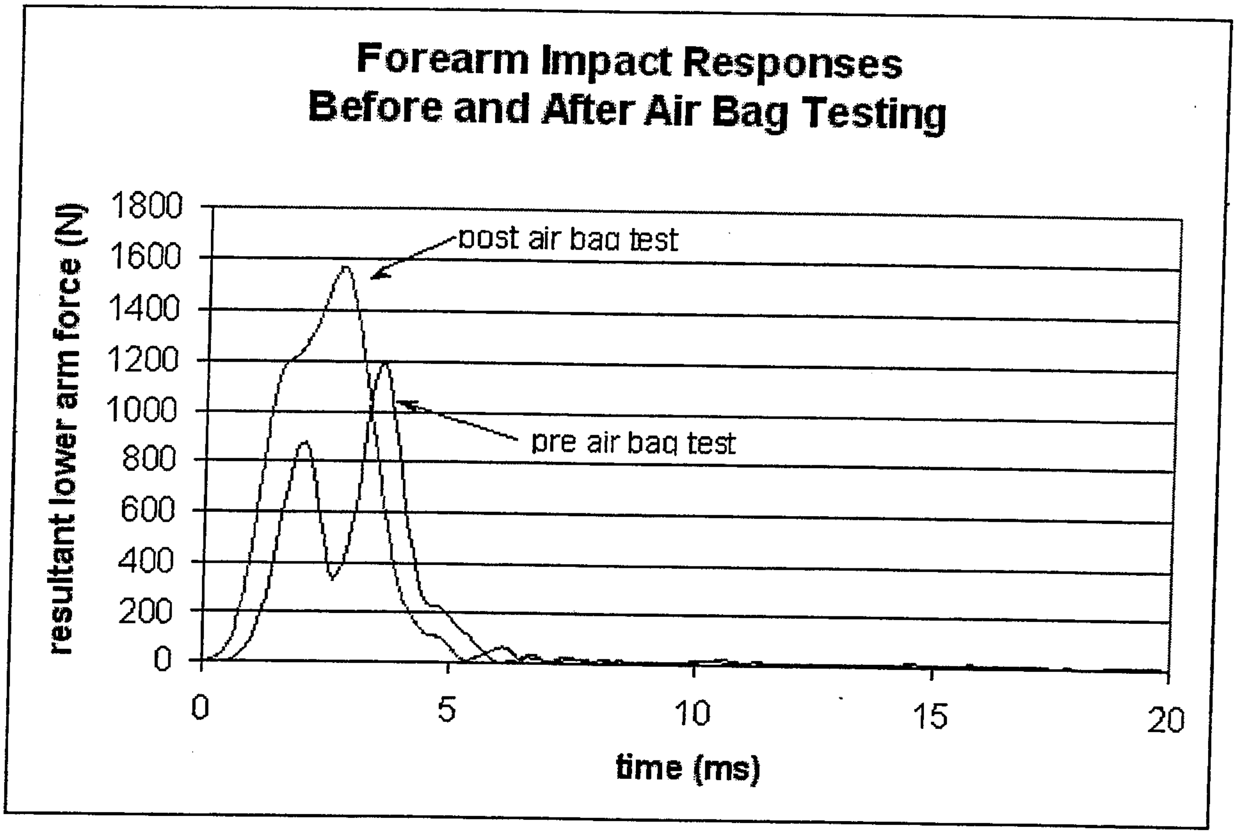

Figure 16. Comparison of the Combined Loading on The Forearm for Tests Conducted Before and After the Air Bag Testing

At this point, it is of interest to compare the post-air bag testing results with the results of the previously conducted repeatability tests. For the forearm segment tests, it is observed that the average combined load increased substantially in the post-air bag tests - 1585.5 versus 1309.3 N - an increase of approximately 21 percent. Also, the shape of the forearm loading response curve changed significantly (see Figure 16). For the initial repeatability tests, the curve contained two distinct peaks occurring within the first 5 milliseconds. Conversely, the response curves for the tests conducted after the air bag tests contained only a single peak.

Post-test calibration of the forearm load cell indicated that the sensitivity of the force channels in the load cell had changed less than 0.4 percent, thus sensitivity and data collection should not have played a role. There are, however, several potential explanations for this change in response. One possible cause is that a combination of effects from air bag loading and aging changed the properties of the arm flesh. Another possible explanation is that the calibration test set-up is excessively sensitive to test factors such as point of impact and positioning of the arm flesh on the arm structural members. Additional testing and evaluation may be required to better understand this phenomena.

For the humerus impacts, the post-air bag test responses were quite similar to the pre-air bag test responses. There was only a slight decrease in bending moment in the post-air bag test responses - 117.8 versus 128.6 Nm - a reduction of approximately 8 percent. Furthermore, the response curves observed for each set of tests displayed a similar, unimodal pattern (see Figure 17).

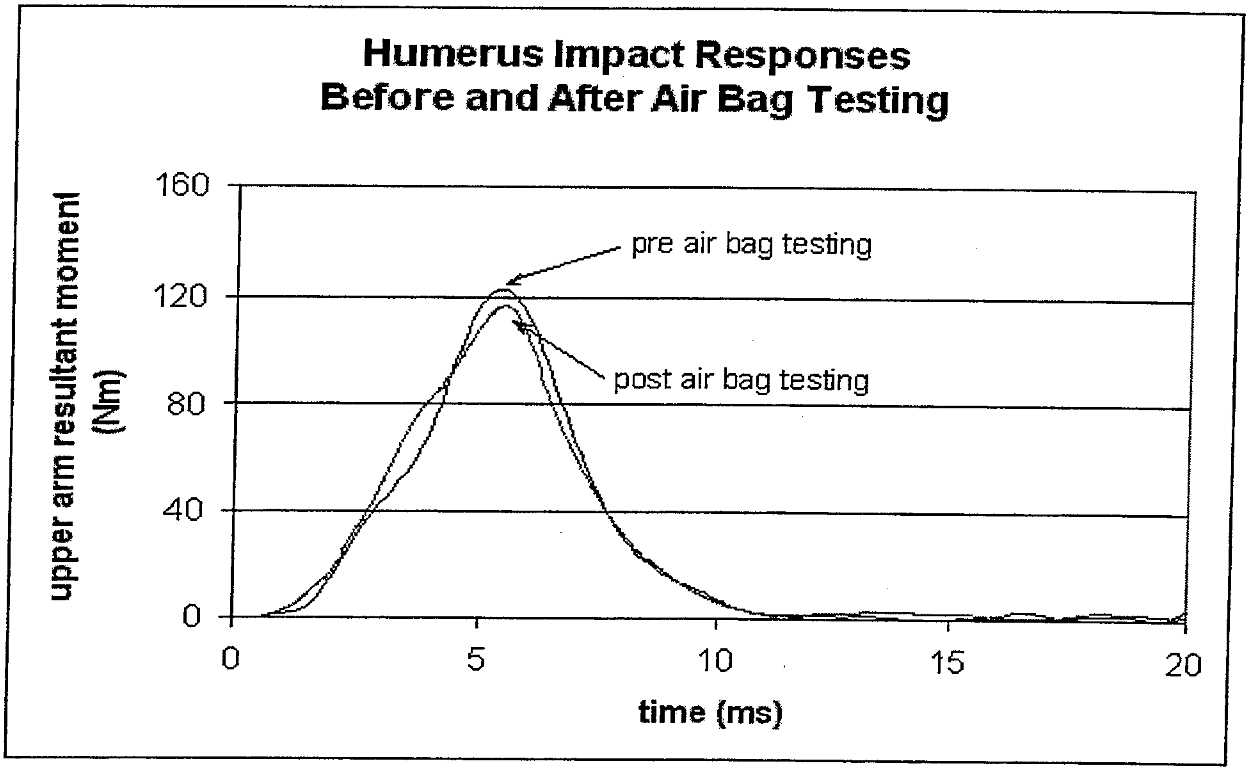

Figure 17. Comparison of Humerus Resultant Moment Responses for Humerus Impacts Conducted Before and After Air Bag Testing

6.0 STATIC AIR BAG TESTING RESULTS

This section summarizes the static air bag test results of the instrumented arm. During a typical air bag test, there were two primary events of interest identified. The first event occurred when the air bag cover and/or the inflating air bag cushion contacted the arm upon deployment, and this is referred to as air bag injury. The second event occurred when the arm was projected by the air bag into the dummy's upper torso. This event is referred to as contact injury. A typical response curve exhibiting primary (peak) injury due to air bag contact is shown in Figure 18, while an example of contact injury is shown in Figure 19.

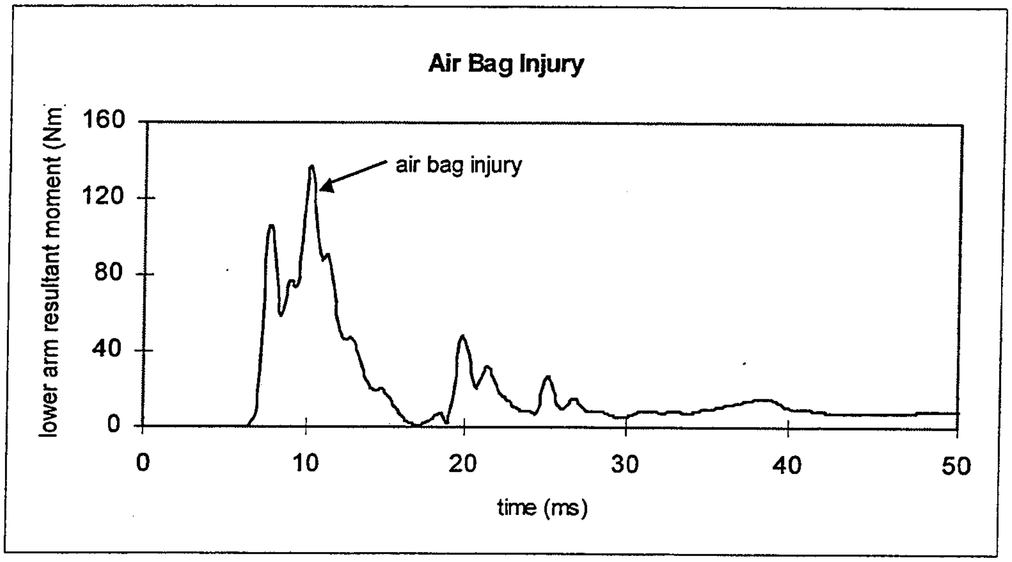

Figure 18. Typical response with air bag injury mechanism. (Test #dab-11)

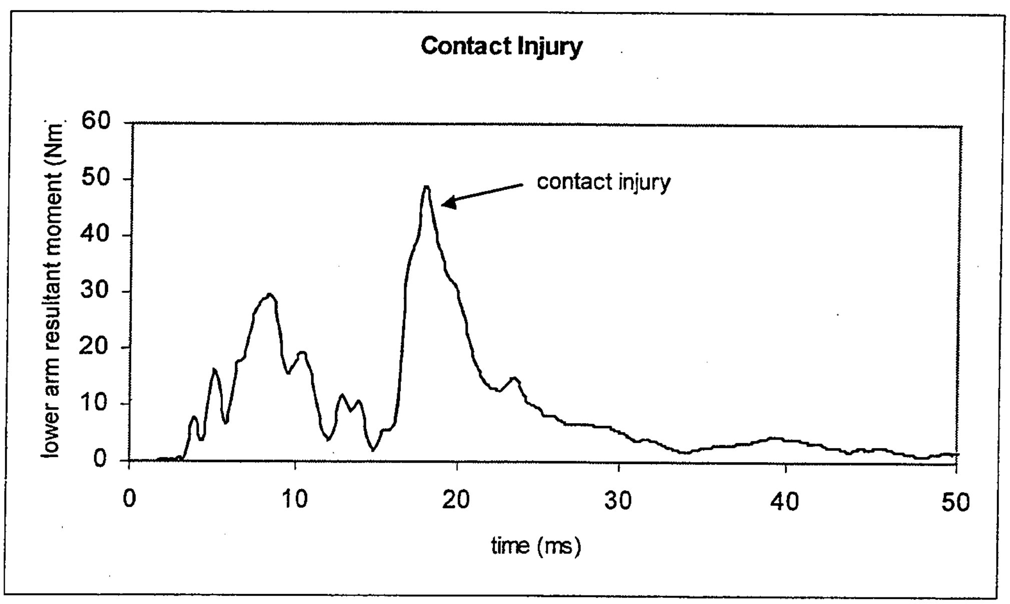

Figure 19. Typical response with contact injury mechanism. (Test #sab-01)

6.1 Static Driver Air Bag Testing

Static air bag tests were conducted to evaluate the performance of the instrumented arm. Three different driver air bag systems were tested - a '95 Ford Explorer, a '98 Ford Explorer, and a '99 Dodge Intrepid. Two tests were conducted with the Intrepid system while 3 tests were conducted with each of the Explorer systems. A summary of the peak results and the time at which the peaks occurred appears in Tables 10 (for the forearm) and 11 (for the humerus).

Table 10. Static Driver Air Bag Peak Responses for the Forearm

Air Bag System	Test Number	Resultant Force (N)		time (ms)	Resultant Moment (Nm)		time (ms)	Resultant Accel. (g)		time (ms)
'99 Intrepid	dab-11	1453.3	@	10.6	137.1	@	10.8	632.1	@	8.0
'99 Intrepid	dab-12	1031.3	@	9.7	116.1	@	7.4	623.6	@	7.0
'95 Explorer	dab-13	422.6	@	10.0	86.9	@	4.4	542.9	@	4.2
'95 Explorer	dab-14	772.2	@	24.8	102.2	@	15.3	519.9	@	3.8
'95 Explorer	dab-15	659.7	@	9.2	172.2	@	18.7	751.9	@	18.5
'98 Explorer	dab-16	275.2	@	11.5	45.9	@	5	392.0	@	4.5
'98 Explorer	dab-17	343.7	@	12.3	38.5	@	5.2	250.2	@	4.7
'98 Explorer	dab-18	478.5	@	11.3	44.4	@	11.6	394.1	@	4.8
range of IARV's		1380			66 - 91			n/a		

Table 11. Static Driver Air Bag Peak Responses for the Humerus

Air Bag System	Test Number	Resultant Force (N)		time (ms)	Resultant Moment (Nm)		time (ms)	Resultant Accel. (g)		time (ms)
'99 Intrepid	dab-11	647.6	@	14.5	89.3	@	14.4	189.6	@	10.6
'99 Intrepid	dab-12	491.8	@	14.4	65.5	@	13.8	164.8	@	9.8
'95 Explorer	dab-13	413.6	@	10.2	65.2	@	10.4	174.4	@	10.2
'95 Explorer	dab-14	766.6	@	25.5	82.0	@	27.1	202.4	@	5.5
'95 Explorer	dab-15	581.9	@	15.3	75.7	@	15.7	231.7	@	18.6
'98 Explorer	dab-16	292.6	@	48.8	28.5	@	22.6	84.7	@	6.2
'98 Explorer	dab-17	246.5	@	23.6	33.4	@	21.9	82.3	@	16.8
'98 Explorer	dab-18	199.1	@	23.6	31.5	@	23.2	95.1	@	6.5
range of IARV's		n/a			128 - 130			n/a		

Plots of selected responses from this test series appear in Appendix B. Review of these plots, Table 10, and high speed digital video of the tests indicate that the majority of the peak forearm responses occurred as a result of the air bag injury mode. The forearm force IARV of 1380 N was exceeded only once (test #dab-11), while the forearm bending moment was either within or exceeded the range of the IARV in 5 of the 8 tests. Conversely, the humerus was not directly contacted by the air bag and therefore the humerus response remained below its bending moment IARV for all 8 tests. Review of the digital video indicates that the humerus appeared to be loaded in compression axially by the force transmitted through the elbow and shoulder joints. A bending moment is then generated as a result of the axial loading, similar to what would be present in a column buckling condition. This observation was confirmed by analysis of the humerus loading response curves, where it was seen that the primary load in the humerus is along the z-axis. Figure 20 illustrates a typical humerus loading response curve. Additional humerus force response curves can be found in Appendix C.

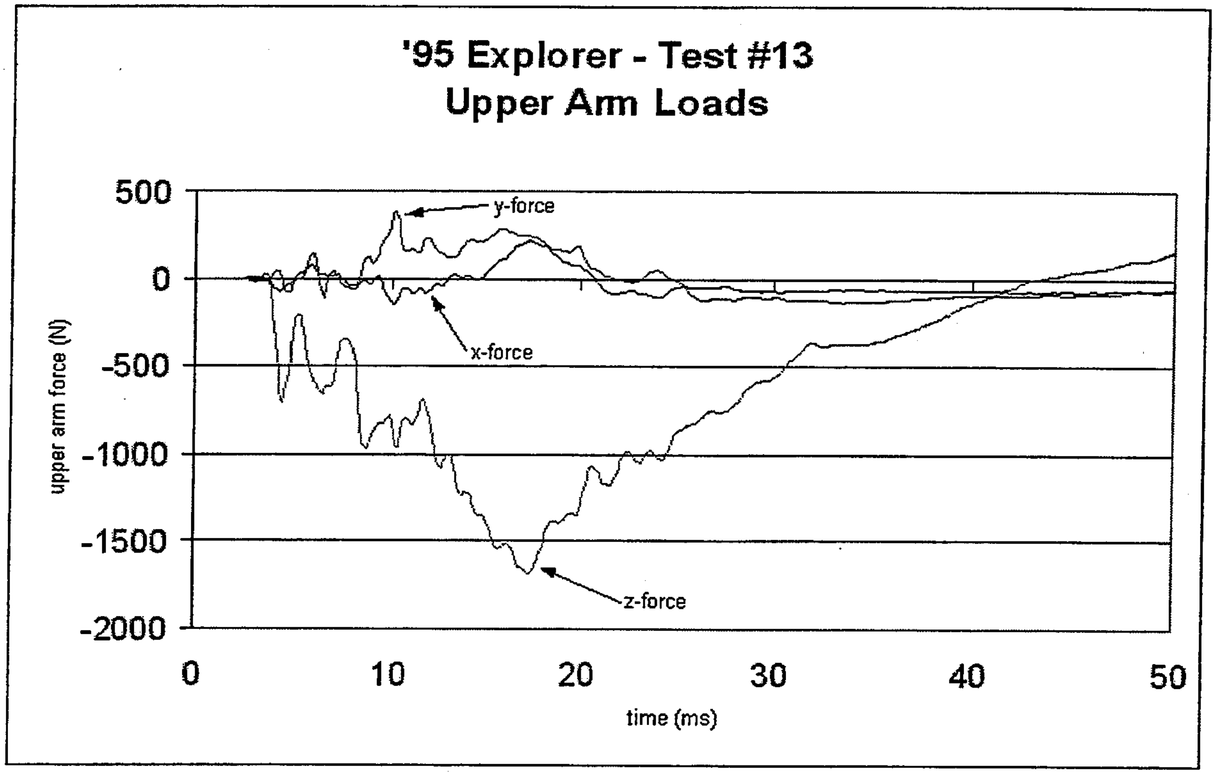

Fig. 20. Typical loading response curve of the humerus in driver air bag test.

One interesting observation made from Tables 10 and 11 is that the responses measured for the Intrepid tests were, in general, higher than those in either of the Explorer test series. This was an unexpected result in light of the inflator tank pressure responses reported in Figure 8. However, as noted in the discussion in Section 4.2, there are factors other than the inflator tank pressure response which determine the overall performance of the air bag system. A teardown analysis of the air bags produced several observations which may help explain these results. One observation was that the Intrepid air cushion did not contain any vent holes while both of the Explorer systems had vent holes present (the '95 system had two ½ inch vents and the '98 system had two 7/8 inch vents). Another observation was that the module cover of the Intrepid seemed to be stiffer than that of the Explorer air bags. This could potentially cause the cushion pressure to be higher in the Intrepid air bag before the cushion breaks out of the module cover, resulting in a more forceful interaction with the arm at the time of cushion "punchout." The fact that most of the peak responses for the Intrepid system occur relatively early in the event seems to indicate that the latter observation may indeed have some credibility.

Another important observation can be made when comparing the '98 Explorer system with the original '95 Explorer system. Physically, these two air bag systems were nearly identical. The air bag covers appeared to have the exact same construction. The construction of the cushions was also the same with the exception of the previously noted vent hole diameter difference. The primary difference was in the inflator performance - the '98 Explorer had a lower onset rate. In the system tests, the peak arm responses for the '98 Explorer system were, in general, less than the corresponding responses recorded for the '95 Explorer system. This observation would indicate that the inflator onset rate played a significant role in the response of the arm. Conversely, the vent hole diameter is likely to have only a small effect on the early response of the arm. The vent hole diameter probably plays a more important role in the deflation or "ride down" segment which occurs later in the event.

6.1.1 Repeatability of Static Driver Air Bag Tests

Due to the small sample sizes, no statistical analysis of the repeatability of responses has been included. Review of Tables 10 and 11 indicate that, from a qualitative perspective, a lack of repeatability exists. There are several factors which likely contributed to this result. One factor is the presence of variation in the air bag deployment event. Examples of key properties which may vary include the air bag unfolding; the inflator performance in terms of peak pressure, initial onset, and the associated gas dynamics; and the module cover punchout force. Some other factors which likely played a role in the poor quantitative repeatability include the lack of complete kinematic biofidelity of the elbow and shoulder joints, the position of the arm relative to the air bag, the location of the skin on the forearm and humerus, and the joint torques at the shoulder and elbow.

From a qualitative standpoint, there are similarities in the shape of the response curves among repeat tests of driver air bag systems. This is a positive indication of the arms's ability to provide similar responses to similar inputs. Figures 21 and 22 illustrate the qualitative repeatability of responses for repeat tests with driver air bag systems. Additional plots can be found in Appendix D.

It should be noted that the instrumented arm suffered some damage during this test series. During test number dab-14, the molded portion of the left hand detached from its metal substructure and was projected approximately 10 feet. The welded steel hand insert remained intact and attached to the wrist assembly. The molded hand and welded steel substructure are shown in Figure 23. The details of this failure were shared with the manufacturer (R. A. Denton, Inc.) so that its design could be reviewed for potential improvements. Since the left hand was now unusable, it was necessary to use the right hand on the left arm to complete the test objectives while a new left hand was ordered from the manufacturer.

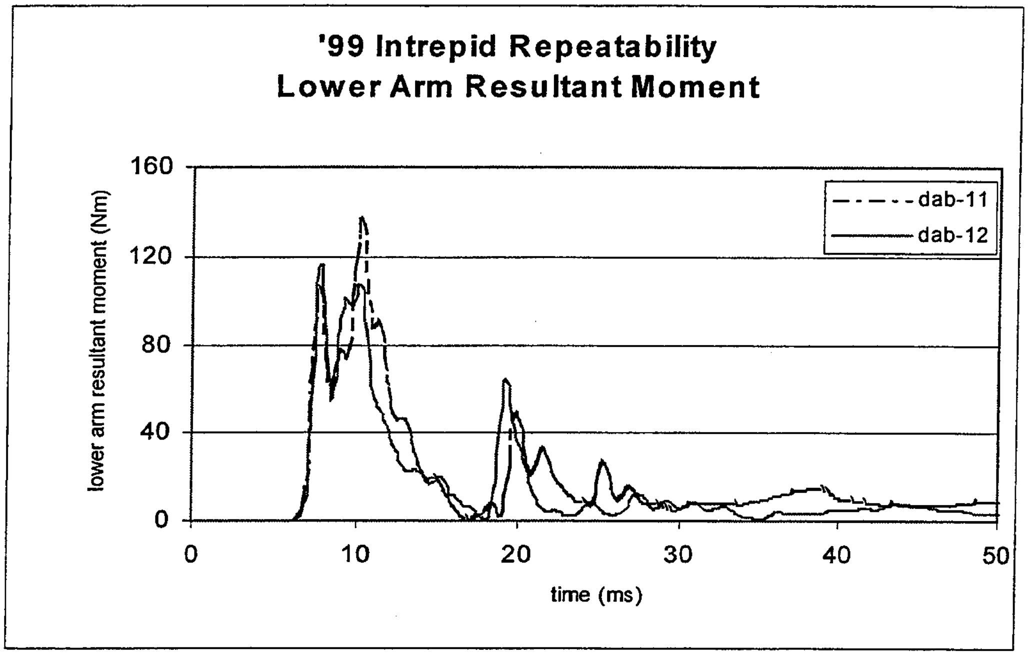

Figure 21. Lower Arm Resultant Moment Responses for Repeat Driver Air Bag Tests

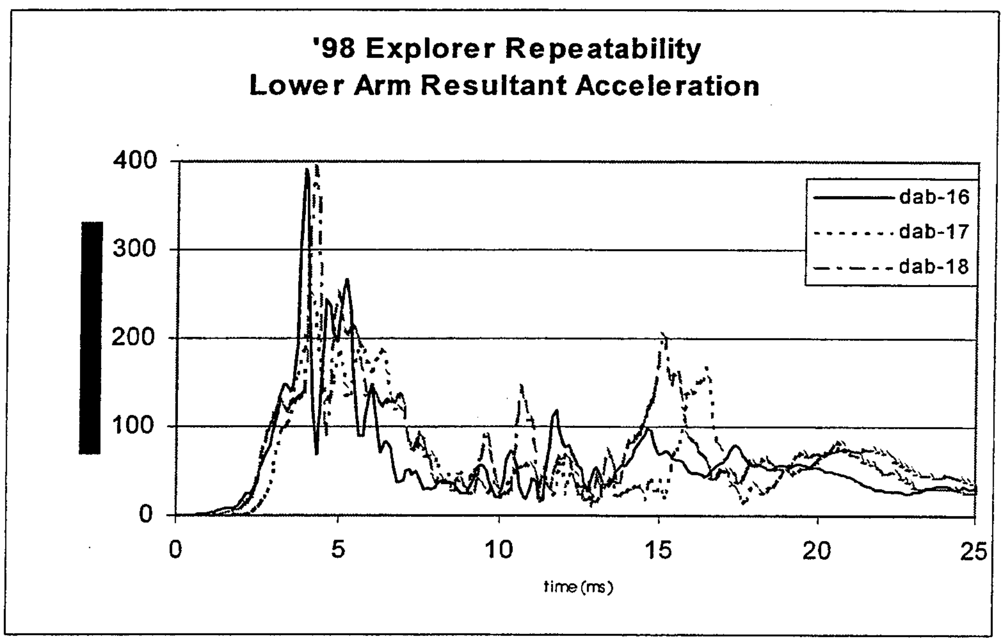

Figure 22. Lower Arm Resultant Acceleration Responses for Repeat Driver Air Bag Tests

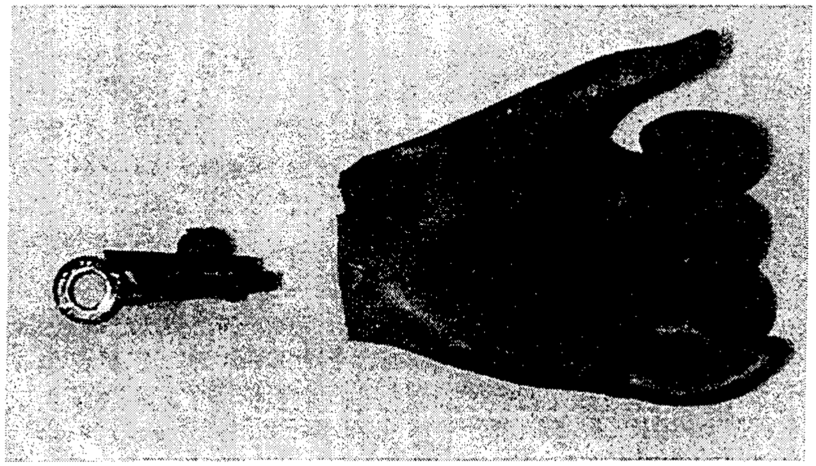

Figure 23. Molded hand and welded steel insert following failure.

6.2 Static Side Impact Air Bag Testing

Side impact air bag tests were conducted using two different air bag systems - a door-mounted '98 Cadillac DeVille and a seat-mounted '98 Chevrolet Venture. Three tests were conducted with each system and a summary of the peak results and the time at which the peaks occurred appear in Tables 12 (for the forearm) and 13 (for the humerus).

Table 12. Static Side Impact Air Bag Peak Responses for the Forearm

Air Bag System	Test Number	Resultant Force (N)		time (ms)	Resultant Moment (Nm)		time (ms)	Resultant Accel. (g)		time (ms)
'98 DeVille	sab-01	910.3	@	18.6	48.8	@	18.0	414.8	@	4.0
'98 DeVille	sab-02	645.1	@	14.6	42.0	@	23.4	312.2	@	3.7
'98 DeVille	sab-03	629.4	@	14.4	33.9	@	8.3	437.4	@	3.9
'98 Venture	sab-04	173.8	@	5.8	13.2	@	6.1	164.7	@	5.7
'98 Venture	sab-05	32.9	@	35.2	20.0	@	35.7	29.8	@	35.3
'98 Venture	sab-06	51.7	@	6.7	4.3	@	6.7	35.0	@	6.0
range of IARV's		1380			66 - 91			n/a		

Table 13. Static Side Impact Air Bag Peak Responses for the Humerus

Air Bag System	Test Number	Resultant Force (N)		time (ms)	Resultant Moment (Nm)		time (ms)	Resultant Accel. (g)		time (ms)
'98 DeVille	sab-01	242.7	@	17.8	46.6	@	19.3	372.9	@	17.9
'98 DeVille	sab-02	231.9	@	13.9	36.2	@	8.4	183.7	@	14.8
'98 DeVille	sab-03	167	@	15.8	51.5	@	15.2	305.4	@	14.3
'98 Venture	sab-04	227.2	@	5.8	28.8	@	5.3	261.1	@	5.8
'98 Venture	sab-05	61.1	@	9.2	8.9	@	10.3	10.7	@	12.6
'98 Venture	sab-06	234.2	@	5.2	24.8	@	6.0	75.1	@	5.2
range of IARV's		n/a			128 - 130			n/a		

As the results in Tables 12 and 13 indicate, the responses of the arm to the Deville air bag (door-mounted system) were generally higher than the responses to the Venture air bag (seat-mounted), particularly the responses of the forearm. This result was expected as the instrumented arm is positioned more directly in the deployment path of the door-mounted air bags.

In the door-mounted air bag tests, the arm is placed relatively close to the dummy's upper torso. As a result, the forearm makes contact with the upper torso very rapidly following air bag deployment. This made it difficult to categorize responses as either air bag or contact injuries.

One observation made from Tables 12 and 13 is that for both the forearm and the humerus, all of the responses were well below the range of IARV's reported in the literature. This is especially true for the seat mounted air bag tests ('98 Venture) where the deployment energy was initially directed away from the arm.

It is also worth noting that the peak responses of the forearm to the door-mounted air bag were within the range of the peak responses observed in the driver air bag systems. This result is somewhat unexpected as the typical door-mounted air bag is much smaller than a driver's air bag. However, the side impact systems are required to inflate much more rapidly than the driver air bag systems, indicating that inflator onset rate again played a significant role in determining the arm's responses.

Plots of selected responses from this test series appear in Appendix E.

7.0 CONCLUSIONS

7.1 Durability

The instrumented arm was subjected to a number of tests in a range of test environments - pendulum impacts, driver air bags, and side impact air bags. A failure of the hand was observed during the evaluation and as a result, it has been recommended to the arm manufacturer that the design of the hand be reviewed. The durability of the remaining components of the arm was acceptable.

7.2 Injury Tolerance of the Upper Extremities

As restraint system technology improves and more lives are saved in traffic accidents, the focus has shifted from not only saving lives but also to reducing debilitating injuries. Previously, the primary concern of restraint design was to protect the major vital organs such as the heart, brain, and central nervous system and thus the focus was on protecting the head, neck, and chest. Now that more and more occupants are surviving severe crashes, the concern is shifting to one of preventing debilitating injuries such as those suffered to the legs and arms.

In the previous research identified by this study, the injury tolerances suggested for the forearm and humerus were relatively consistent. Research from both Duma and Kirkish recommend a bending moment tolerance for the humerus in the range of 128 - 131 Nm. Papers by Saul, Bass, and Pintar propose a bending moment tolerance for the forearm in the range of 66 - 91 Nm. Pintar's work also documents a force tolerance for the forearm at 1380 N. However, there is very little upper extremity injury tolerance data in existence. It is likely that the IARV's used in this study may need to be updated as the biomechanics community gathers data and knowledge of the arm's injury tolerance.

7.3 Calibration Tests

After determining the impact parameters, repeatability tests were conducted. It was determined that the component impact tests provided more repeatable responses than the tests conducted with the assembled arms. This result was attributed to the variations in joint torque observed in conducting the assembled arm tests.

The initial repeatability results for the component tests was very good. However, when a second series of calibration tests was conducted following the air bag testing, the response of the forearm was significantly different in both the peak response and the shape of the response curve. The cause of this result has not been clearly identified, however, it is hypothesized that the properties of the flesh may have changed due to use and aging or that the test is overly sensitive to slight changes in the test parameters. The humerus component tests displayed more repeatability when comparing pre- and post-air bag test calibration responses.

7.4 Air Bag Tests

For the air bag tests, two primary events of interest were observed. The first event occurred when the air bag cover and/or the inflating air bag cushion contacted the arm upon deployment and this is referred to as air bag injury. The second event occurred when the arm was projected by the air bag into the dummy's upper torso. This event is referred to as contact injury.

Driver air bag tests were conducted with three different systems. Review of the responses and high speed digital video of the driver air bag tests indicate that the majority of the peak forearm responses occurred as a result of the air bag injury mode. The forearm force IARV was exceeded only once, while the forearm bending moment was either within or exceeded the range of the IARV in 5 of the 8 tests. The humerus was not directly contacted by the air bag, and therefore the humerus response remained below its bending moment IARV for all 8 tests.

Prior to conducting the driver air bag tests, an attempt was made to quantify the performance of each system by tank testing the inflator from each air bag. Later, after conducting the air bag tests, conclusions were drawn regarding the ability to predict the performance of the air bag system based on the inflator pressure curves. In tests comparing a de-powered driver air bag ('98 Explorer) with its predecessor ('95 Explorer), the measured responses of the arm were reduced. This indicated that when most other characteristics of the air bag's design are kept constant, a reduction in inflator onset rate produced a corresponding reduction in the responses of the arm.

However, when comparing air bag systems of significantly different designs (such as the Intrepid versus the Explorer), it was determined that the inflator tank test results alone were a poor predictor of system performance with regard to arm injury. Other factors, including air bag cover designs, cushion fold patterns, cushion materials, presence of tethers, cushion venting, and inflator type, also play a significant role in determining the overall system performance and subsequent response of the instrumented arm.

While no statistical analysis was presented, the responses of the instrumented arm measured in the driver air bag tests appeared to exhibit a lack of quantitative repeatability. Possible sources of variation include the air bag unfolding; the inflator performance in terms of peak pressure, initial onset, and the associated gas dynamics; and the module cover punchout force. Some other factors which likely played a role in the poor repeatability include the lack of complete kinematic biofidelity of the elbow and shoulder joints, the position of the arm relative to the air bag, the location of the skin on the forearm and humerus, and the joint torques at the shoulder and elbow. Even though there was a lack of quantitative repeatability, the responses exhibited good qualitative repeatability. For repeated test conditions, the arm provided similarly shaped response curves.

Tests were also conducted with both seat-mounted and door-mounted side impact air bags. The seat-mounted air bags imparted very little force to the arm. This is because the deployment energy for the seat-mounted systems was not directed primarily at the arm, but rather at the vehicle door. On the other hand, the door-mounted systems provided a significant amount of energy to the arm. In both cases, the responses measured by the instrumented arm were substantially below the recommended IARV's.

8.0 ACKNOWLEDGMENTS

The authors would like to express their sincere gratitude to all of the people who contributed to this project. From VRTC, we would like to recognize Brad Arn, Rob Jacobs, and Mike Ward for electronics and data acquisition support; Herman Jooss and Matt Hostetler for high speed digital video and photographic support; Dick Levan, Gene Faut, and David Hyder for mechanical technician support; and Dr. Roger Saul and Heather Rhule for engineering and technical reference. The authors would also like to thank Paul Depinet of Robert A. Denton, Inc. for providing AutoCAD drawings of the instrumented arm and for technical support. We would also like to acknowledge Stefan M. Duma of the University of Virginia, Automotive Safety Laboratory and Sarah Kirkish of Ford Motor Company for providing technical references. Finally, the authors also express their gratitude to Susie Weiser for compiling and formatting this document.

9.0 References

1. Kuppa, S.M., Yeiser, C.W., Olson, M.B., Taylor, L., Morgan, R., Eppinger, R., *RAID- An Investigation Tool to Study Air Bag/Upper Extremity Interactions*, SAE Paper 970399, SAE International Congress and Exposition, Detroit, MI, 1997.

2. Johnston, K.L., Klinich, K.D., Rhule, D.A., Saul, R.A., *Assessing Arm Injury Potential From Deploying Air Bags*, SAE Paper 970400, 1997.

3. Kirkish, S.L., Begeman, P.C., Paravasthu, N.S., *Proposed Provisional Reference Values for the Humerus for Evaluation of Injury Potential*, SAE Paper 962416, 40th Stapp International Car Crash Conference, Albuquerque, New Mexico, 1996.

4. Duma, S. M., Crandall, J. R.,Hurwitz, S.R., Pilkey, W. D.; *Small Female Upper Extremity Interaction with a Deploying Side Air Bag*, SAE Paper 983148, 1998.

5. Saul, R.A., Backaitis, S.H., Beebe, M.S., Ore, L., *Hybrid III Dummy Instrumentation and Assessment of Arm Injuries During Air Bag Deployment*, SAE Paper 962417, 40th Stapp International Car Crash Conference, Albuquerque, New Mexico, 1996.

6. Bass, C.R., Duma, S.M., Crandall, J.R., Morris, R., Martin, P., Pilkey, W.D., Hurvitz, S., Khaewpong, N., Eppinger, R., Sun, E., *The Interaction of Air Bags with Upper Extremities*, SAE Paper 973324, 41st Stapp International Car Crash Conference, Orlando, Florida, 1997.

7. Pintar, F. A., Eppinger, R. H., and Yoganandan, N, *Response and Tolerance of the Human Forearm to Impact Loading*, SAE Paper 983149, 1999.

8. ISO Technical Draft, Report 15827, ISO/TC22/SC10/WG3N175.

Appendix A

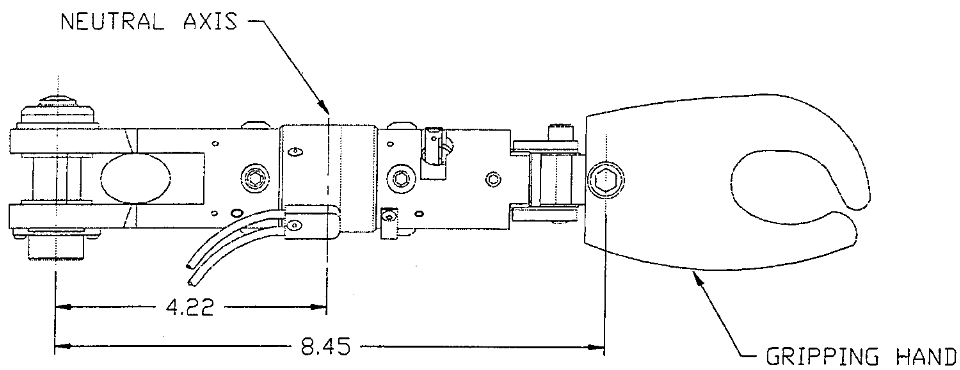

Fig. A.1. Location of Load Cell Neutral Axis in the Forearm.

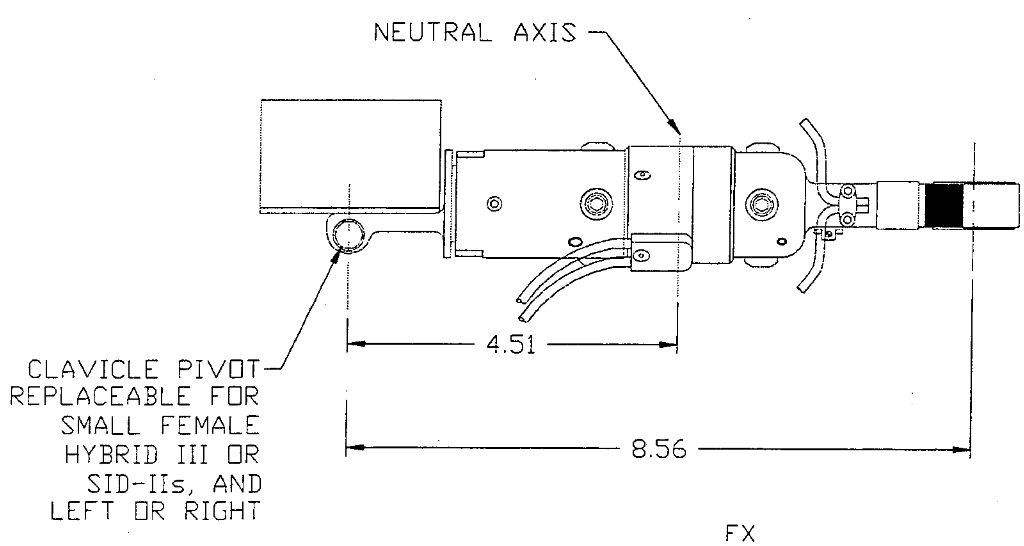

Fig. A.2. Location of Load Cell Neutral Axis in the Upper Arm.

Appendix B

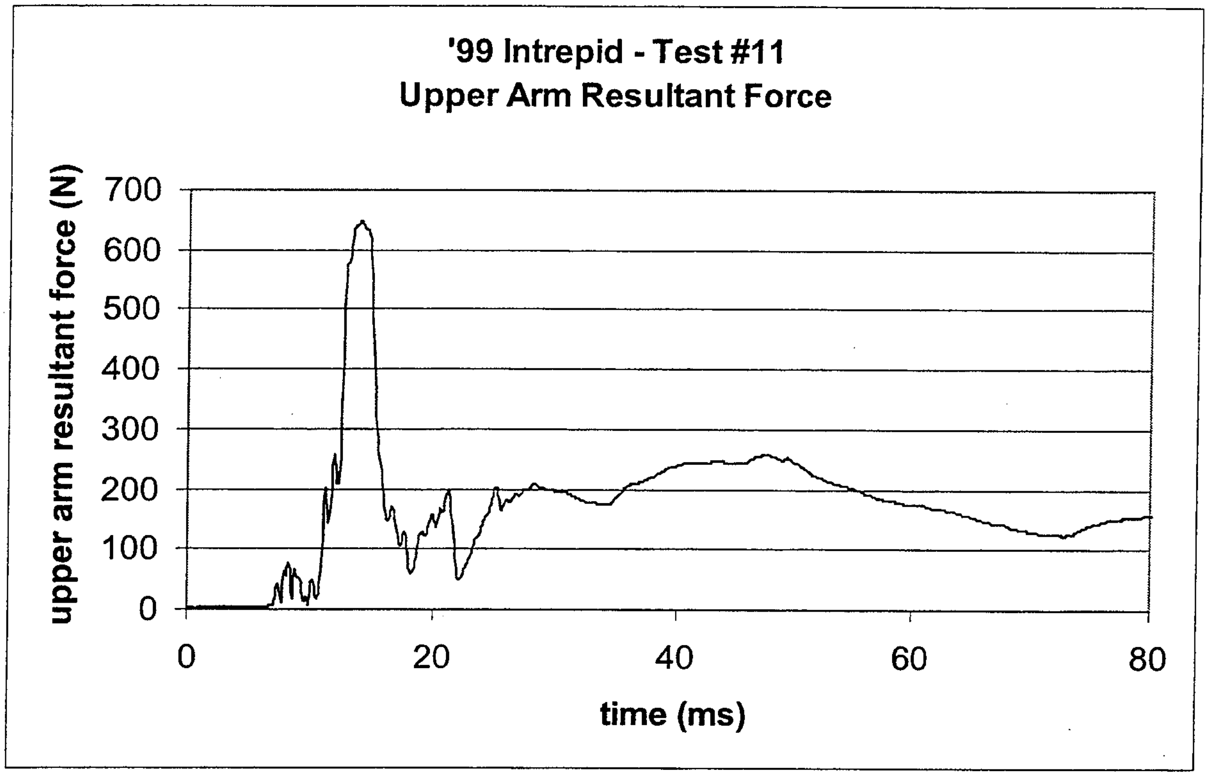

Fig. B.1. '99 Intrepid - Test 11. Upper Arm Resultant Force

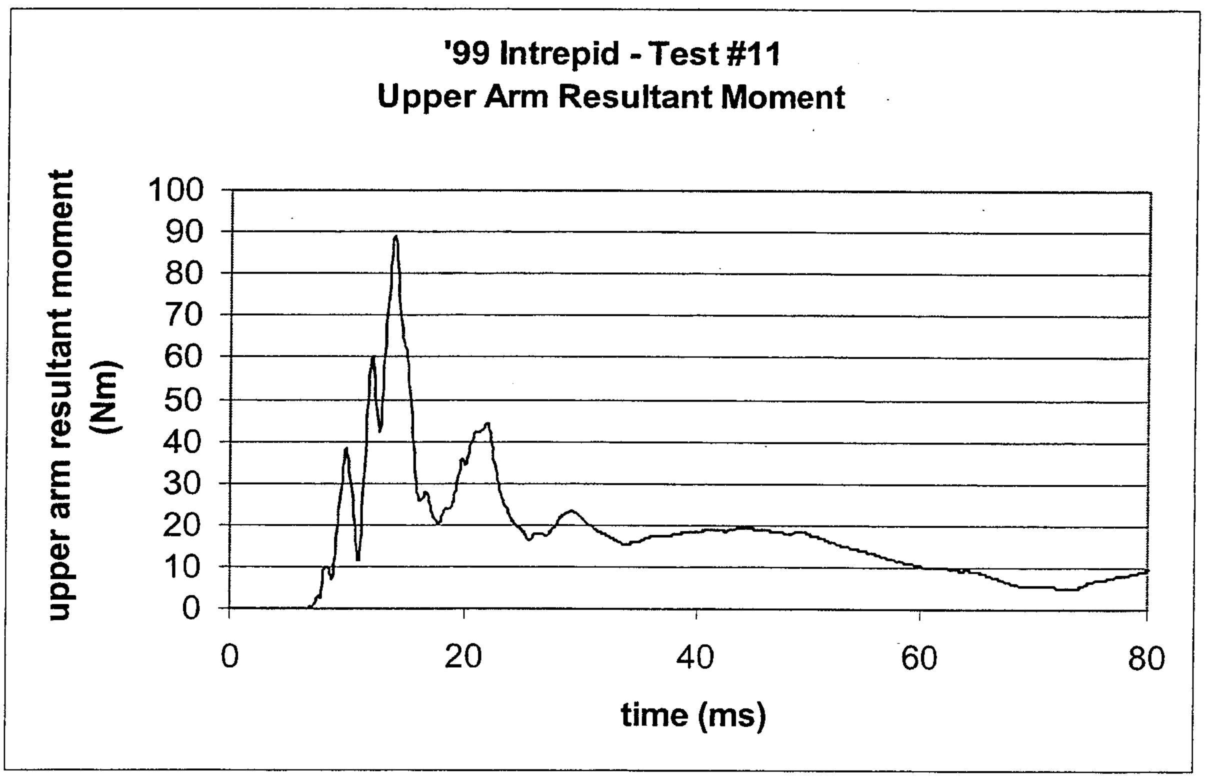

Fig. B.2. '99 Intrepid - Test 11. Upper Arm Resultant Moment.

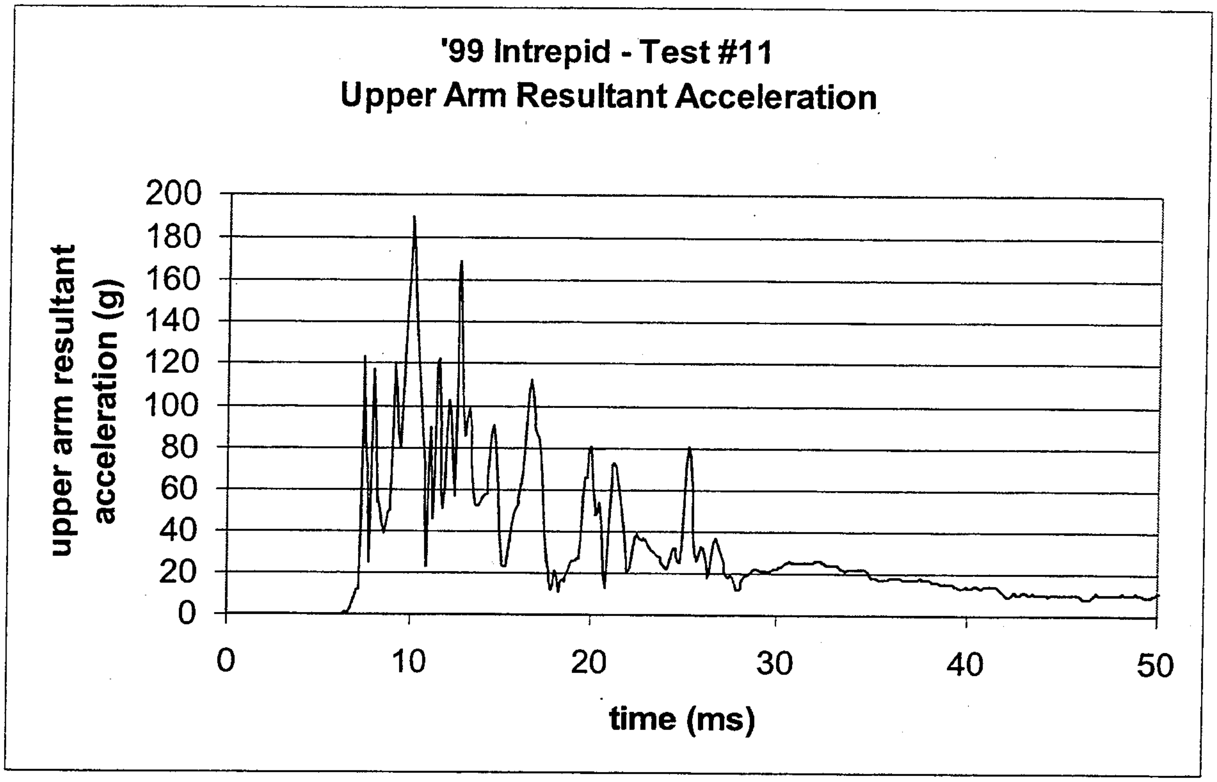

Fig. B.3. '99 Intrepid - Test 11. Upper Arm Resultant Acceleration

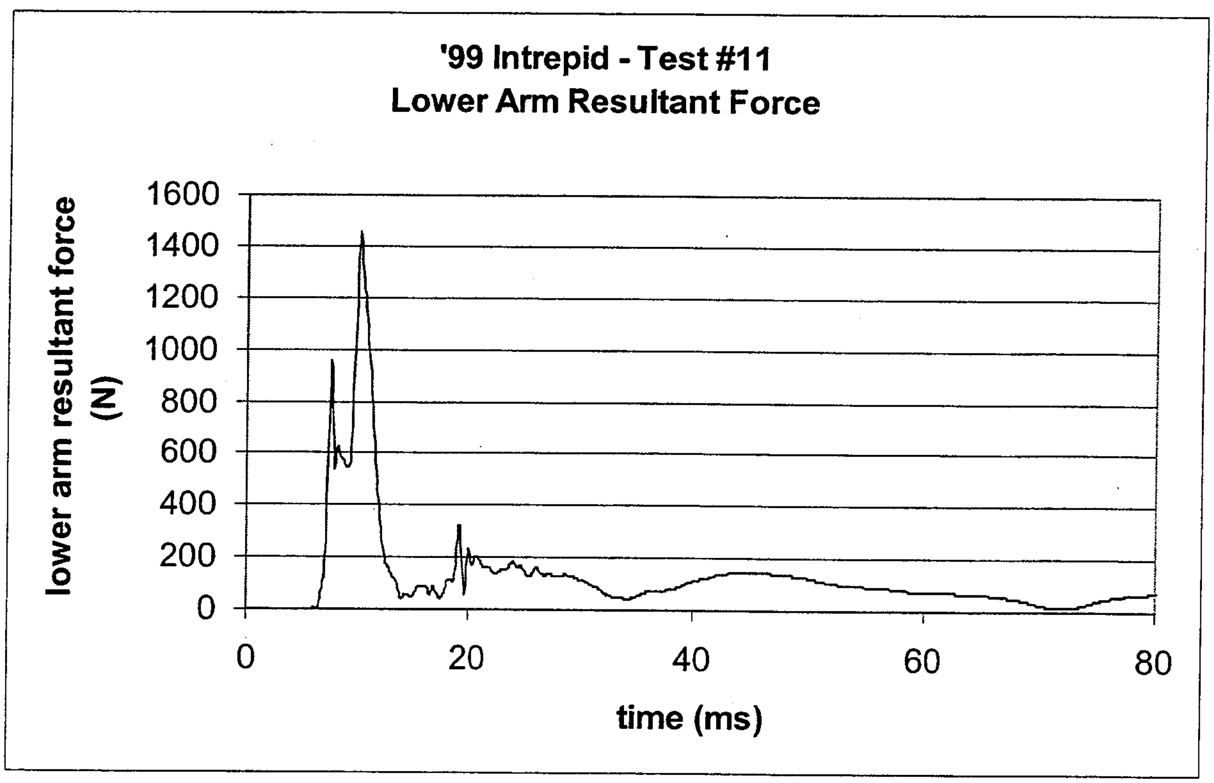

Fig. B.4. '99 Intrepid - Test 11. Lower Arm Resultant Force.

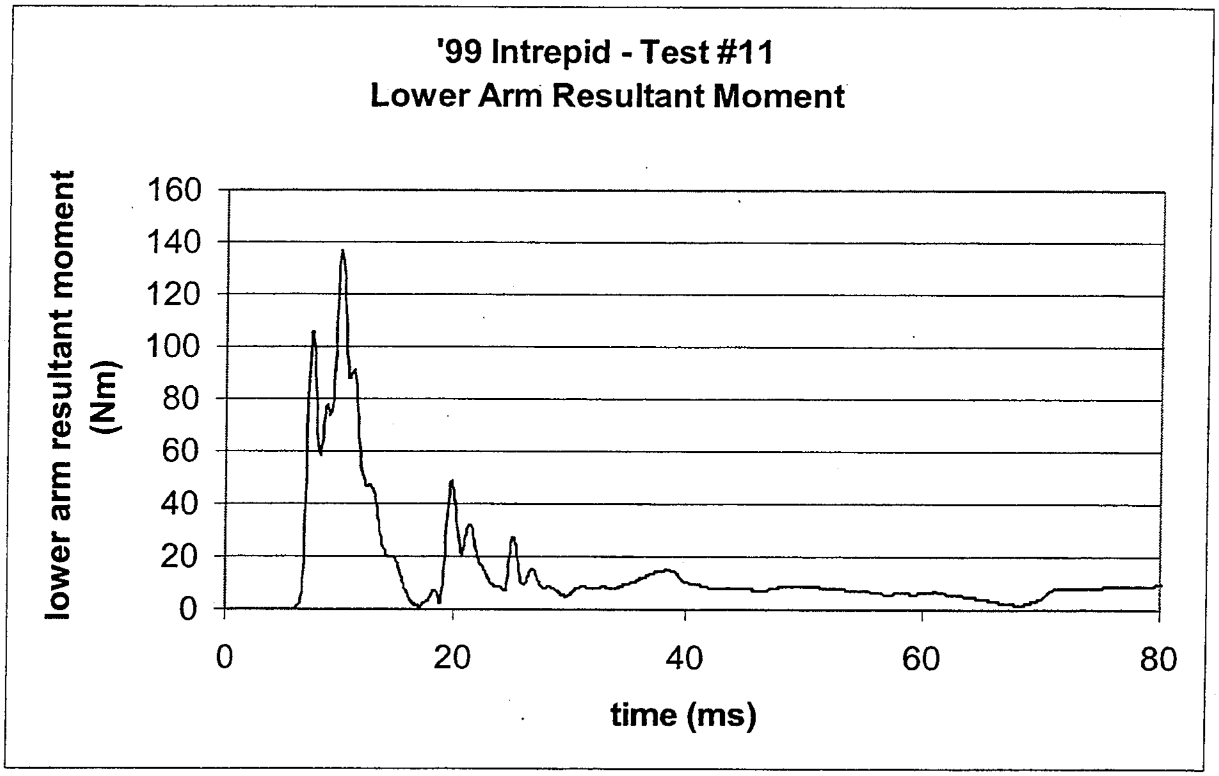

Fig. B.5. '99 Intrepid - Test 11. Lower Arm Resultant Moment.

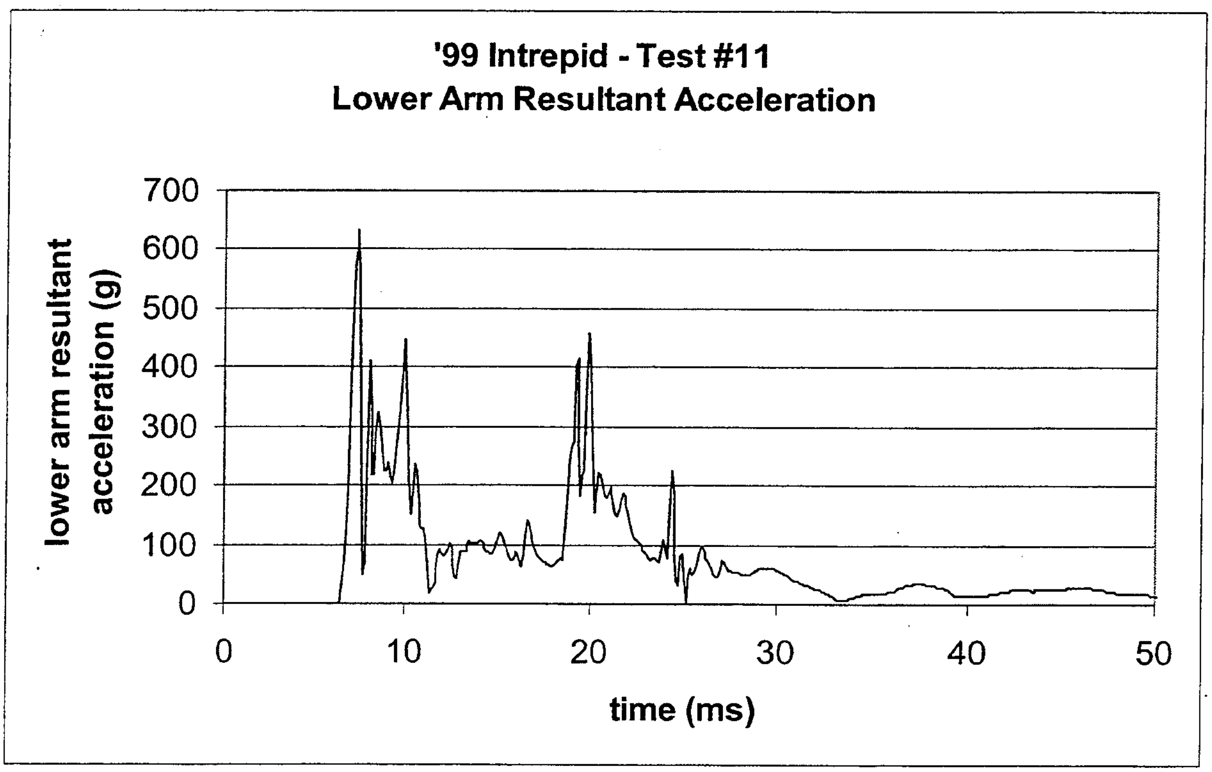

Fig. B.6. '99 Intrepid - Test 11. Lower Arm Resultant Acceleration.

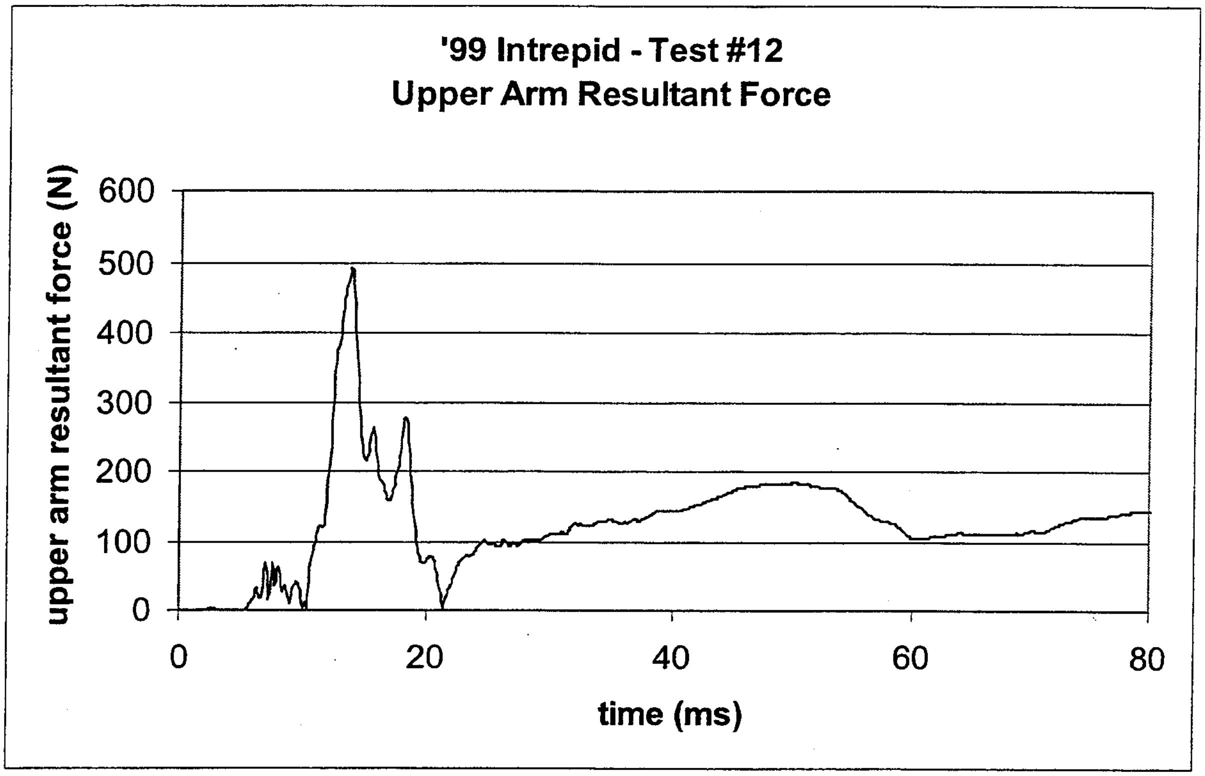

Fig. B.7. '99 Intrepid - Test 12. Upper Arm Resultant Force

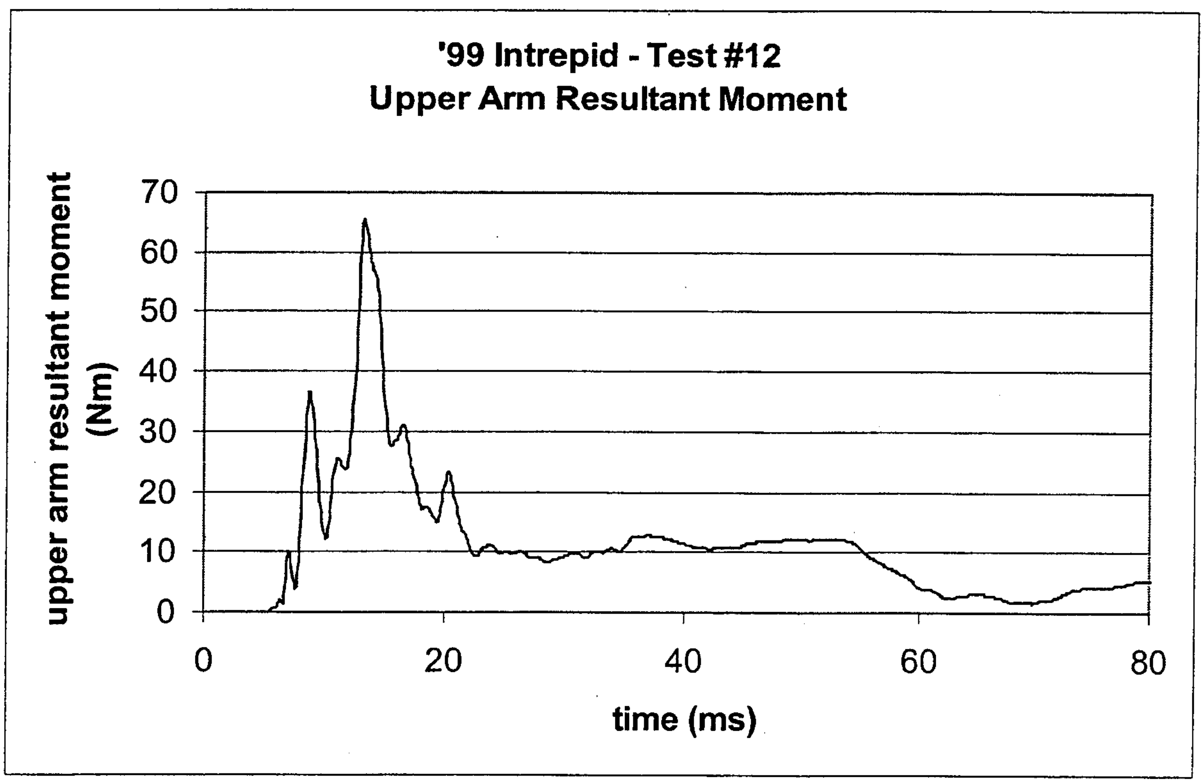

Fig. B.8. '99 Intrepid - Test 12. Upper Arm Resultant Moment

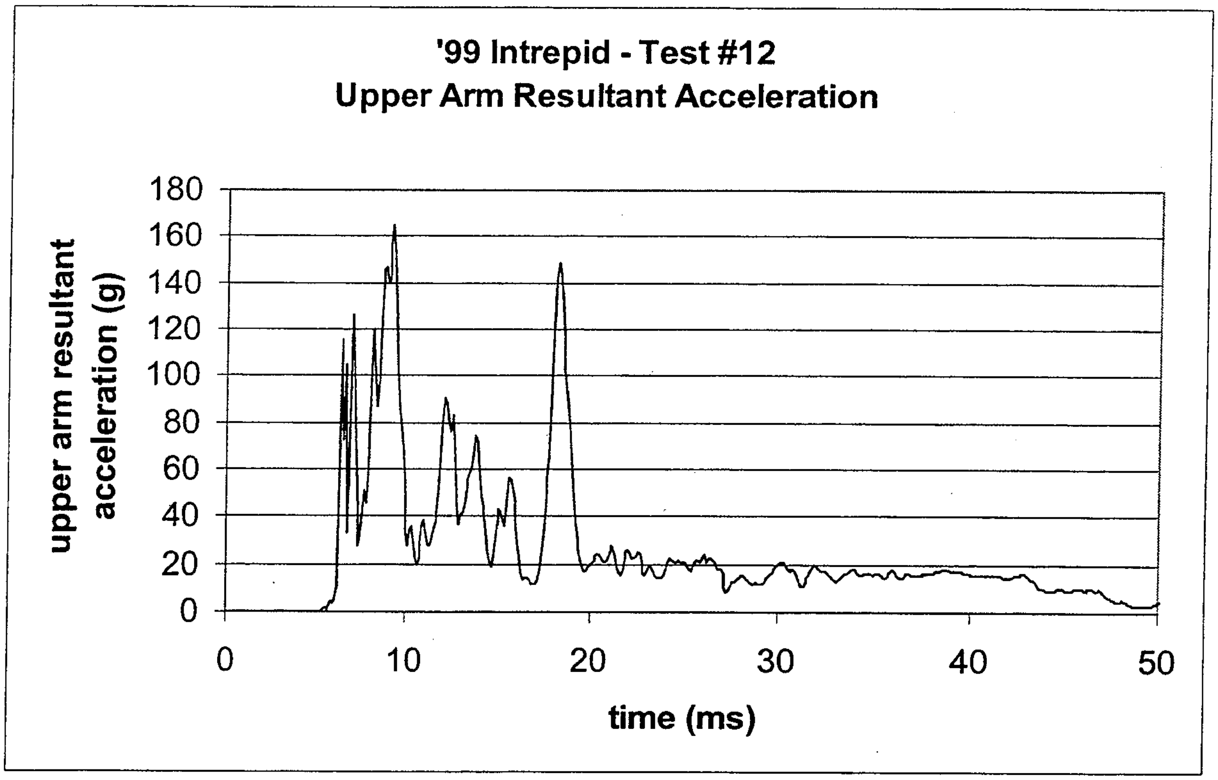

Fig. B.9. ‘99 Intrepid - Test 12. Upper Arm Resultant Acceleration.

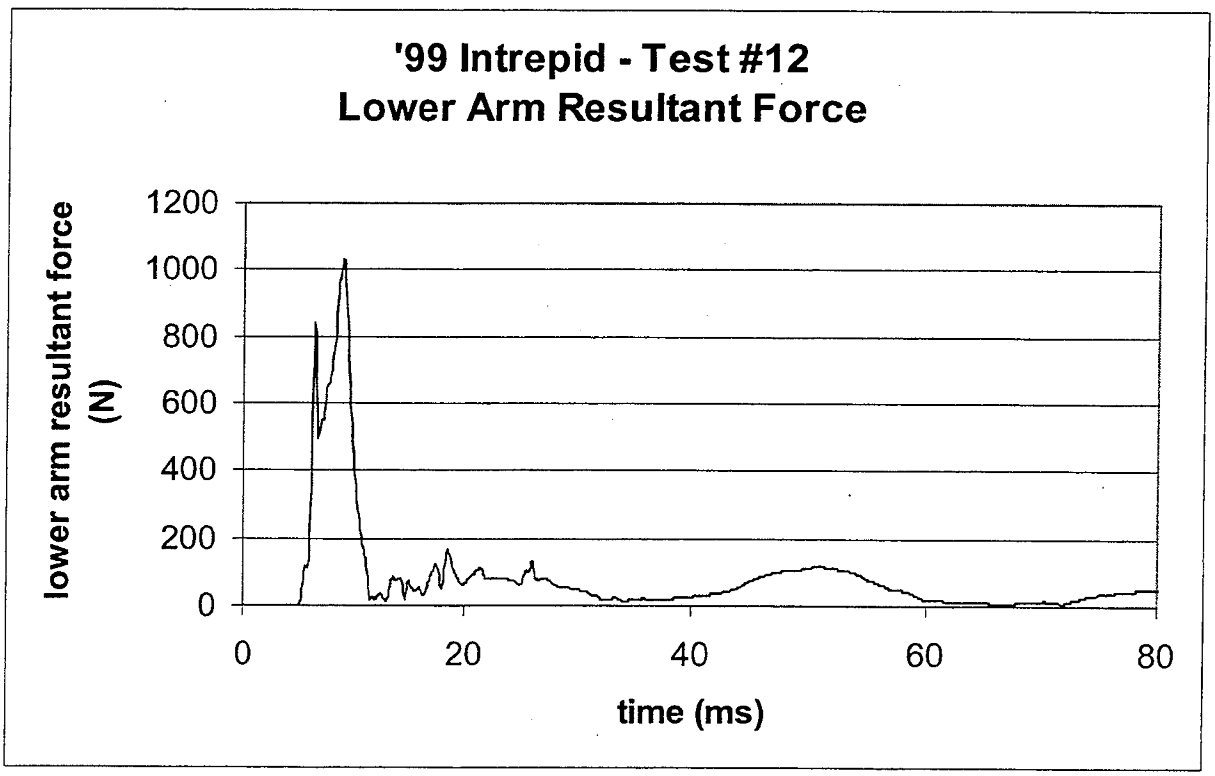

Fig. B.10. ‘99 Intrepid - Test 12. Lower Arm Resultant Force.

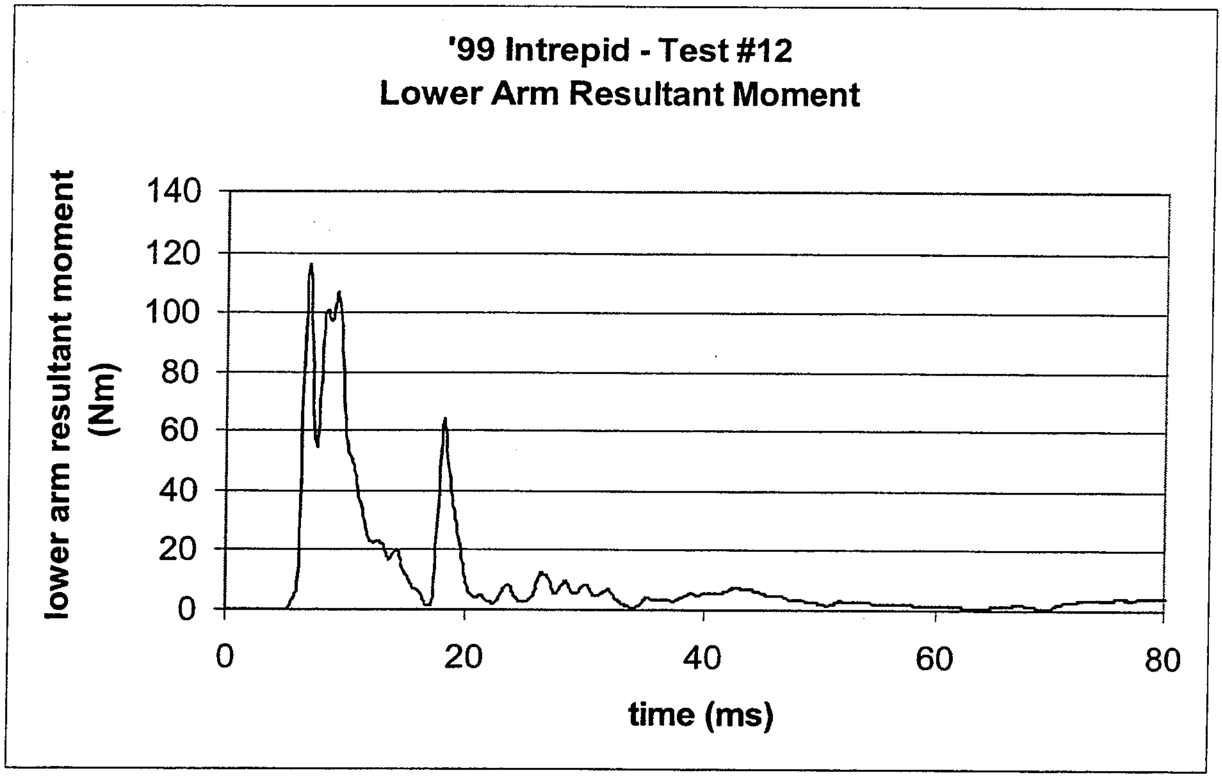

Fig. B.11. '99 Intrepid - Test 12. Lower Arm Resultant Moment.

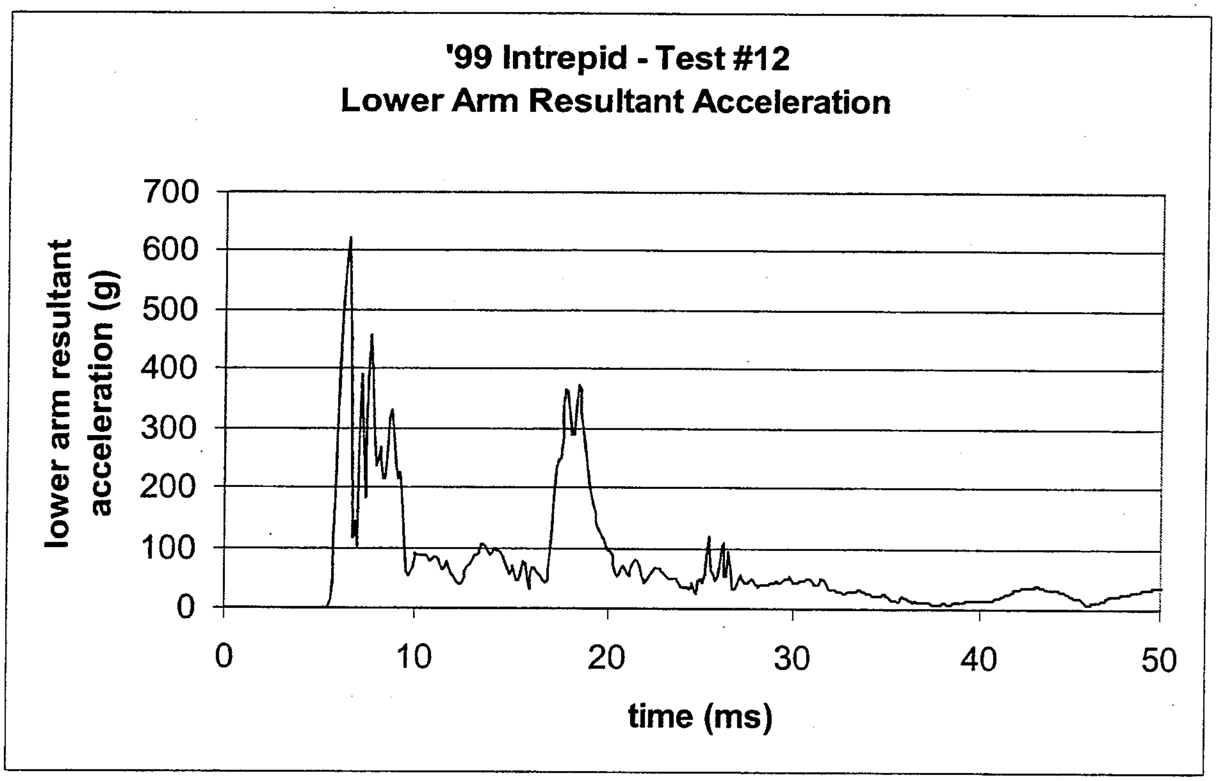

Fig. B.12. '99 Intrepid - Test 12. Lower Arm Resultant Acceleration.

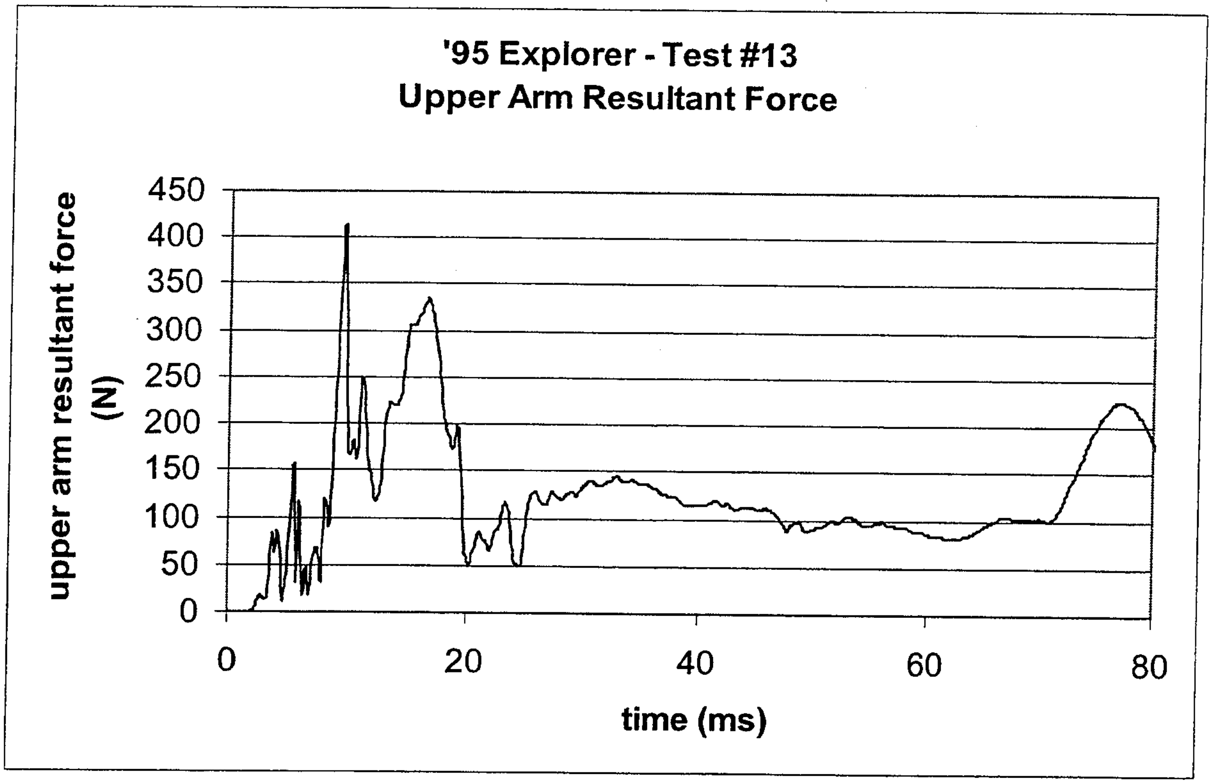

Fig. B.13. '95 Explorer - Test 13. Upper Arm Resultant Force.

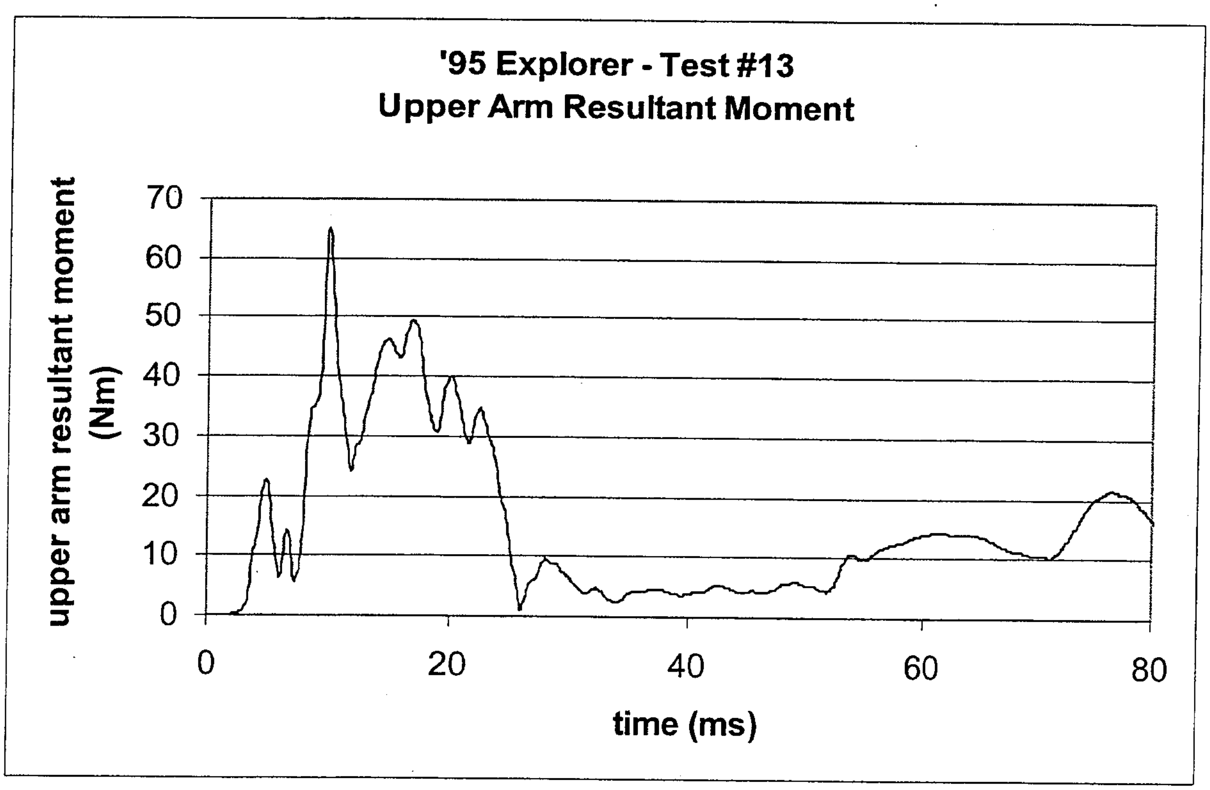

Fig. B.14. '95 Explorer - Test 13. Upper Arm Resultant Moment

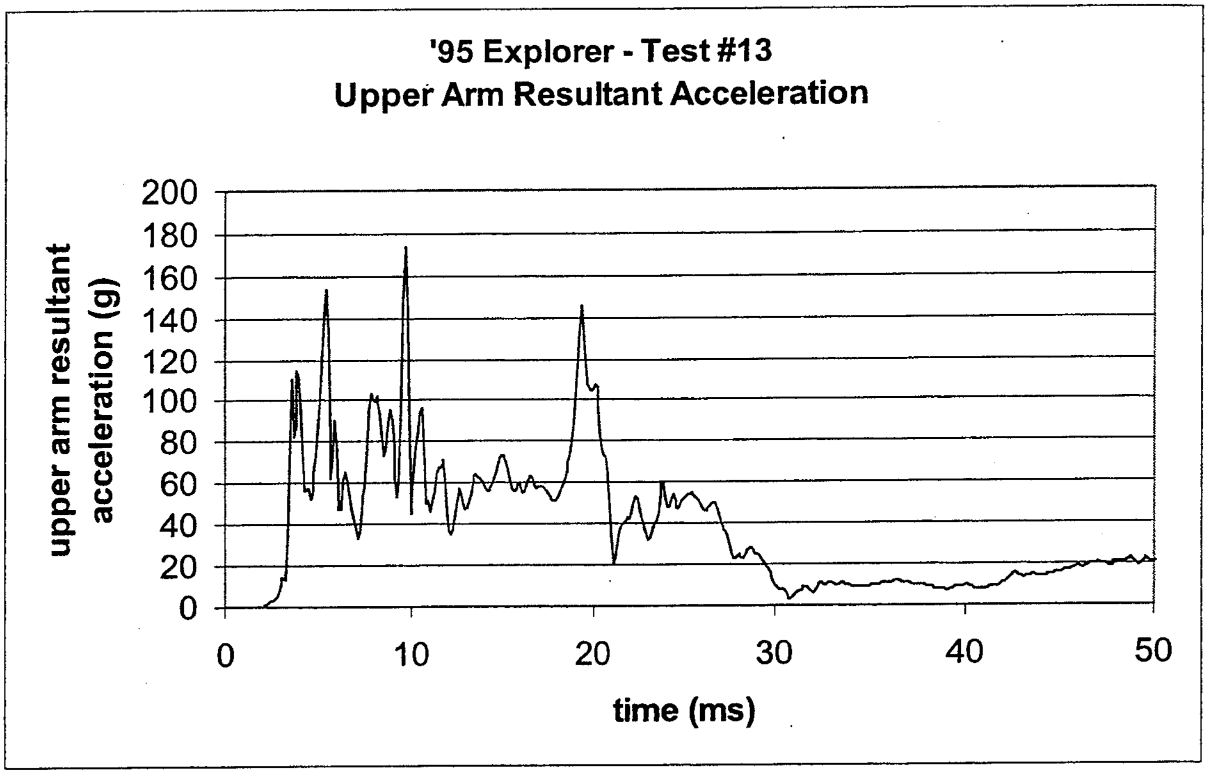

Fig. B.15. '95 Explorer - Test 13. Upper Arm Resultant Acceleration.

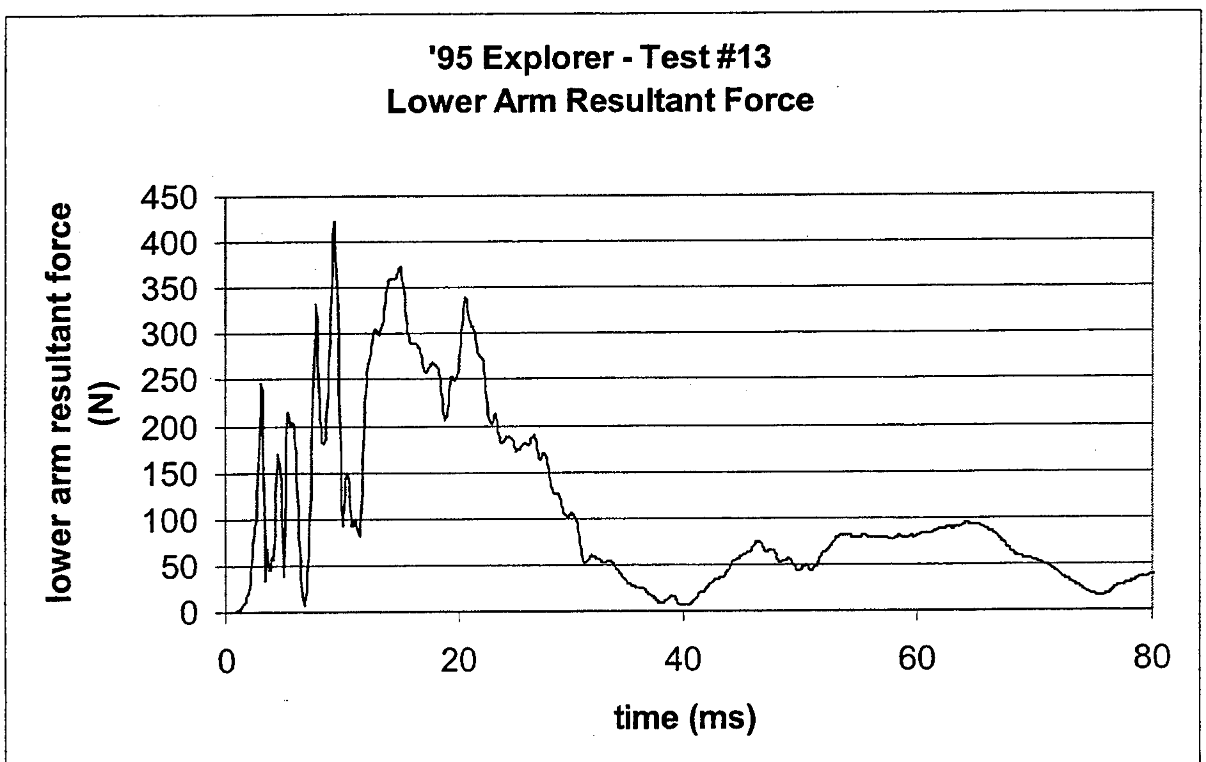

Fig. B.16. '95 Explorer - Test 13. Lower Arm Resultant Force.

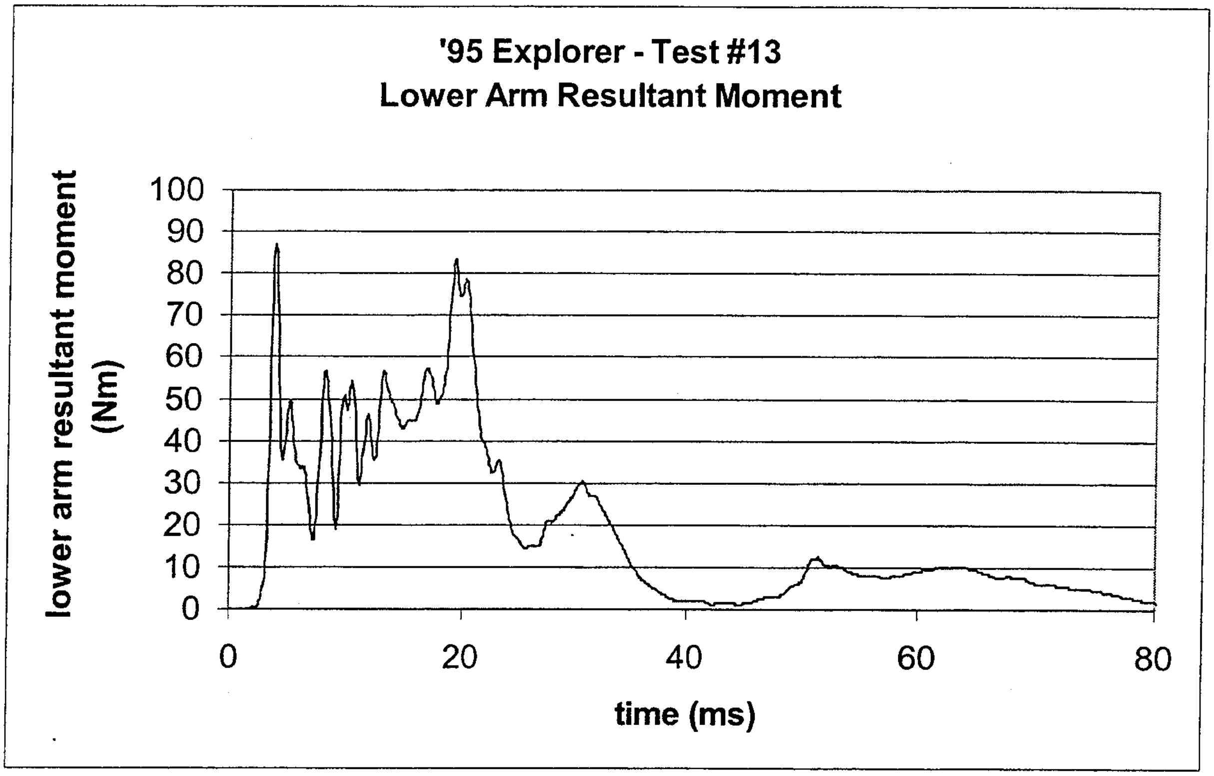

Fig. B.17. ‘95 Explorer - Test 13. Lower Arm Resultant Moment.

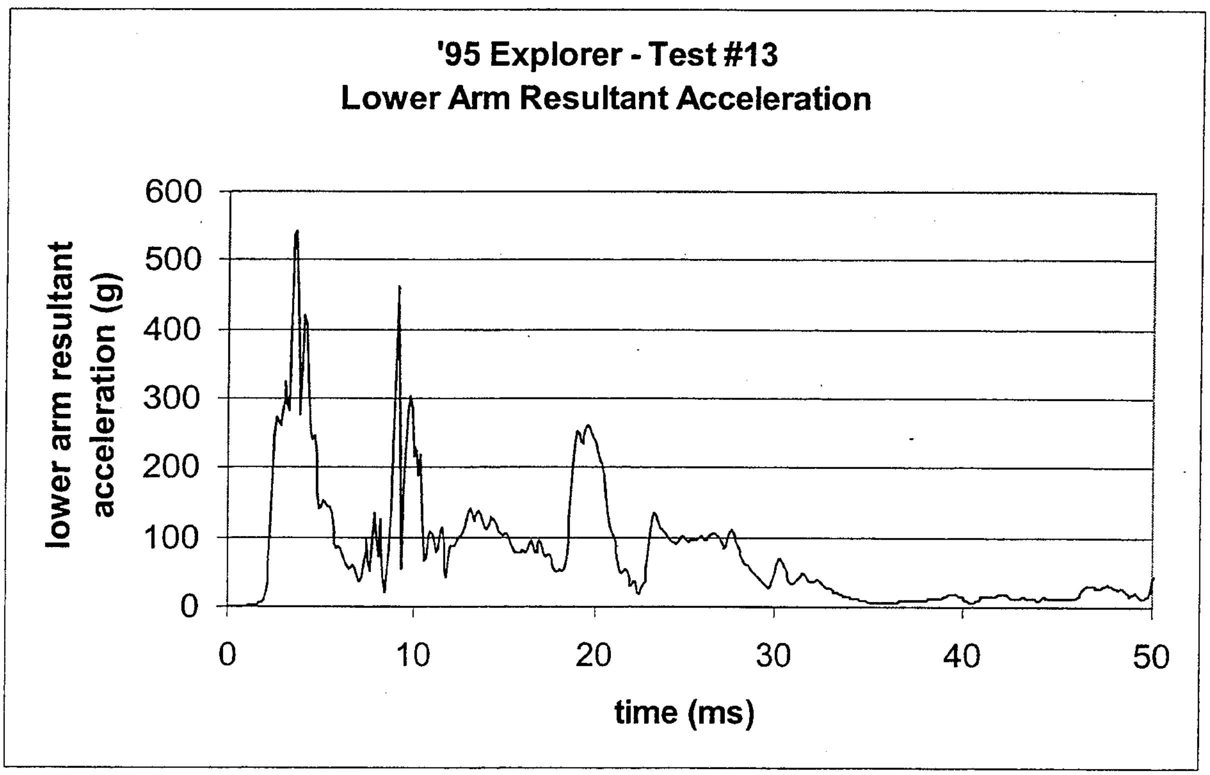

Fig. B.18. ‘95 Explorer - Test 13. Lower Arm Resultant Acceleration.

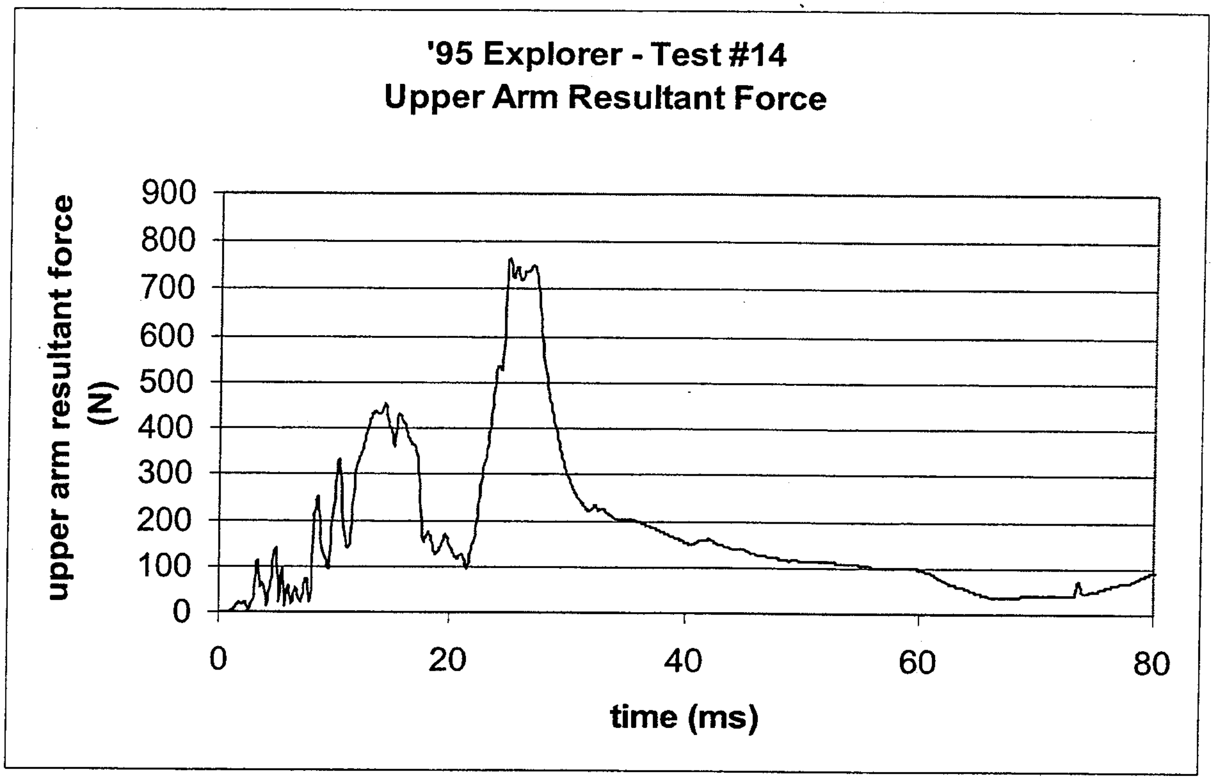

Fig. B.19. '95 Explorer - Test 14. Upper Arm Resultant Acceleration.

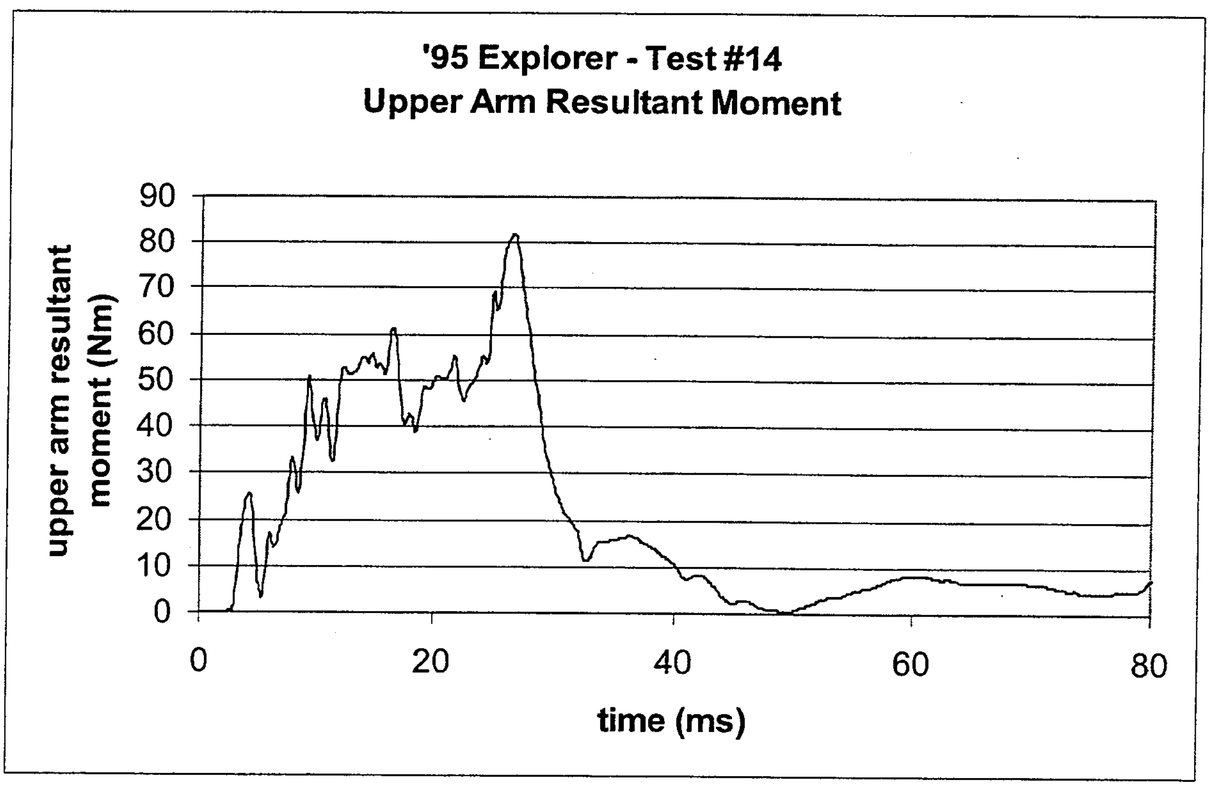

Fig. B.20. '95 Explorer - Test 14. Upper Arm Resultant Moment

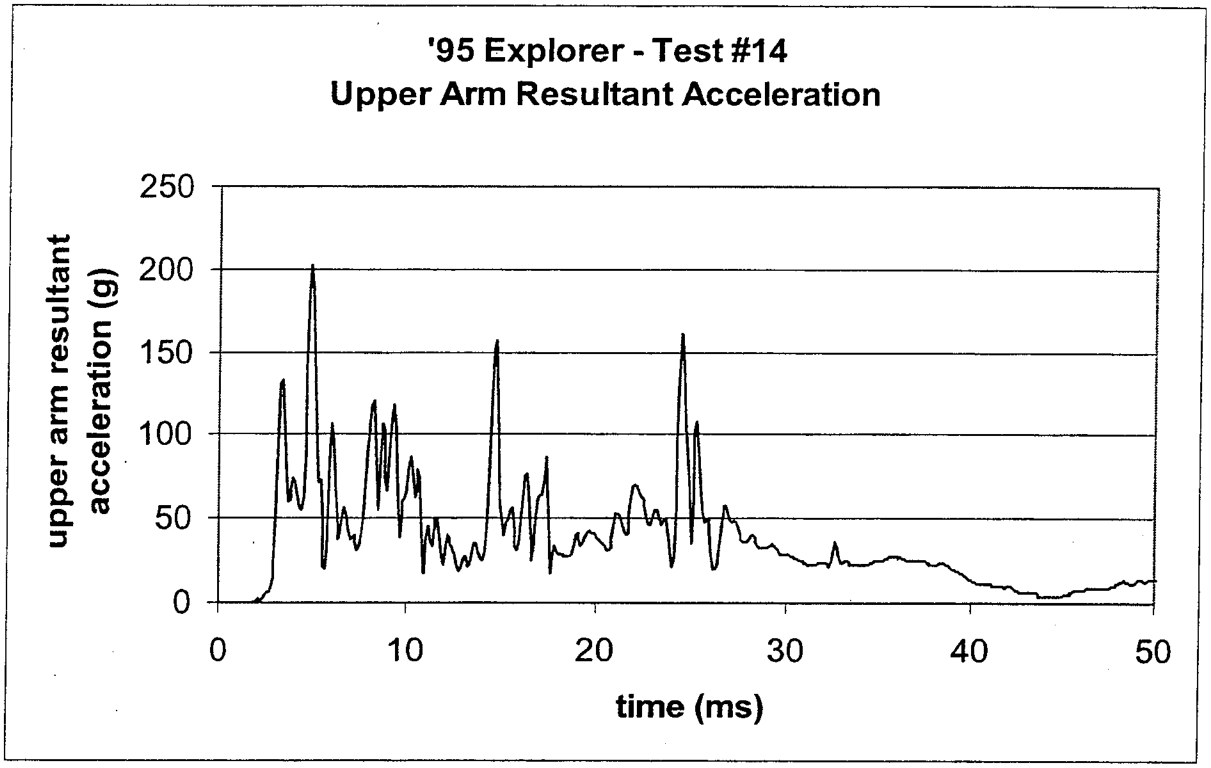

Fig. B.21. '95 Explorer - Test 14. Upper Arm Resultant Acceleration.

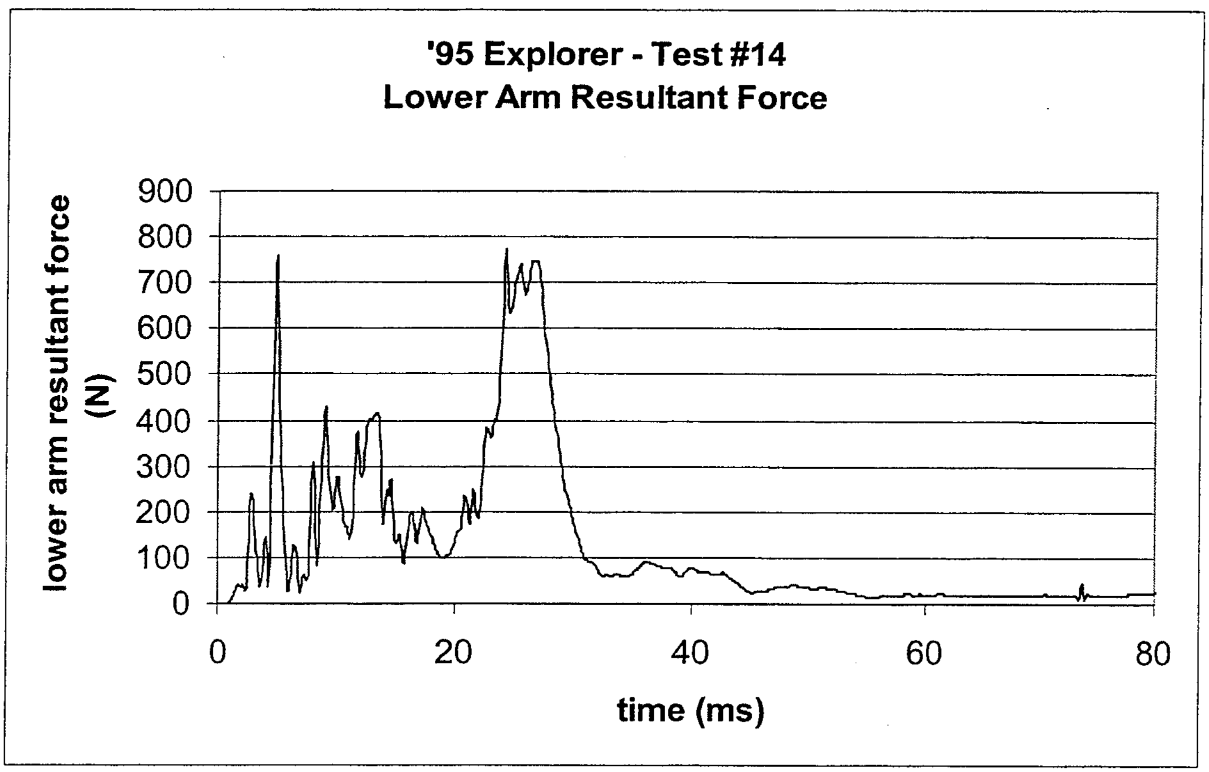

Fig. B.22. '95 Explorer - Test 14. Lower Arm Resultant Force.

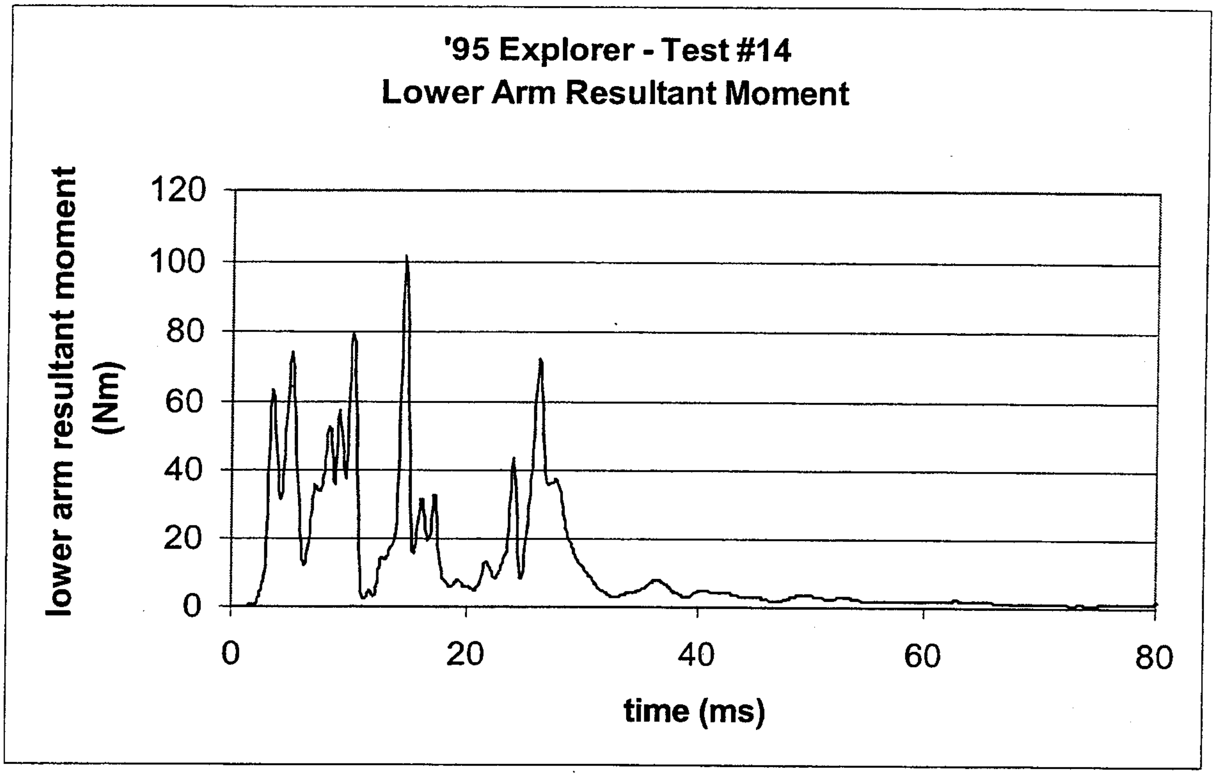

Fig. B.23. '95 Explorer - Test 14. Lower Arm Resultant Moment.

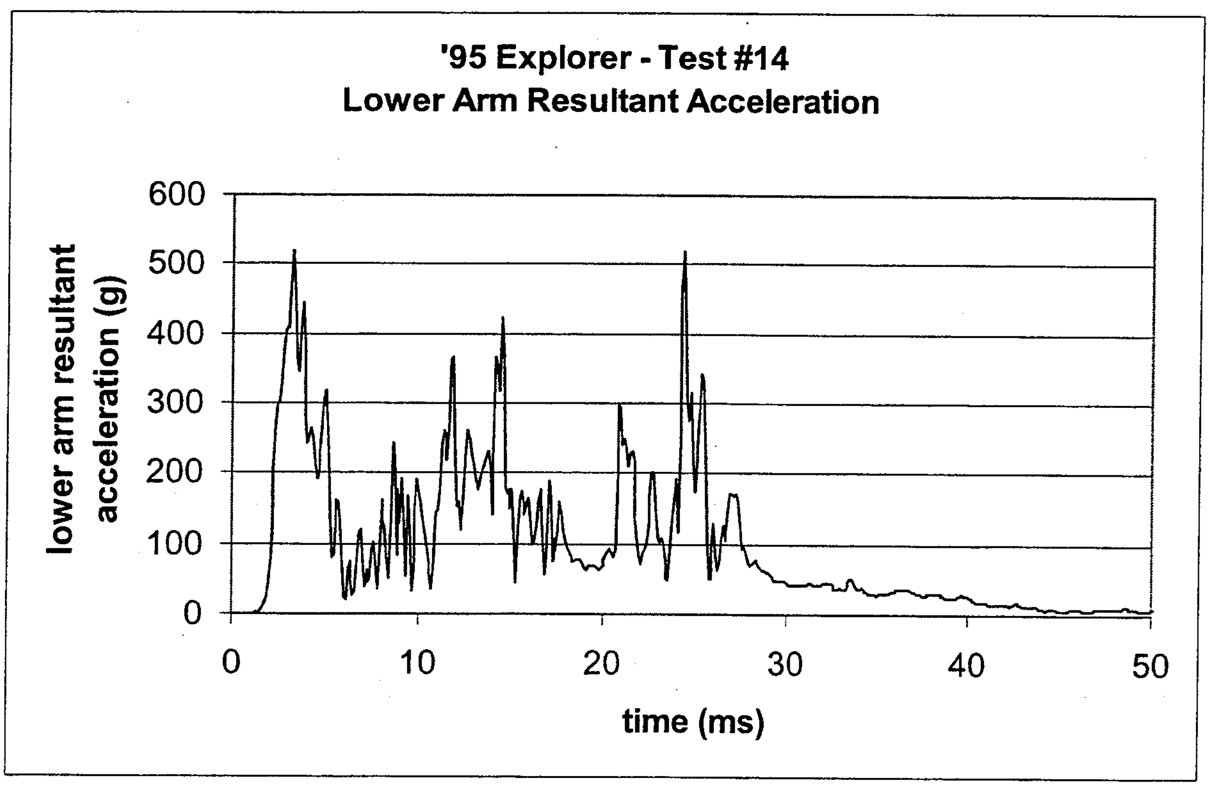

Fig. B.24. '95 Explorer - Test 14. Lower Arm Resultant Acceleration.

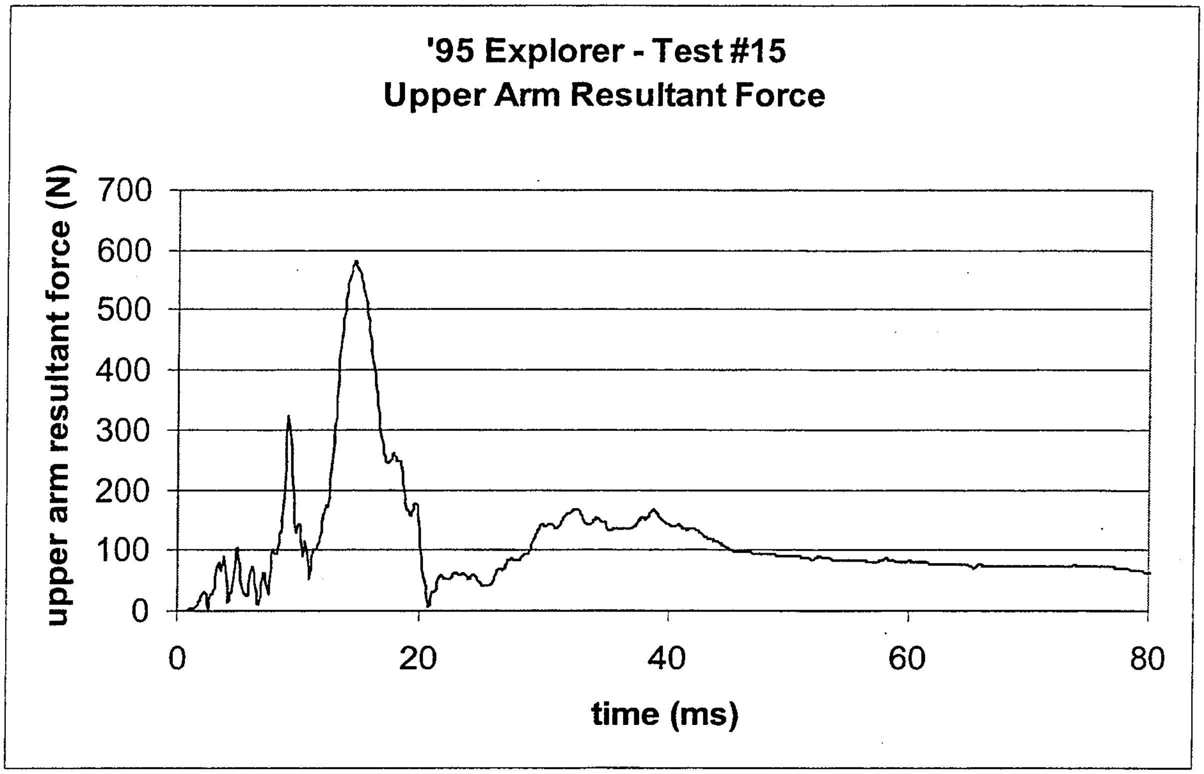

Fig. B.25. '95 Explorer - Test 15. Upper Arm Resultant Force.

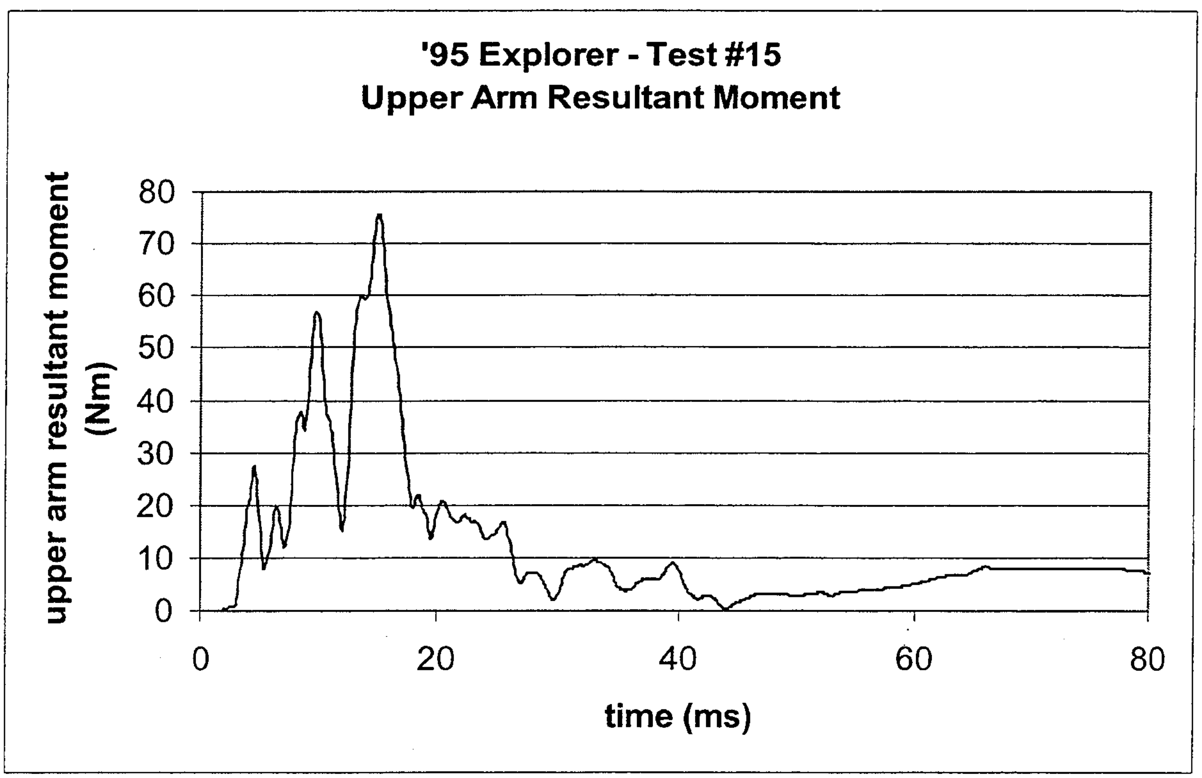

Fig. B.26. '95 Explorer - Test 15. Upper Arm Resultant Moment.

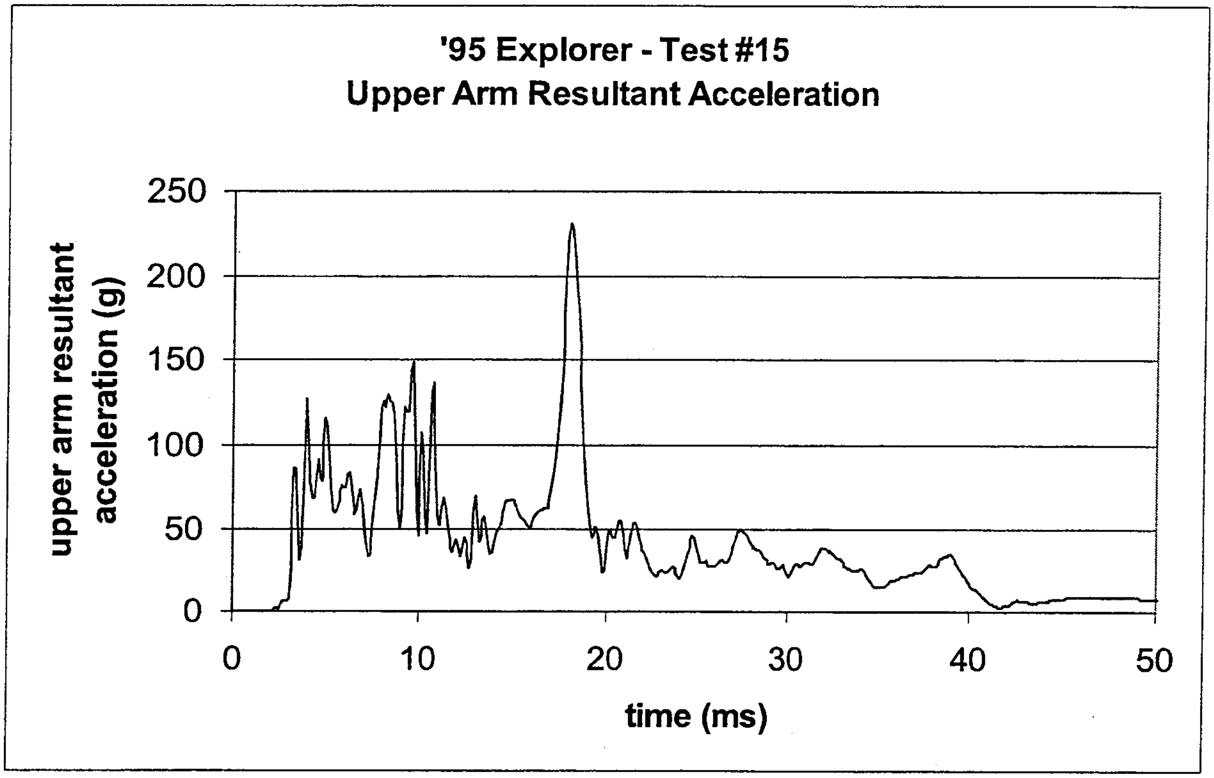

Fig. B.27. '95 Explorer - Test 15. Upper Arm Resultant Acceleration.

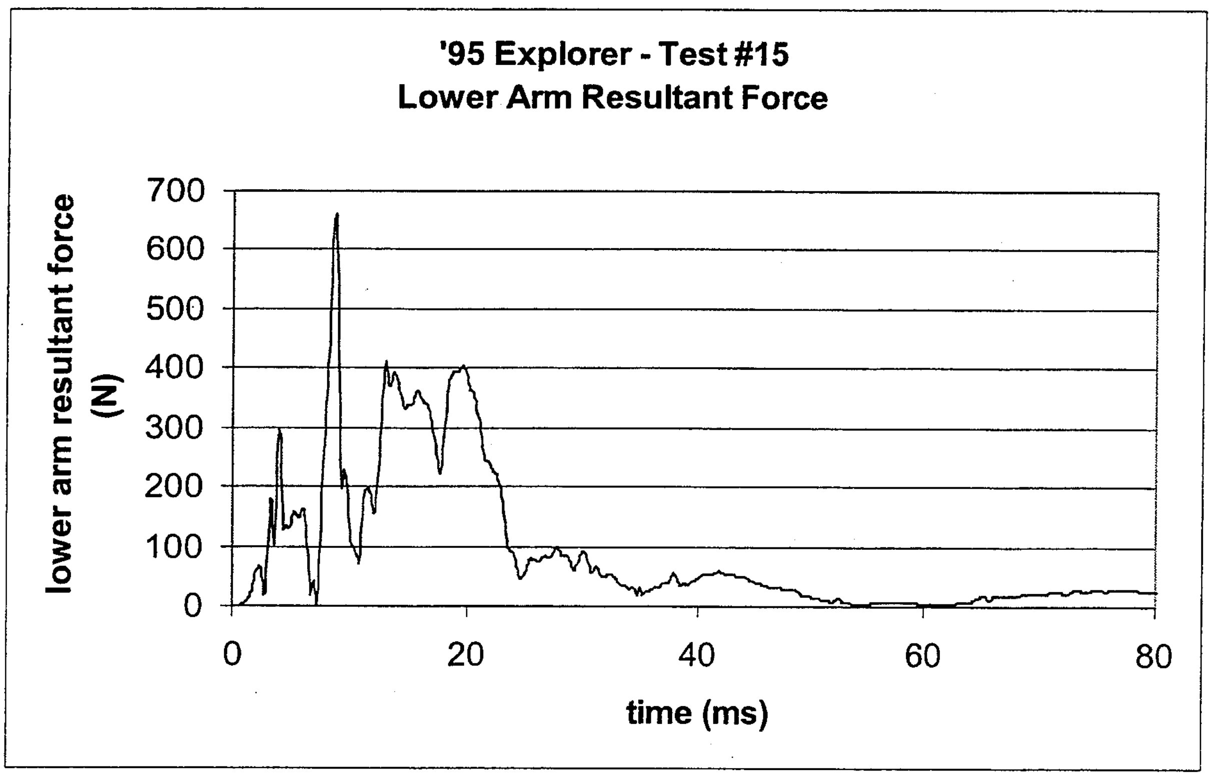

Fig. B.28. '95 Explorer - Test 15. Lower Arm Resultant Force.

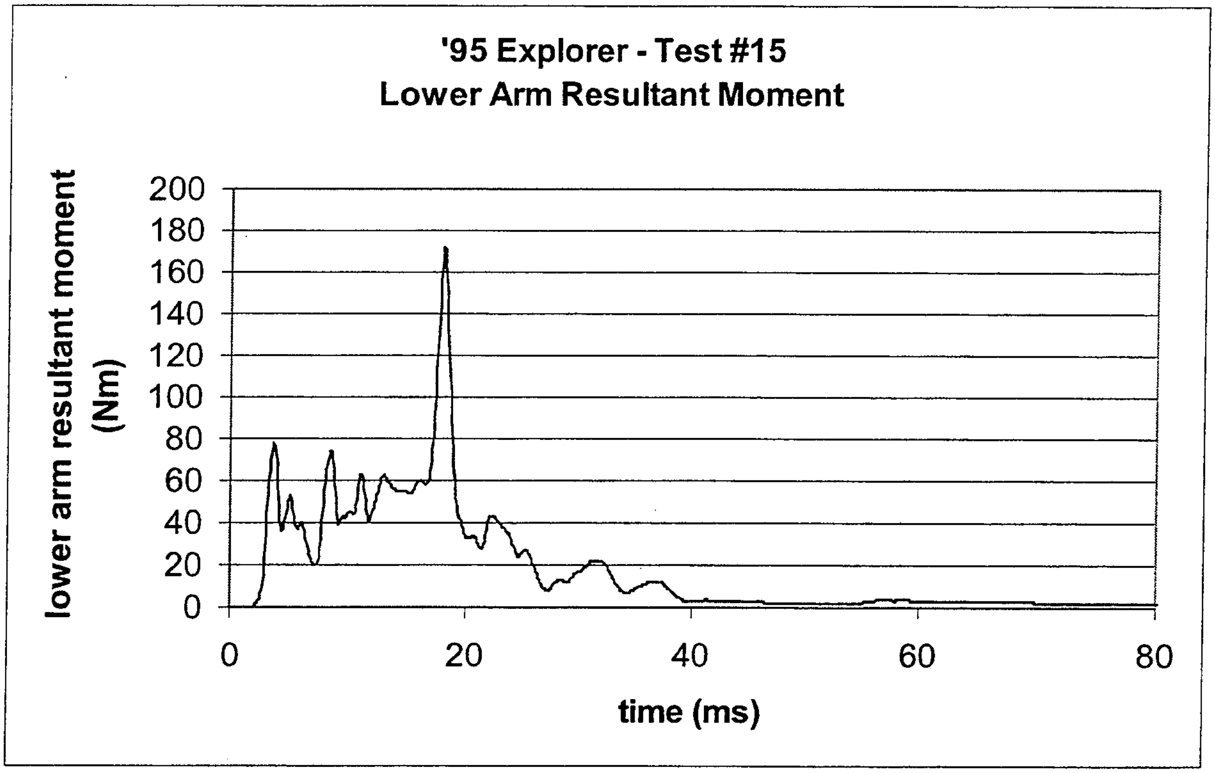

Fig. B.29. '95 Explorer - Test 15. Lower Arm Resultant Moment.

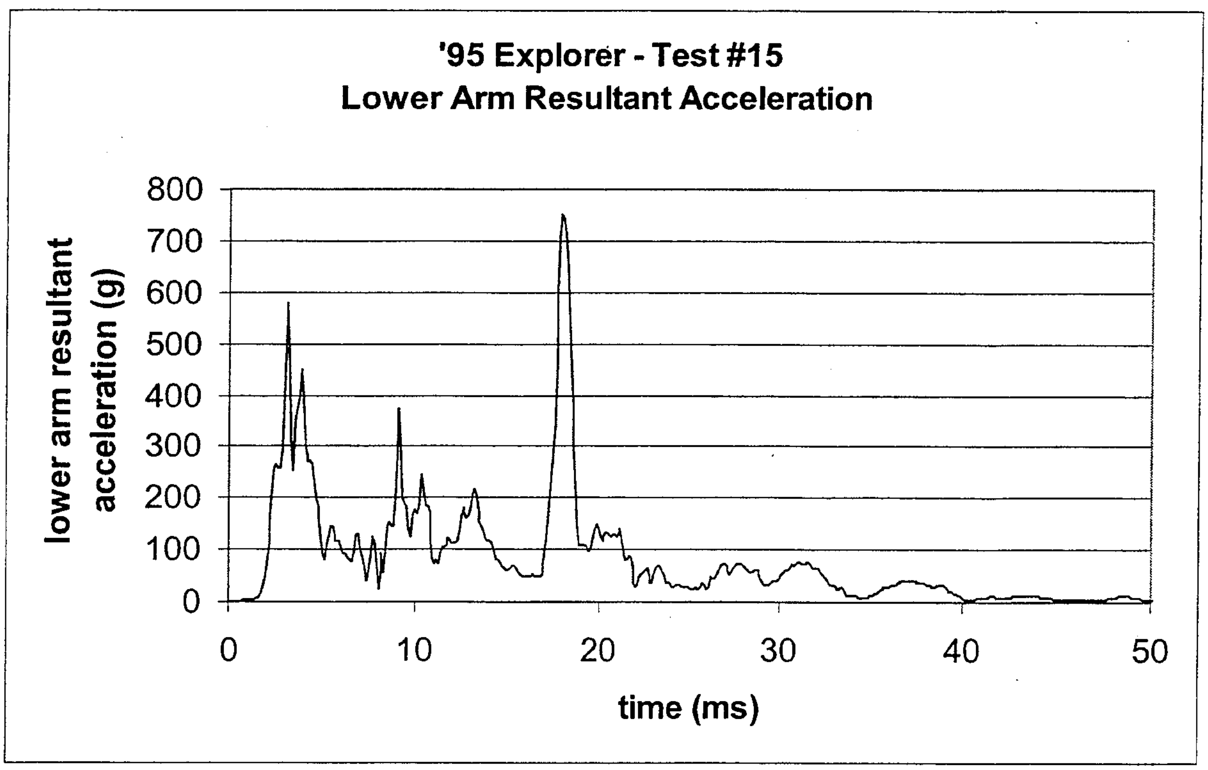

Fig. B.30. '95 Explorer - Test 15. Lower Arm Resultant Acceleration.

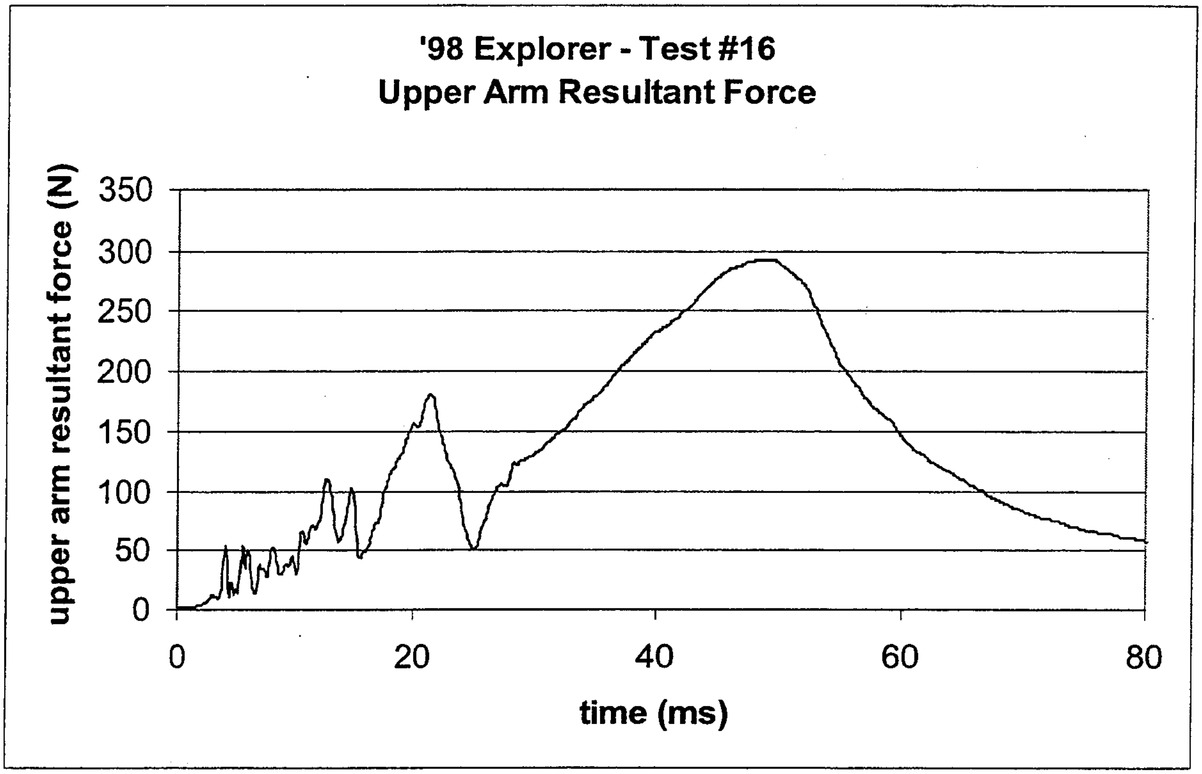

Fig. B.31. '98 Explorer - Test 16. Upper Arm Resultant Force.

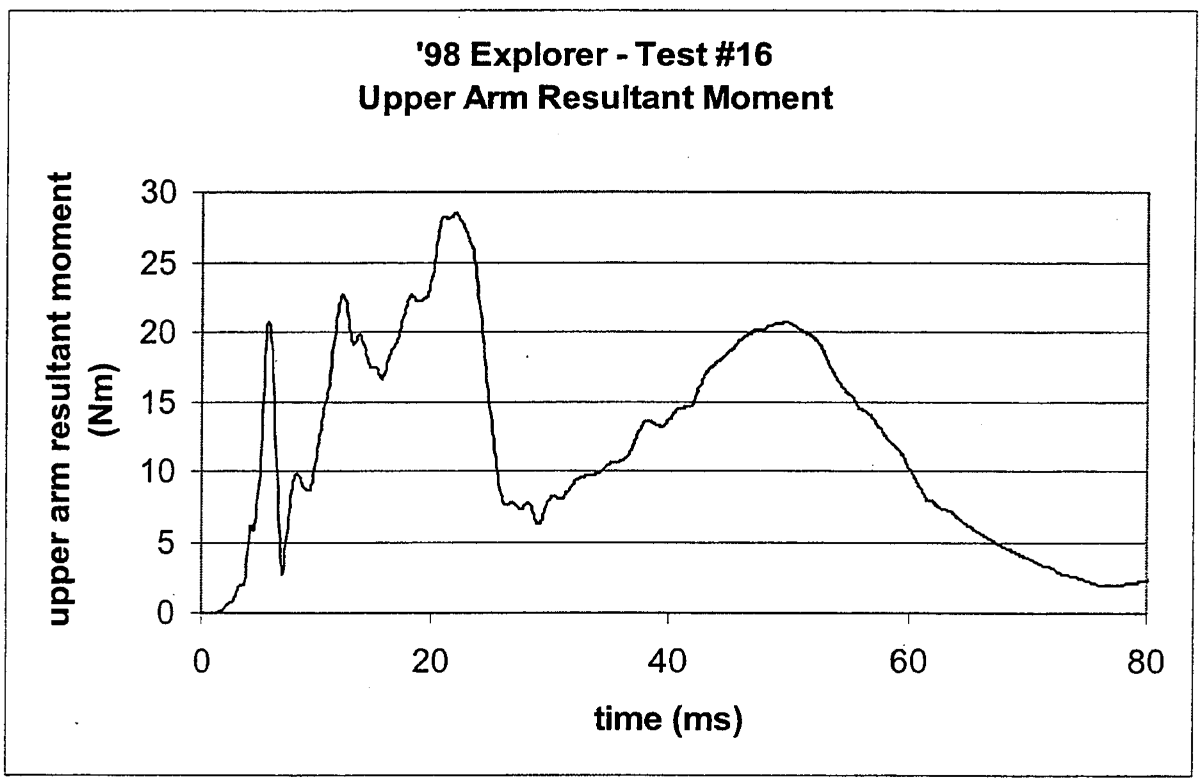

Fig. B.32. '98 Explorer - Test 16. Upper Arm Resultant Moment.

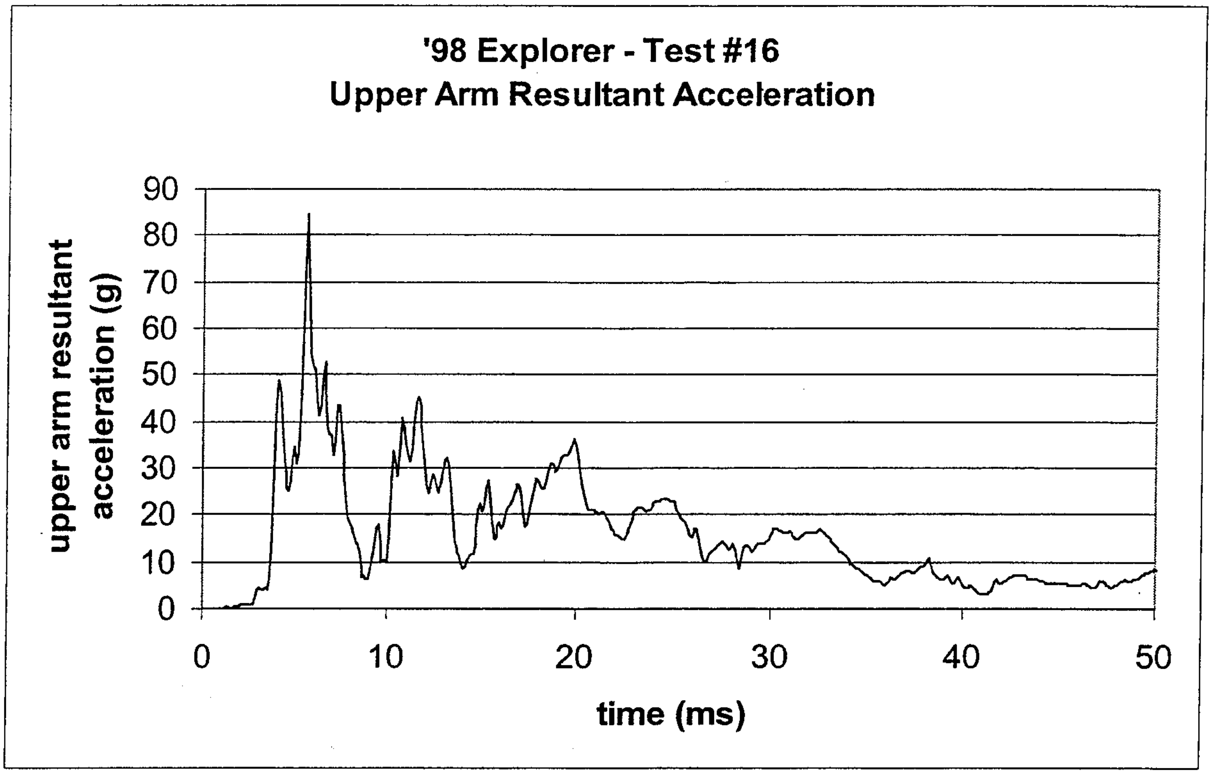

Fig. B.33. '98 Explorer - Test 16. Upper Arm Resultant Acceleration.

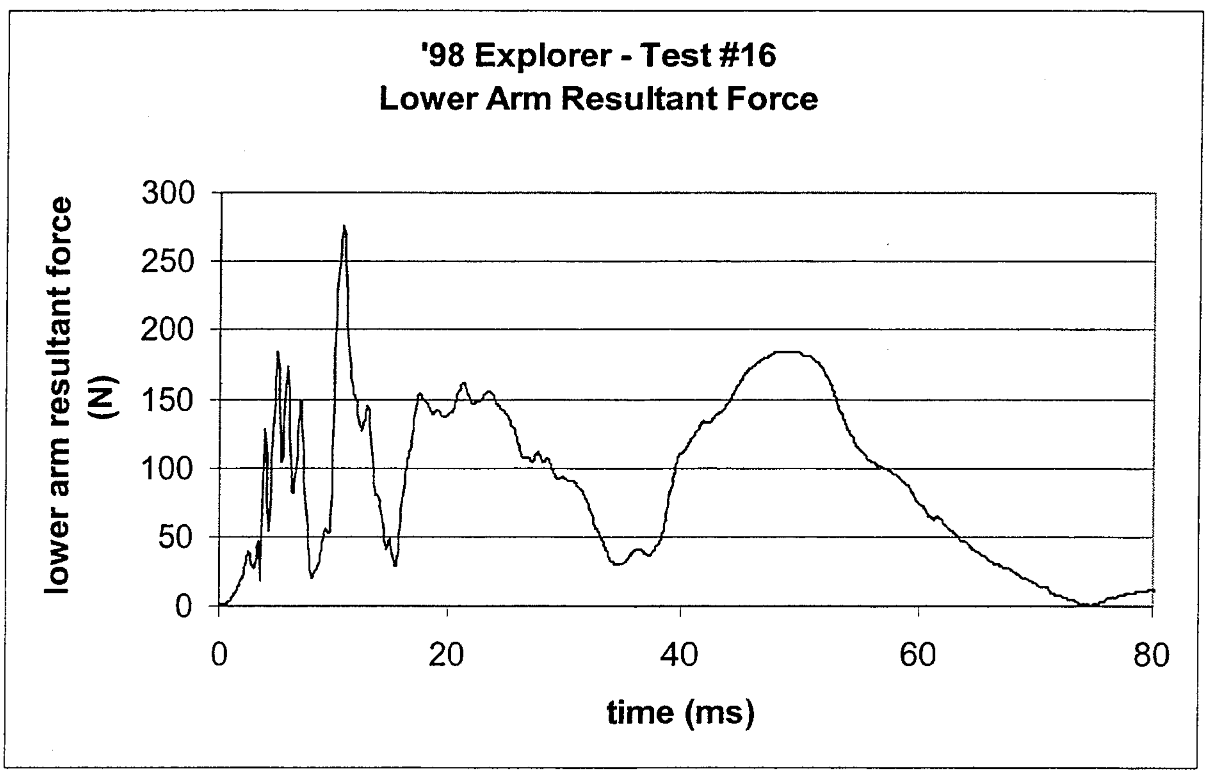

Fig. B.34. '98 Explorer - Test 16. Lower Arm Resultant Force.

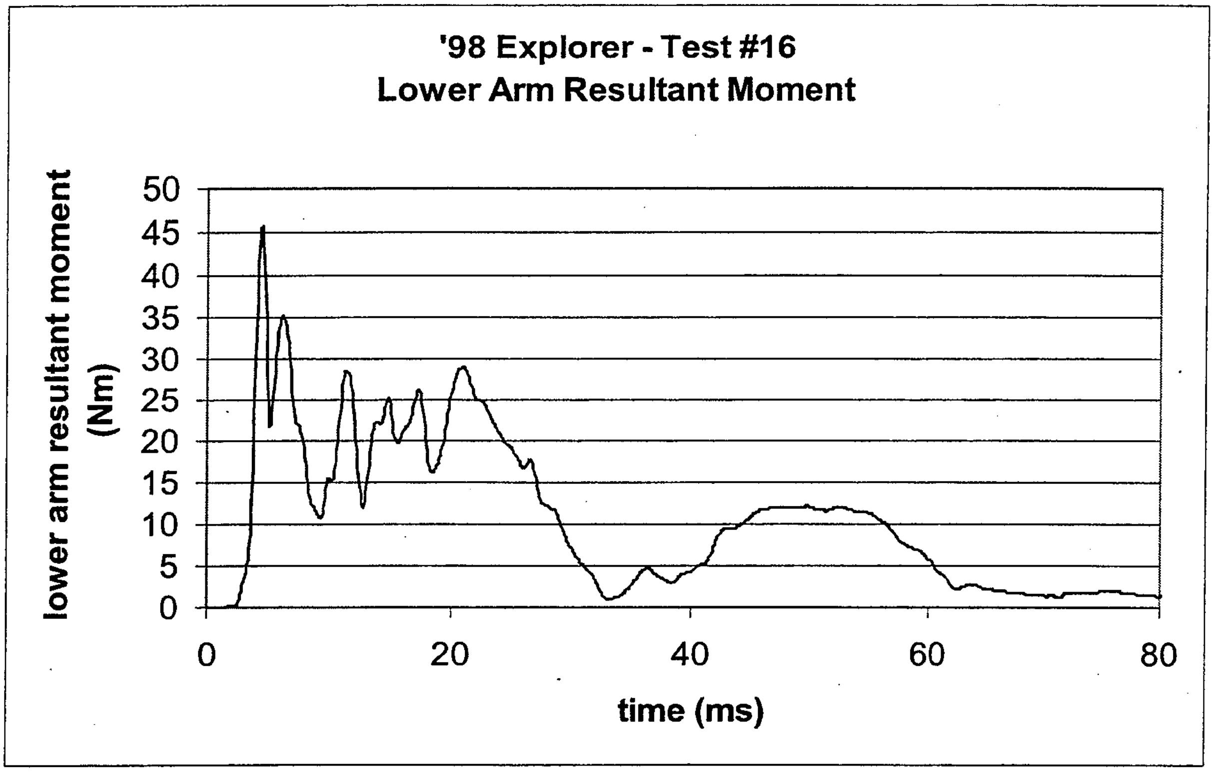

Fig. B.35. '98 Explorer - Test 16. Lower Arm Resultant Moment.

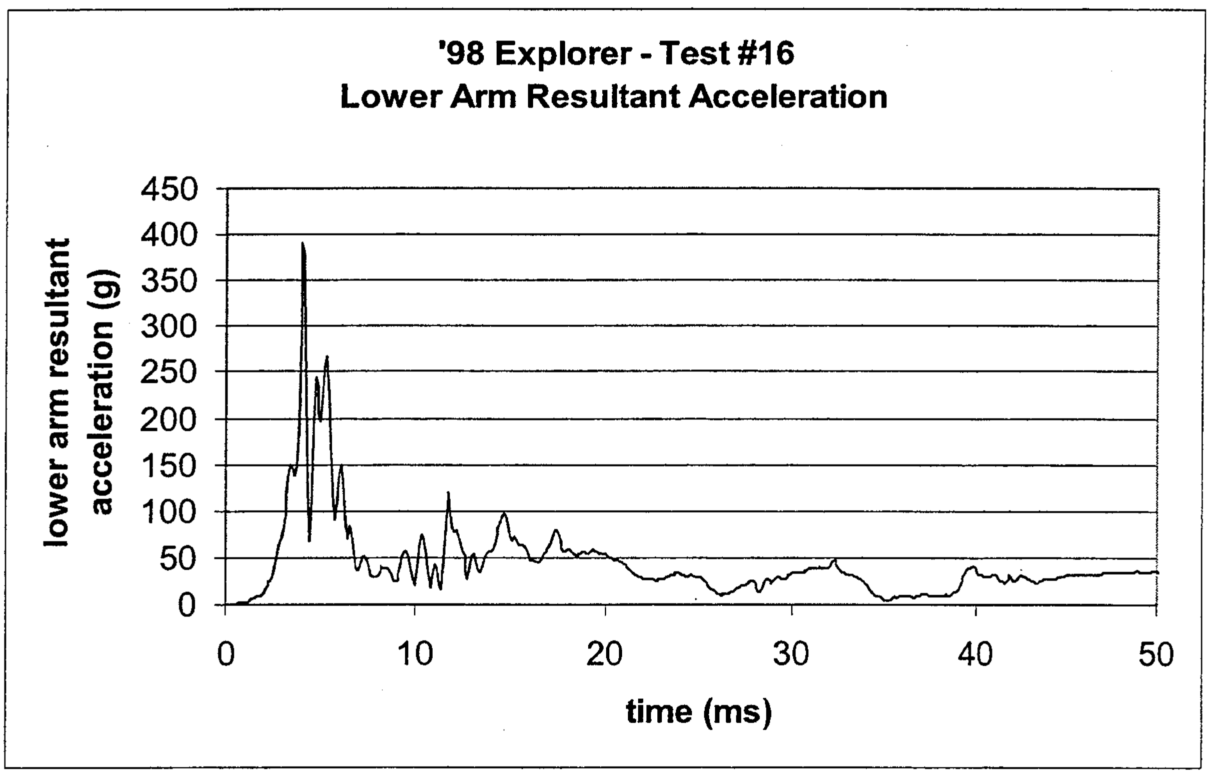

Fig. B.36. '98 Explorer - Test 16. Lower Arm Resultant Acceleration.

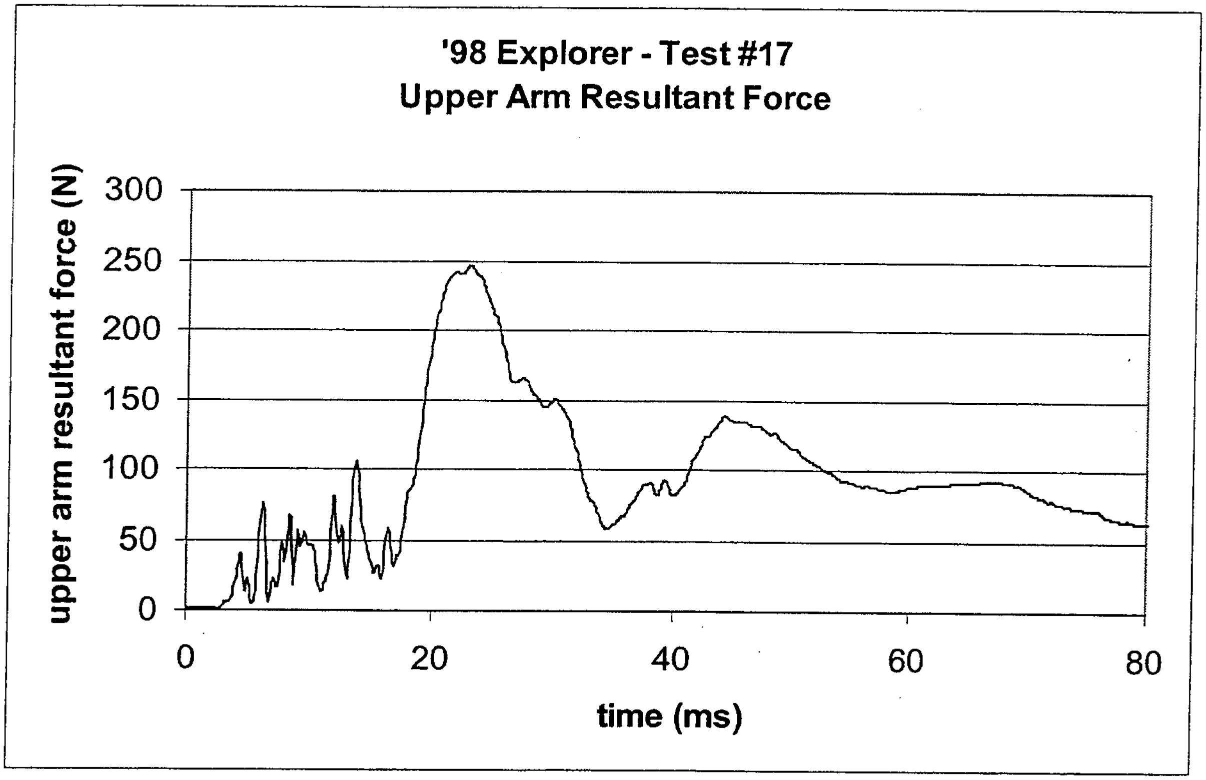

Fig. B.37. '98 Explorer - Test 17. Upper Arm Resultant Force.

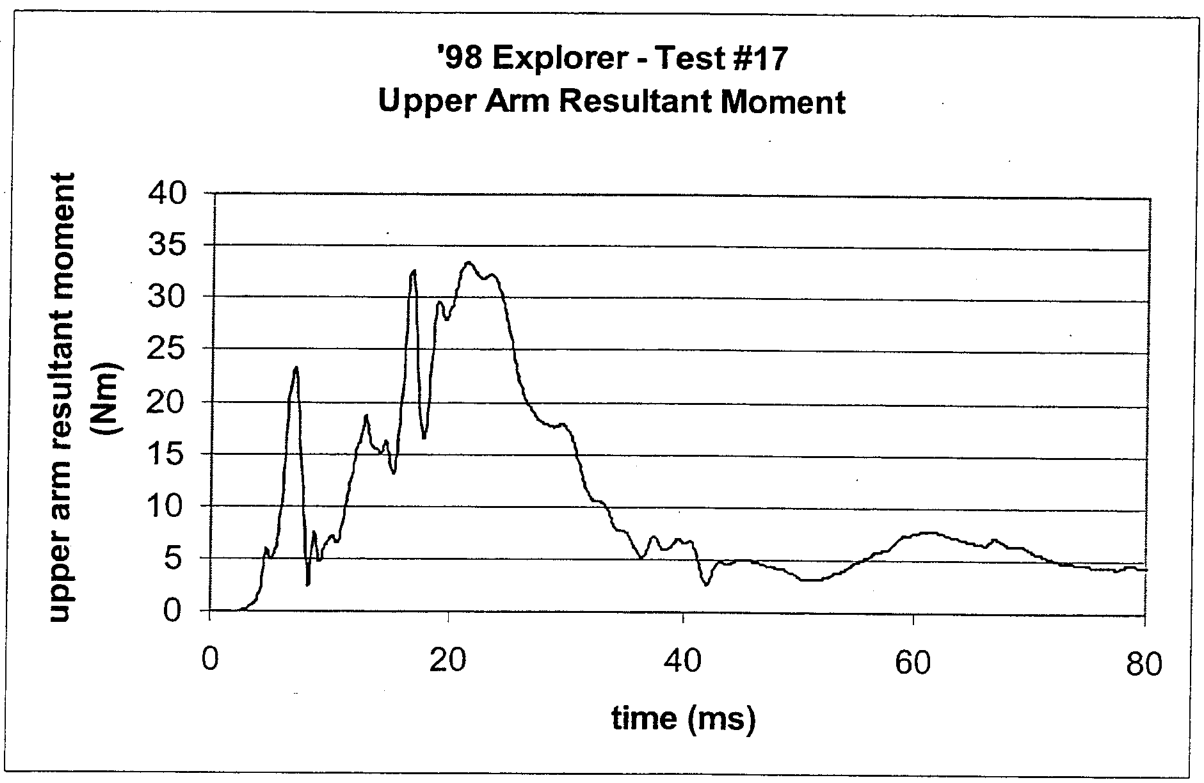

Fig. B.38. '98 Explorer - Test 17. Upper Arm Resultant Moment.

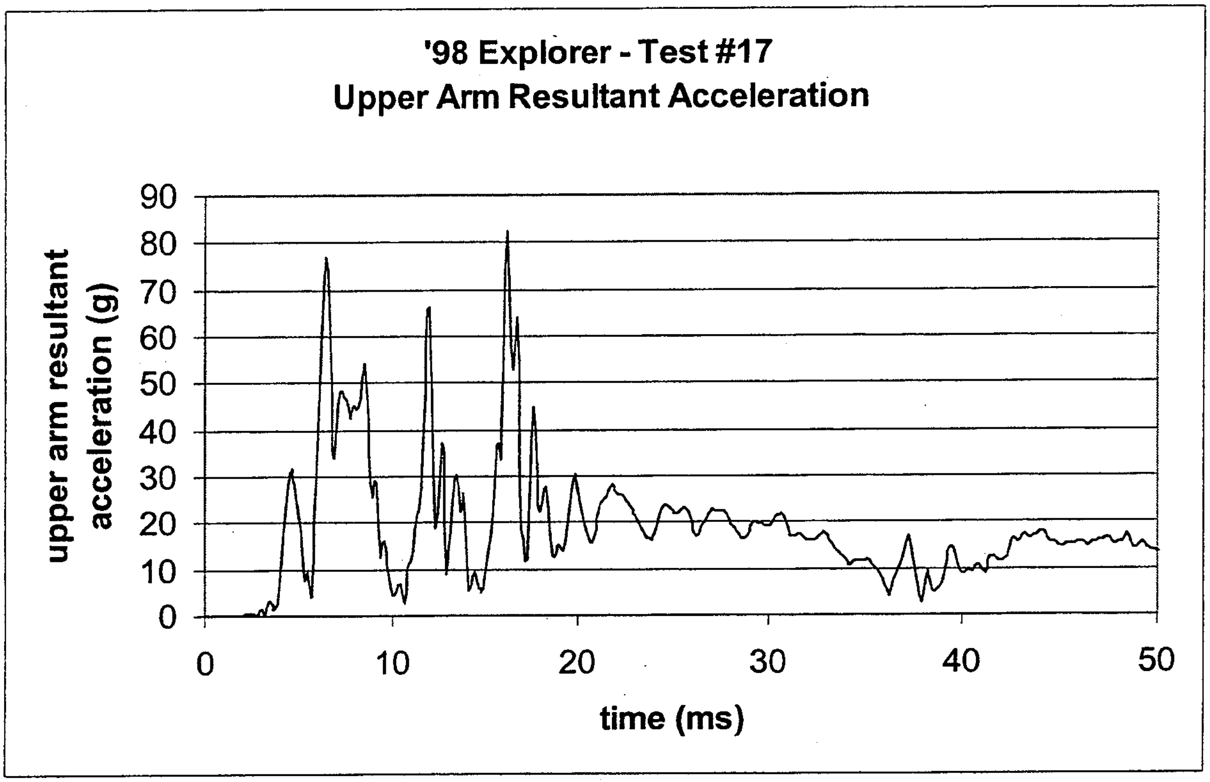

Fig. B.39. '98 Explorer - Test 17. Upper Arm Resultant Acceleration.

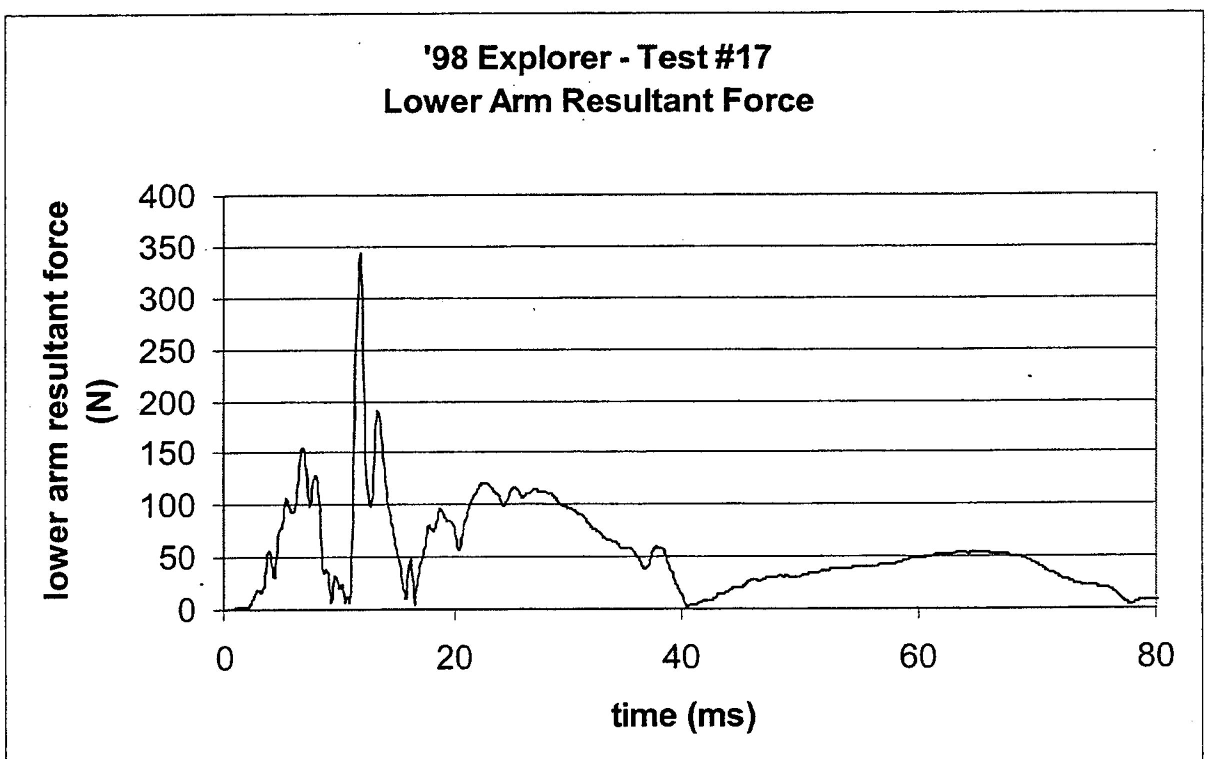

Fig. B.40. '98 Explorer - Test 17. Lower Arm Resultant Force.

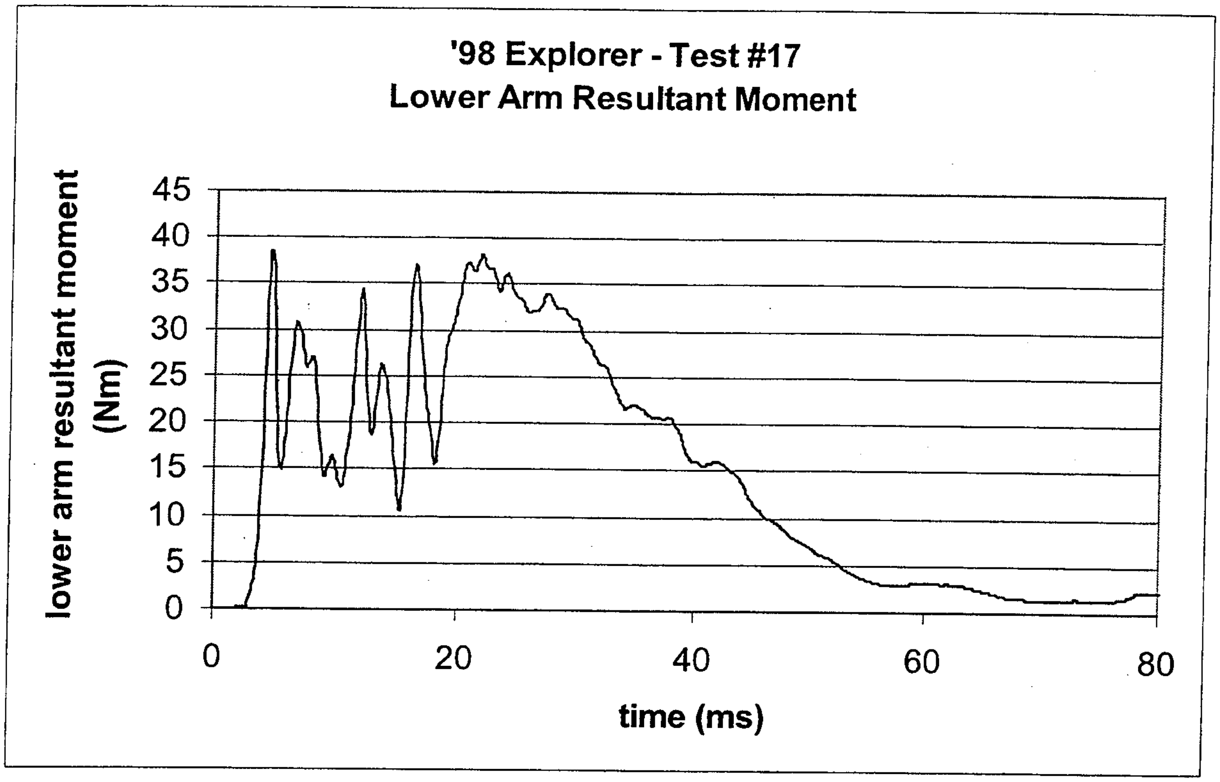

Fig. B.41. '98 Explorer - Test 17. Lower Arm Resultant Moment.

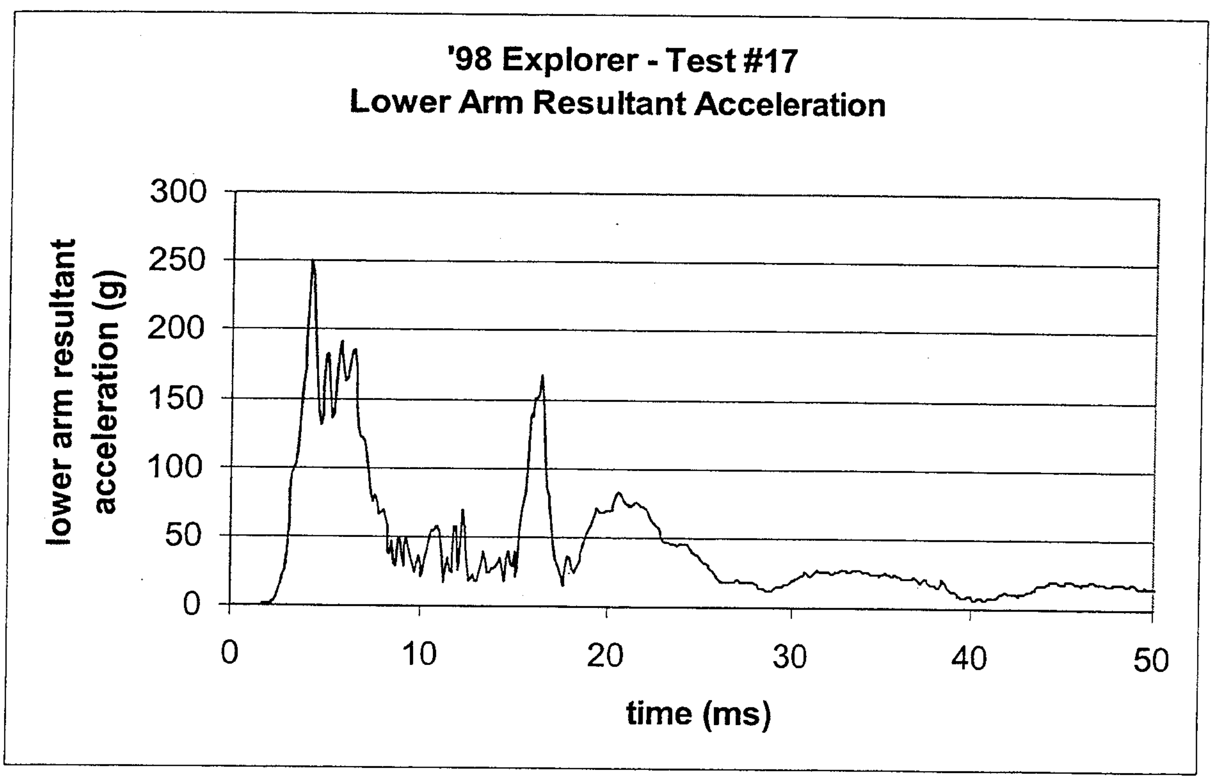

Fig. B.42. '98 Explorer - Test 17. Lower Arm Resultant Acceleration.

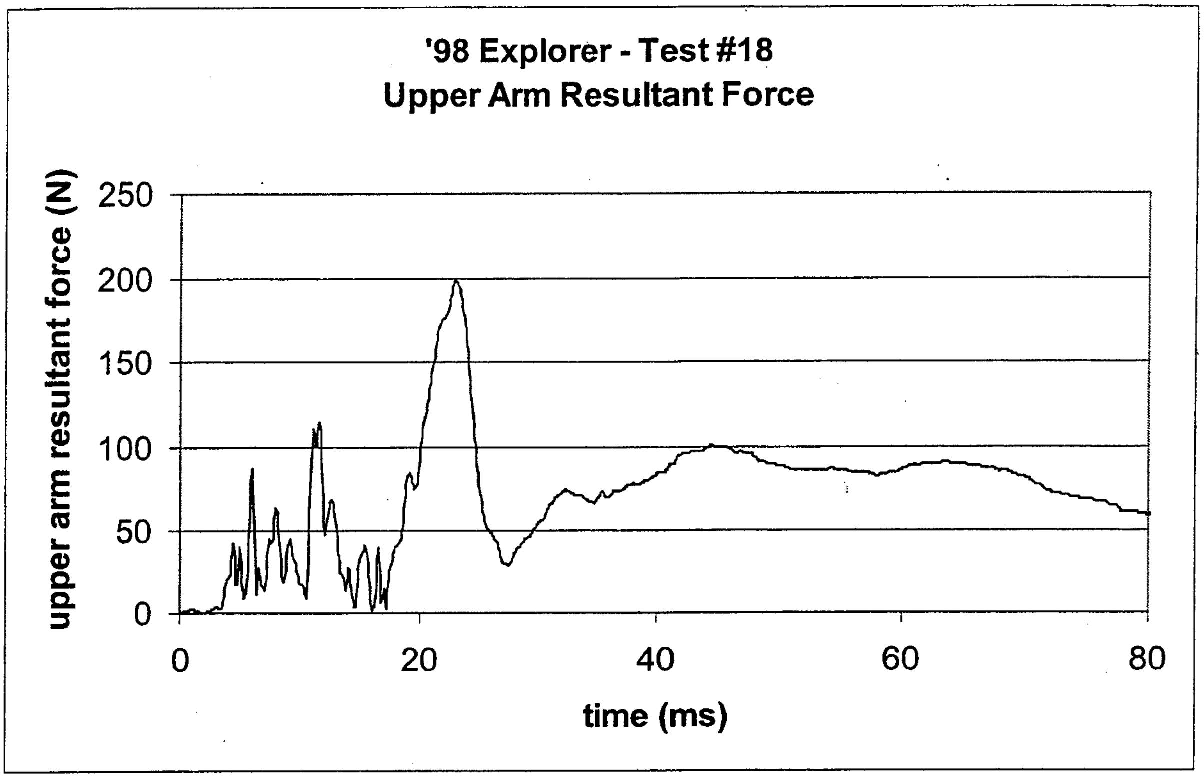

Fig. B.43. '98 Explorer - Test 18. Upper Arm Resultant Force.

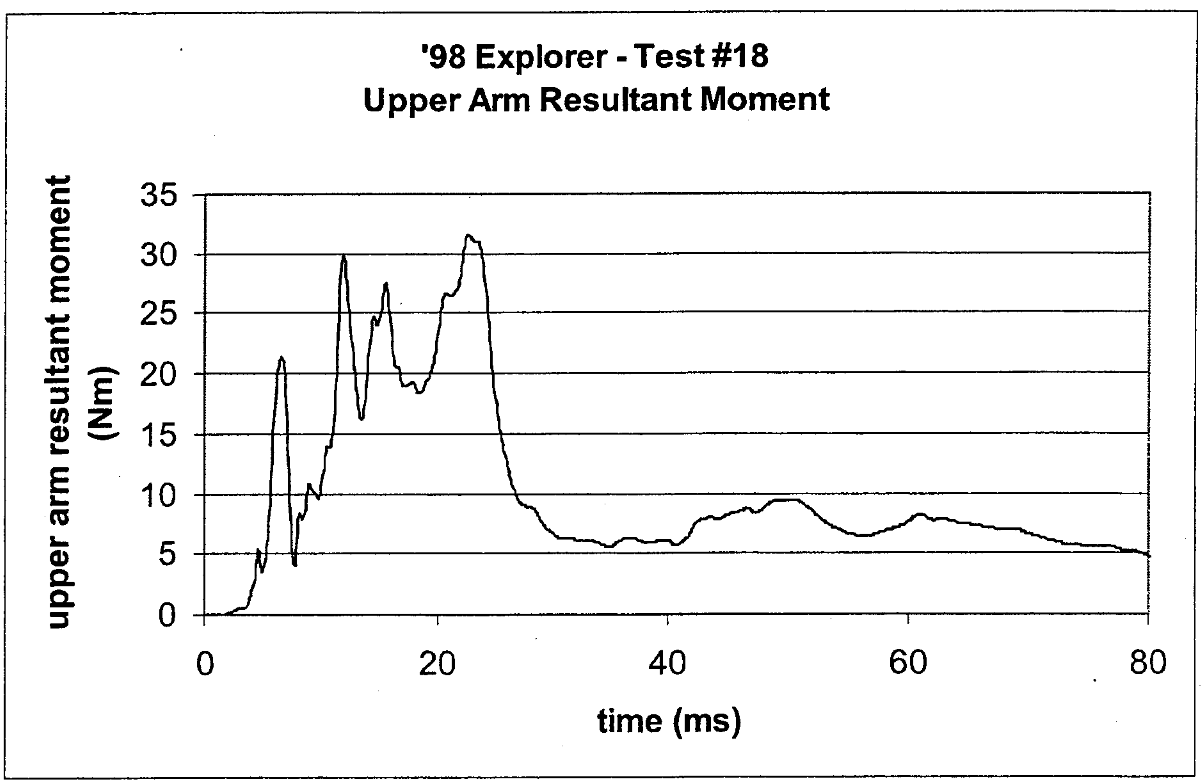

Fig. B.44. '98 Explorer - Test 18. Upper Arm Resultant Moment.

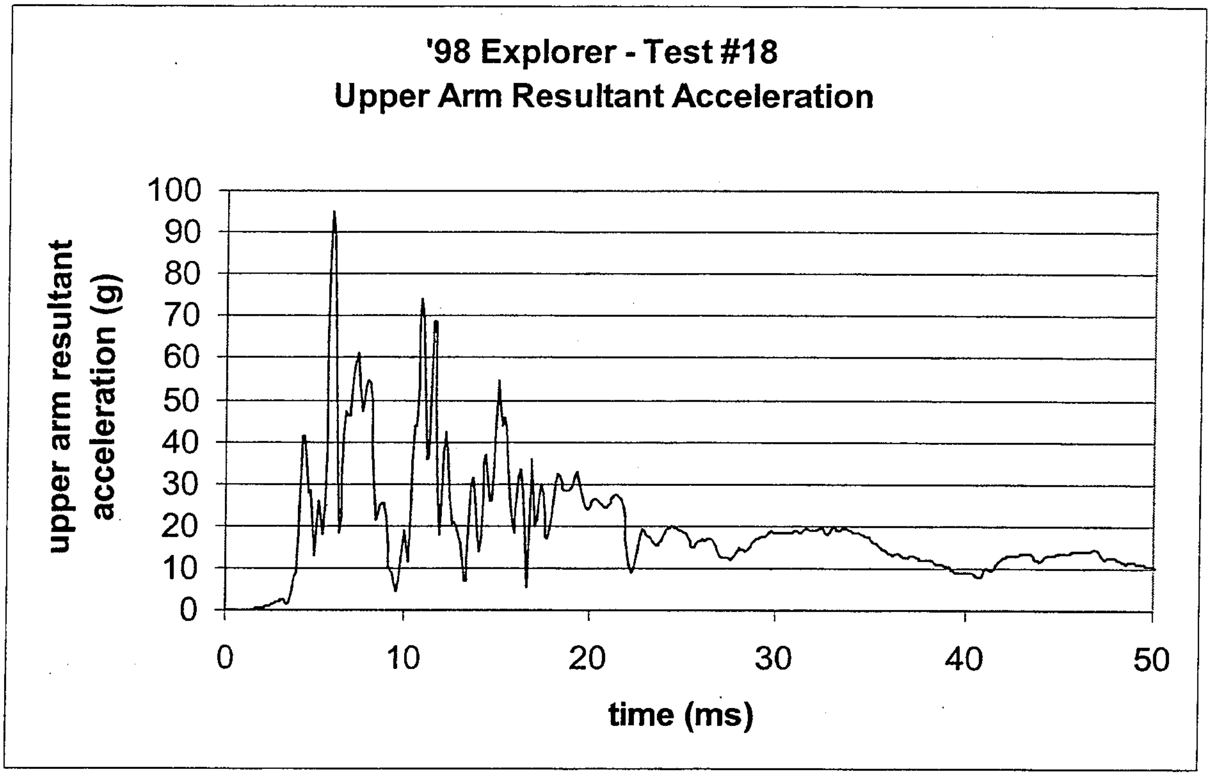

Fig. B.45. '98 Explorer - Test 18. Upper Arm Resultant Acceleration

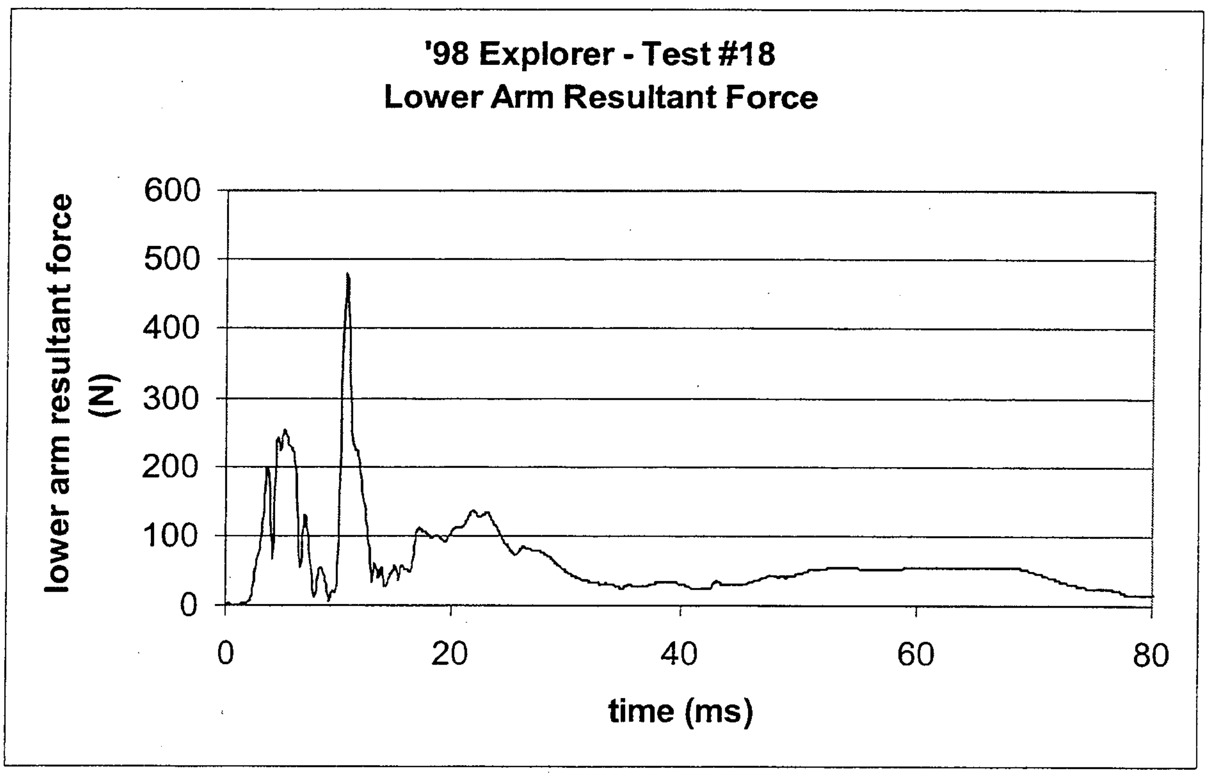

Fig. B.46. '98 Explorer - Test 18. Lower Arm Resultant Force.

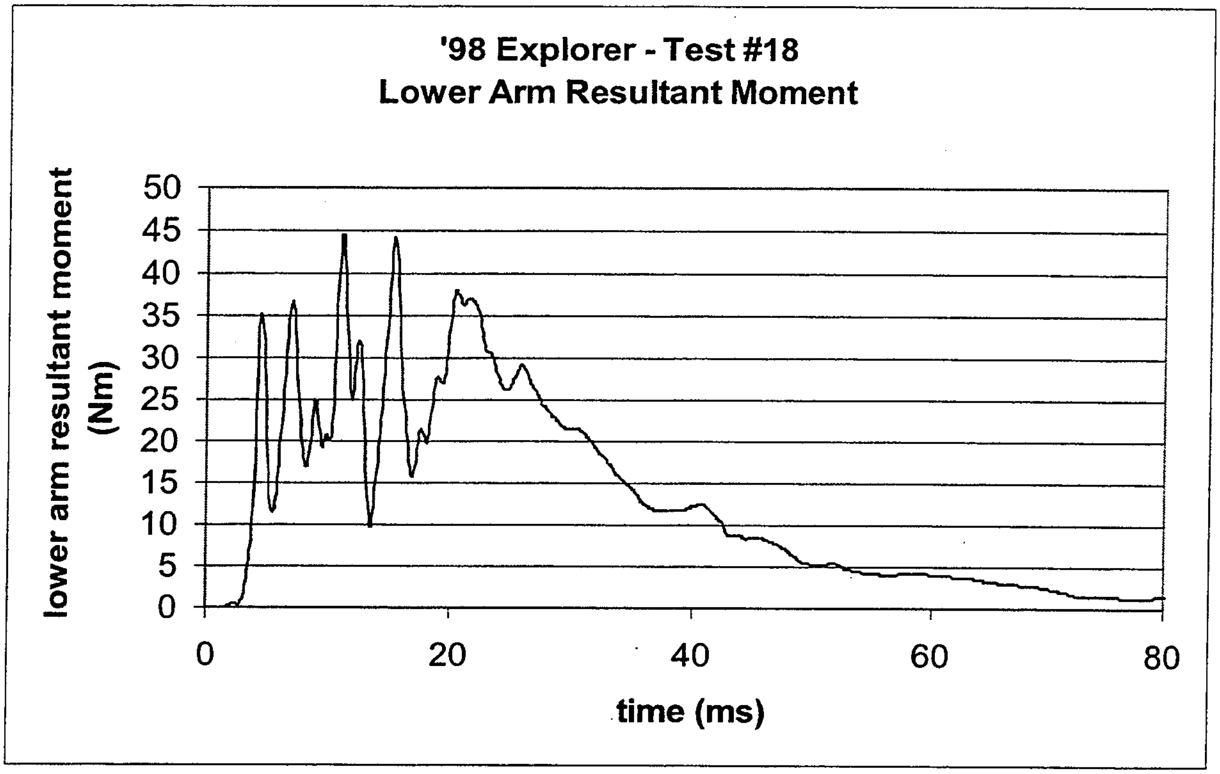

Fig. B.47. '98 Explorer - Test 18. Lower Arm Resultant Moment.

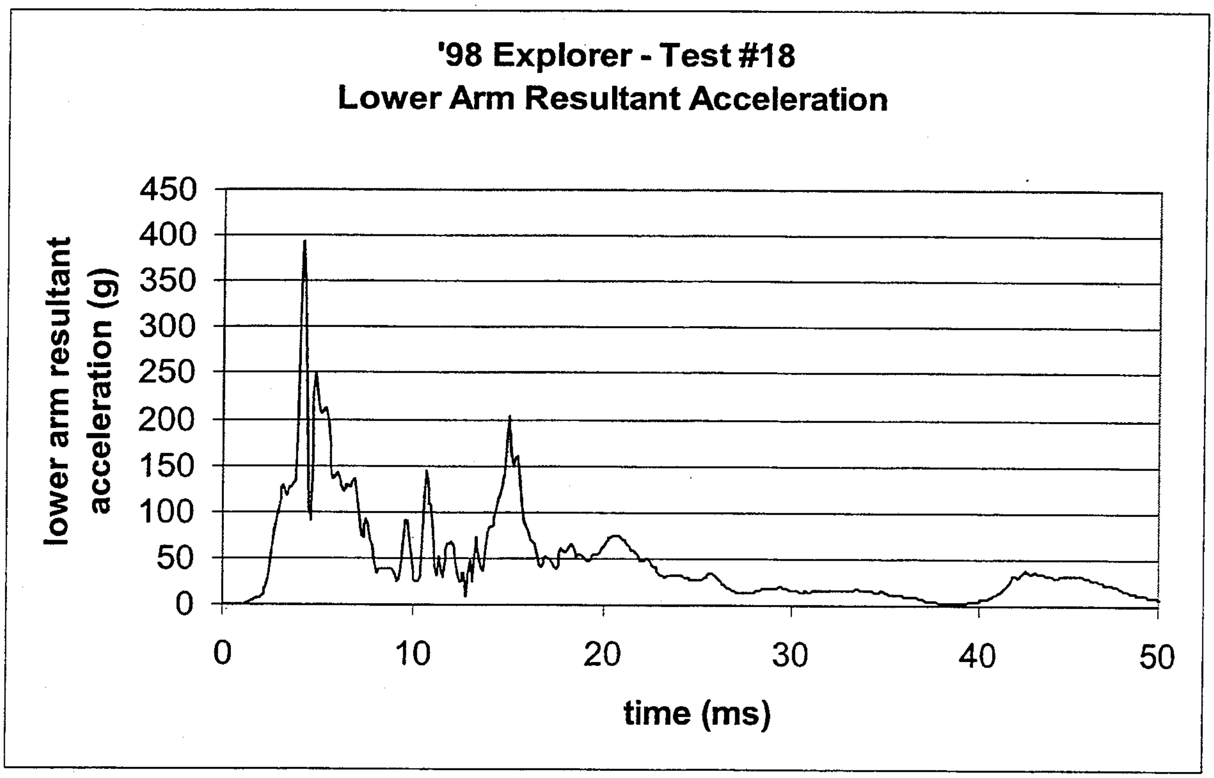

Fig. B.48. '98 Explorer - Test 18. Lower Arm Resultant Acceleration.

Appendix C

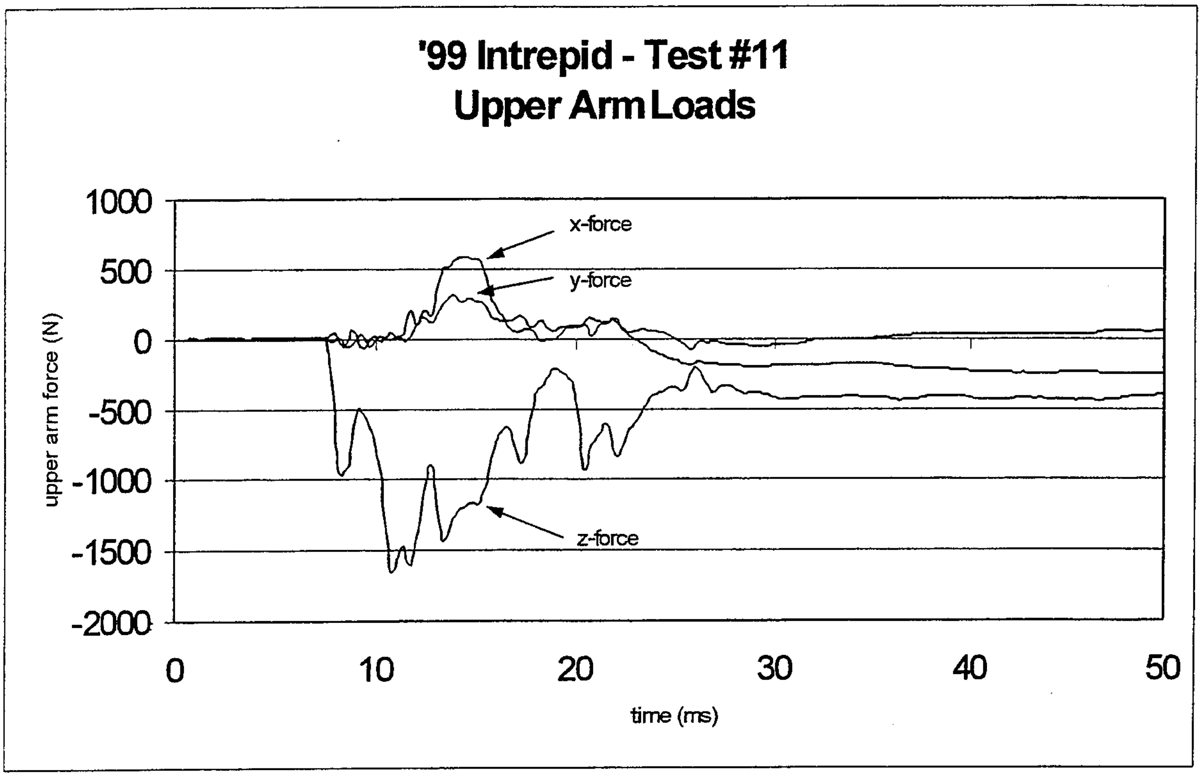

Fig. C.1. Upper Arm Loads for '99 Intrepid Test dab-11

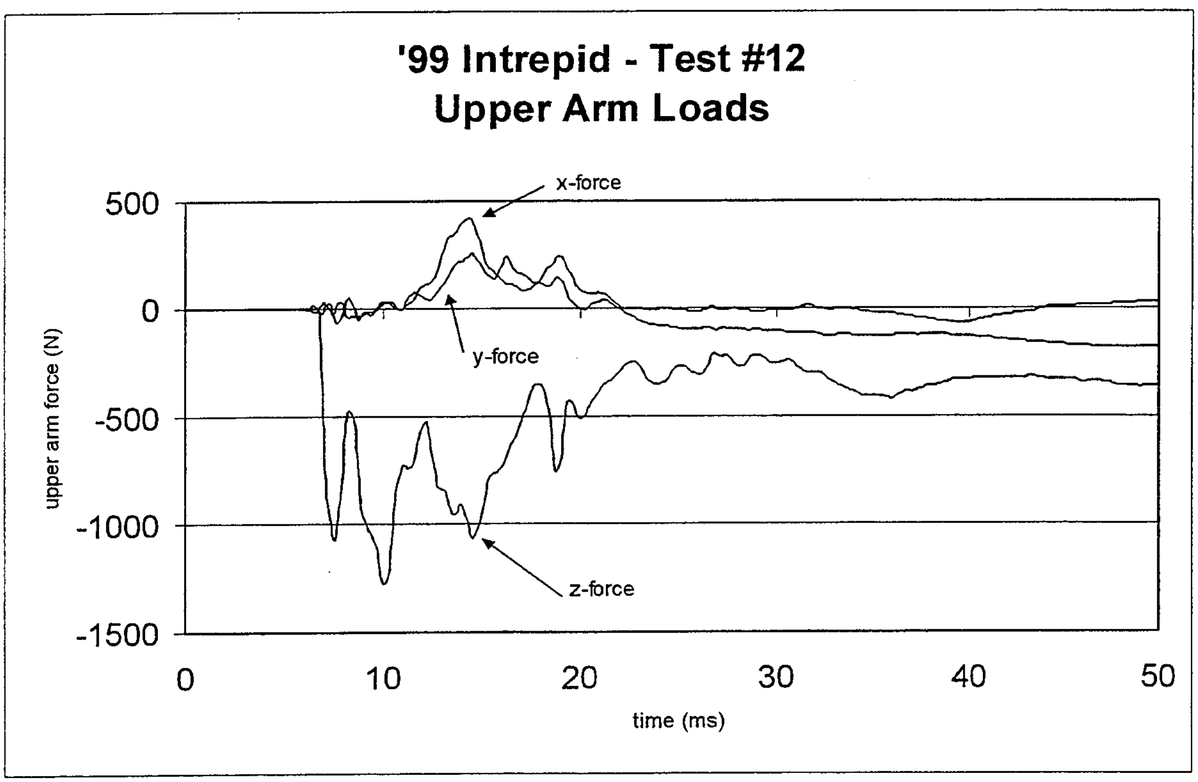

Fig. C.2. Upper Arm Loads for '99 Intrepid Test dab-12

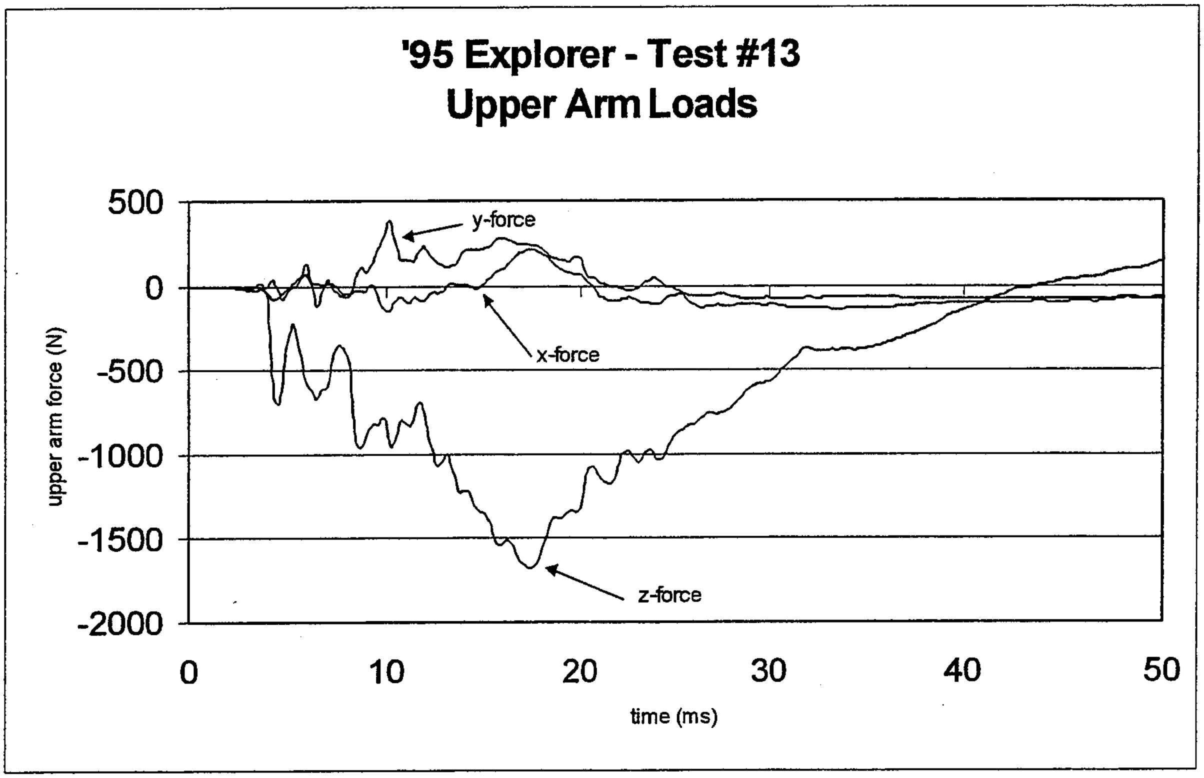

Fig. C.3. Upper Arm Loads for '95 Explorer Test dab-13

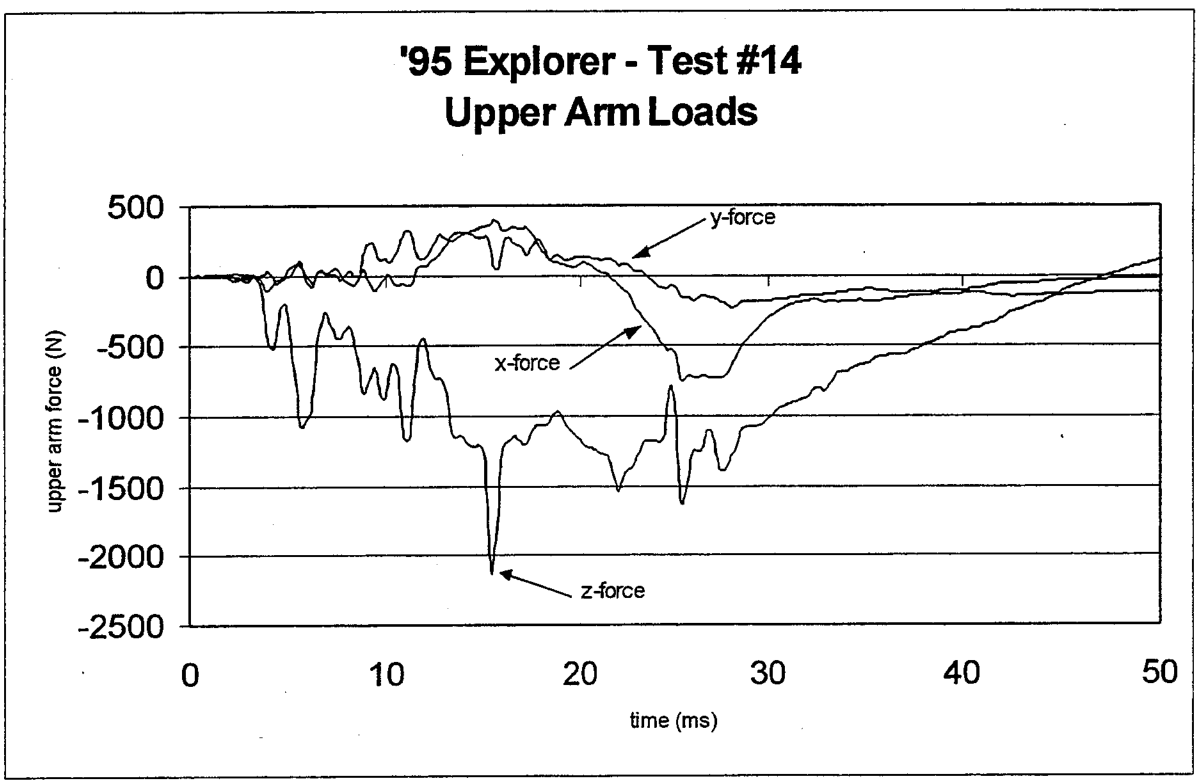

Fig. C.4. Upper Arm Loads for '95 Explorer Test dab-14

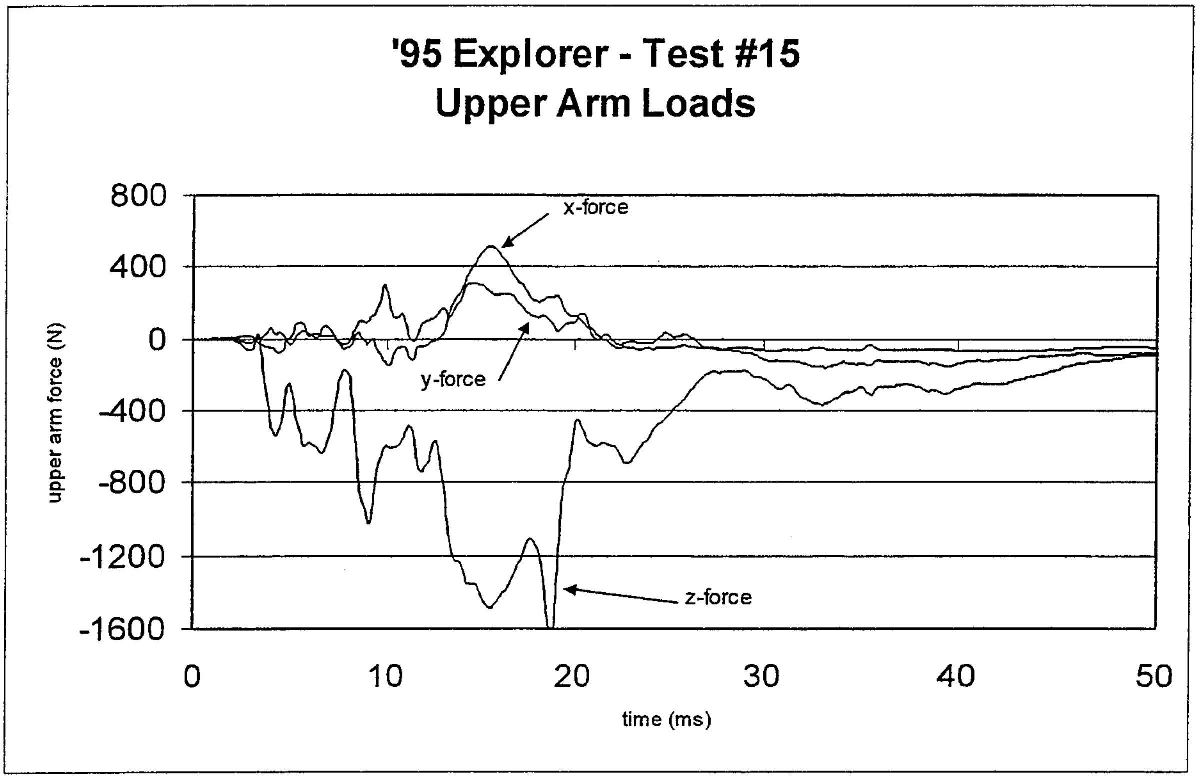

Fig. C.5. Upper Arm Loads for '95 Explorer Test dab-15

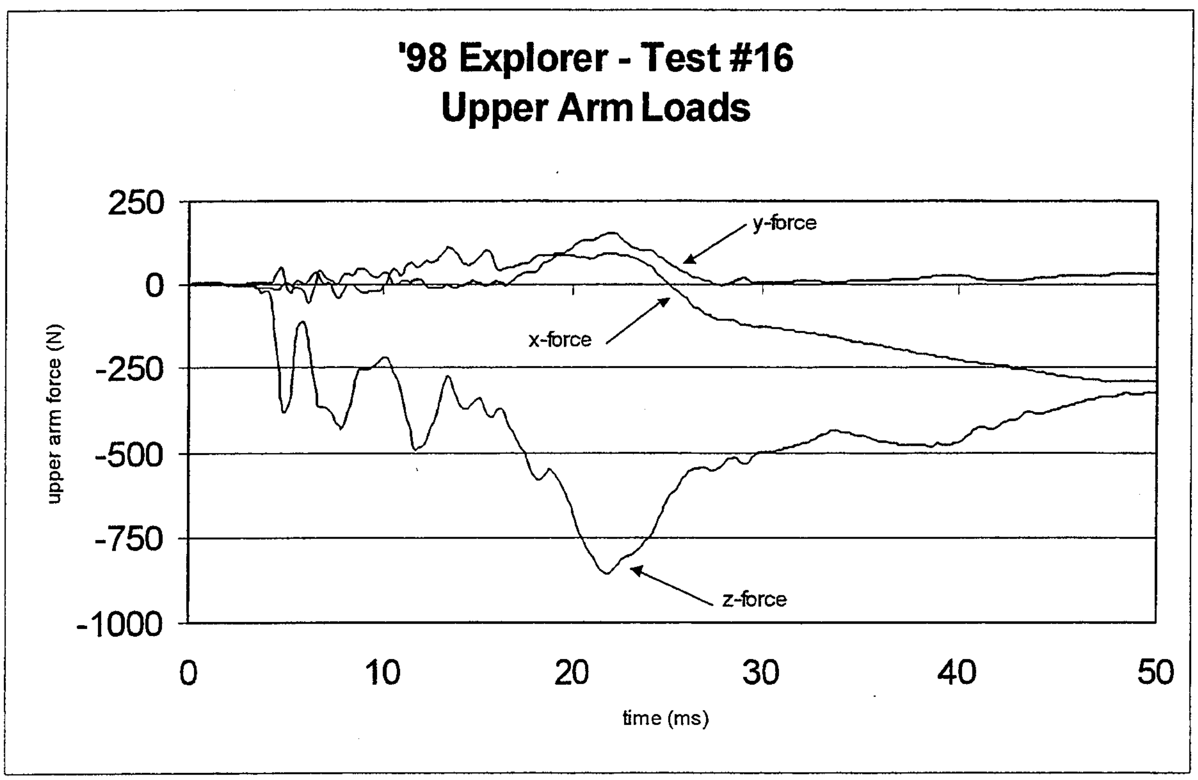

Fig. C.6. Upper Arm Loads for '98 Explorer Test dab-16

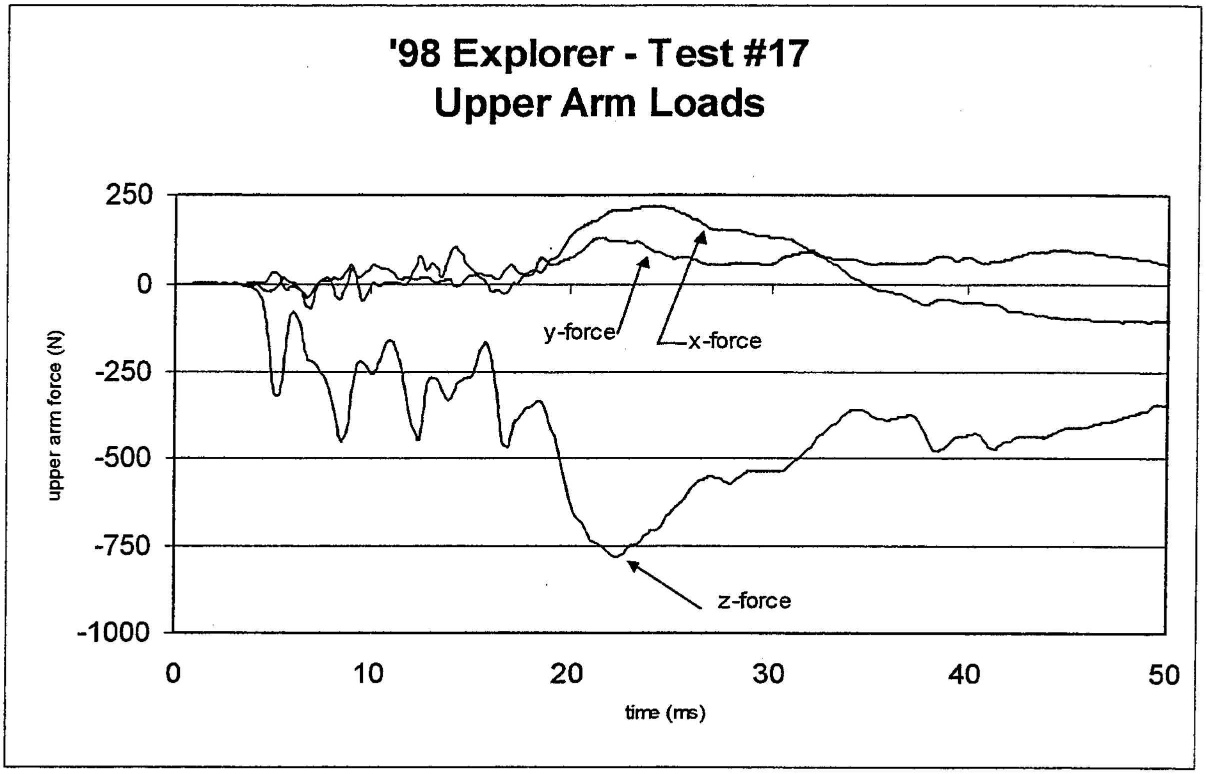

Fig. C.7. Upper Arm Loads for '98 Explorer Test dab-17

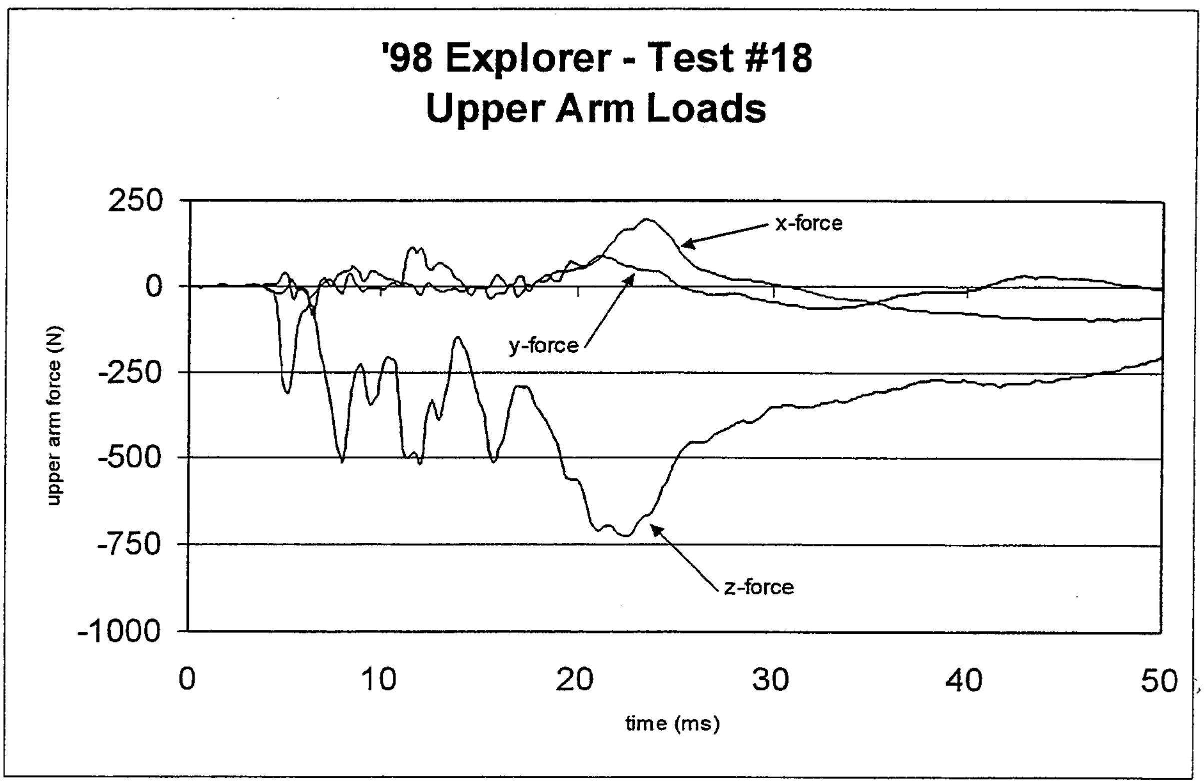

Fig. C.8. Upper Arm Loads for '98 Explorer Test dab-18

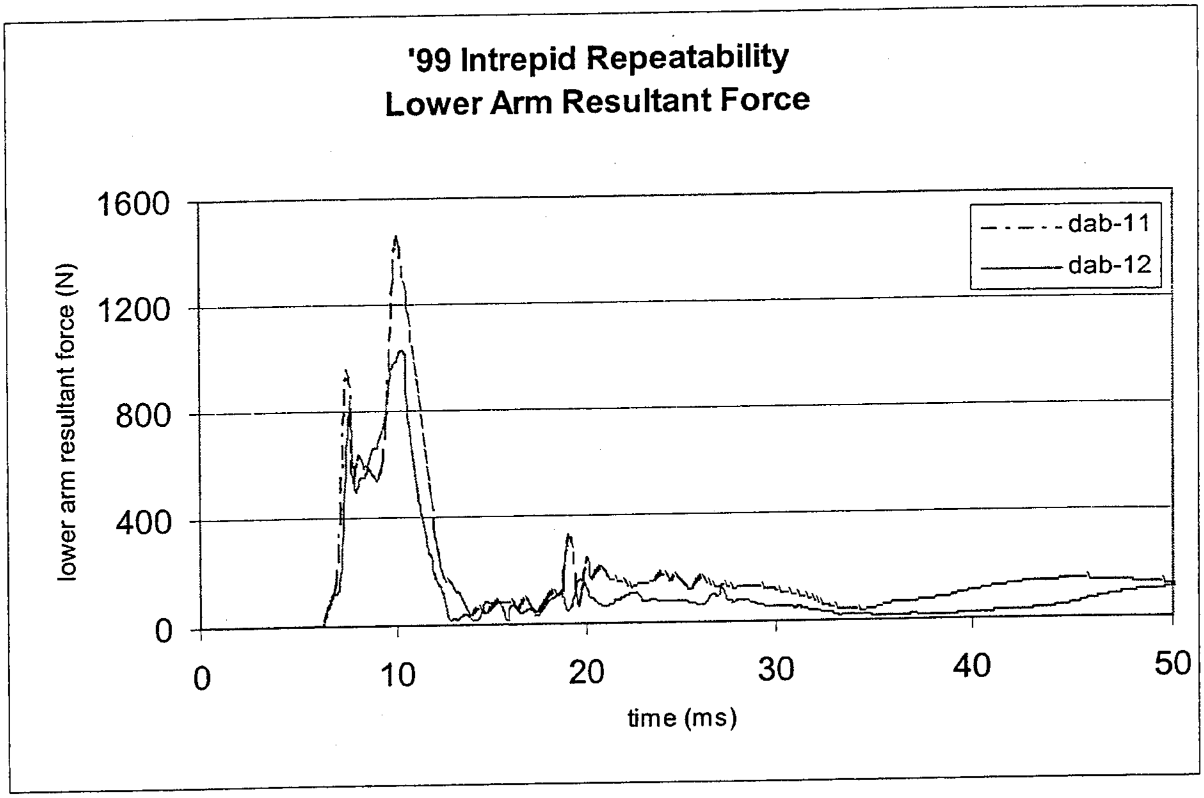

Fig. D.1. '99 Intrepid Repeatability - Lower Arm Resultant Force

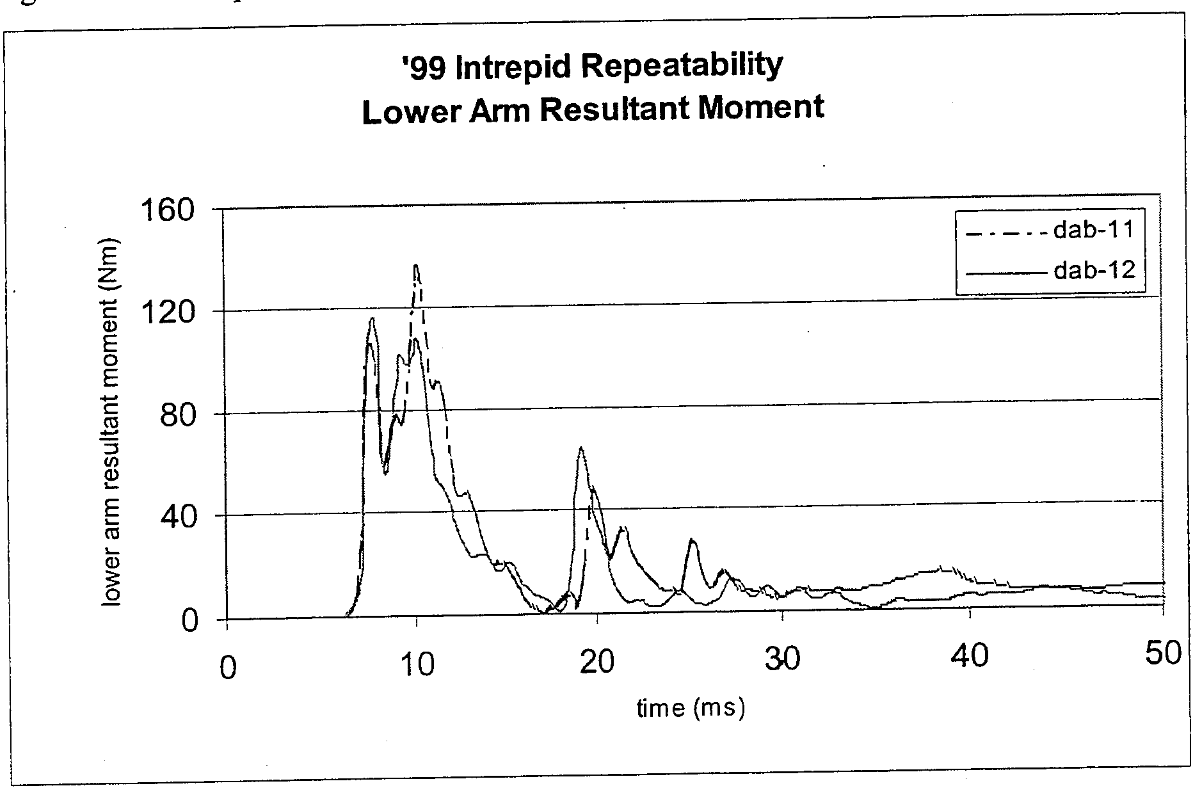

Fig. D.2. '99 Intrepid Repeatability - Lower Arm Resultant Moment

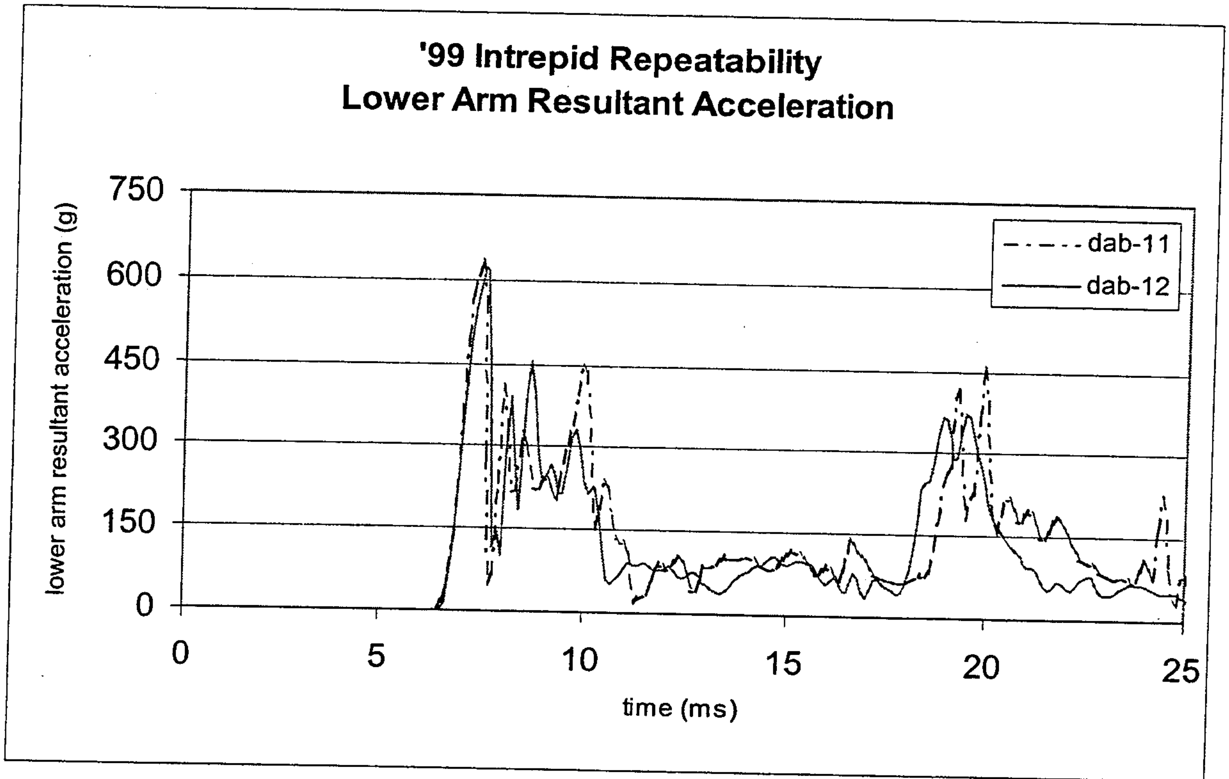

Fig. D.3. '99 Intrepid Repeatability - Lower Arm Resultant Acceleration

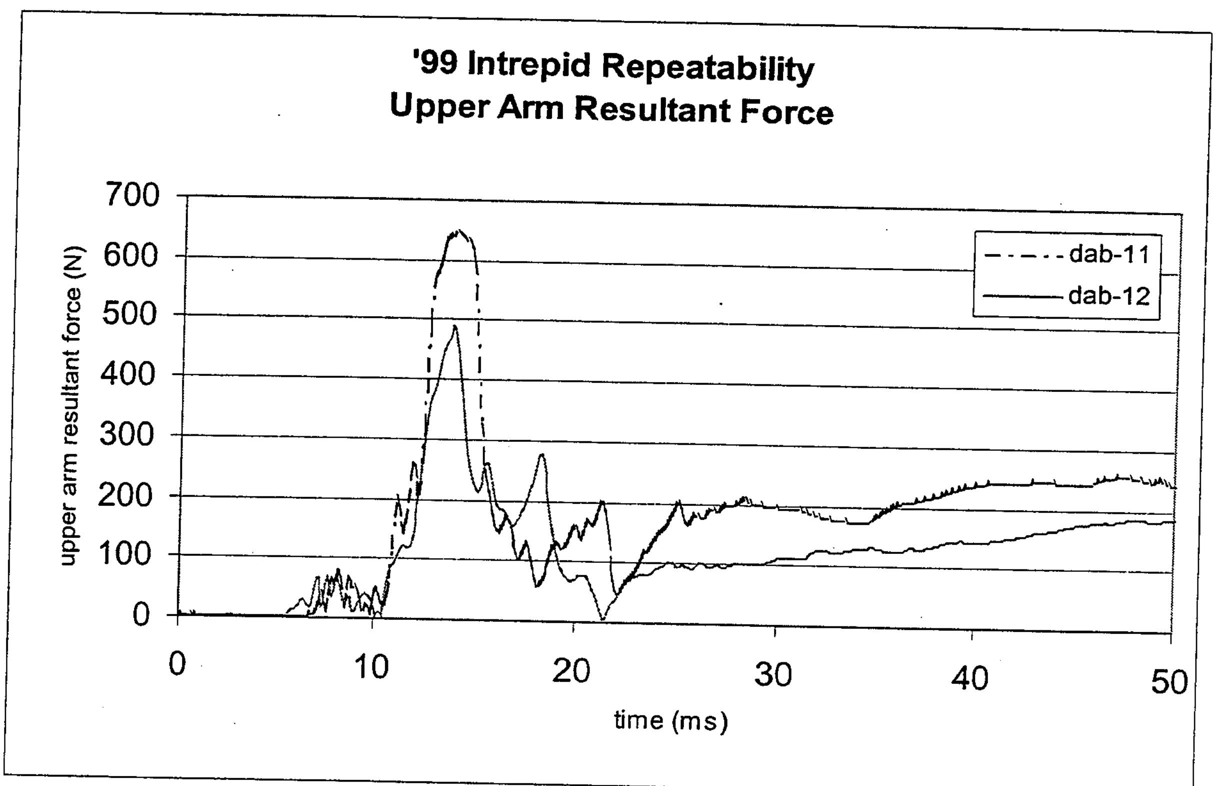

Fig. D.4. '99 Intrepid Repeatability - Upper Arm Resultant Force

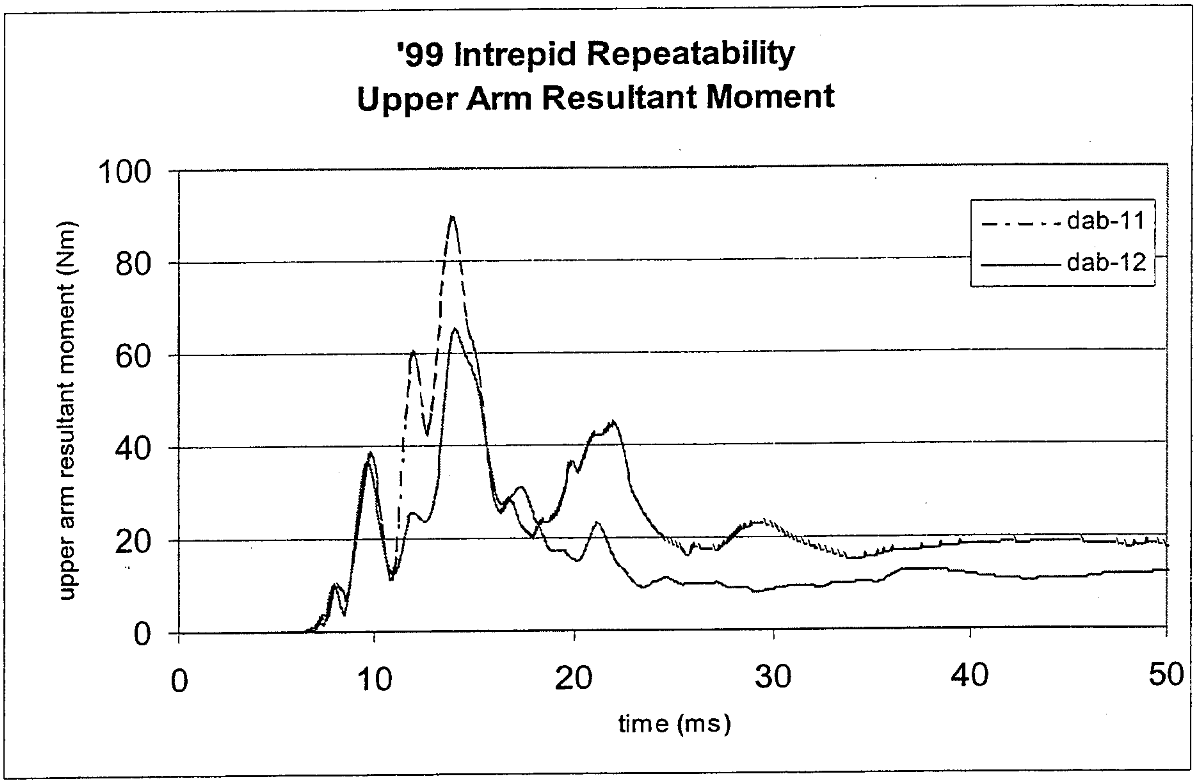

Fig. D.5. '99 Intrepid Repeatability - Upper Arm Resultant Moment

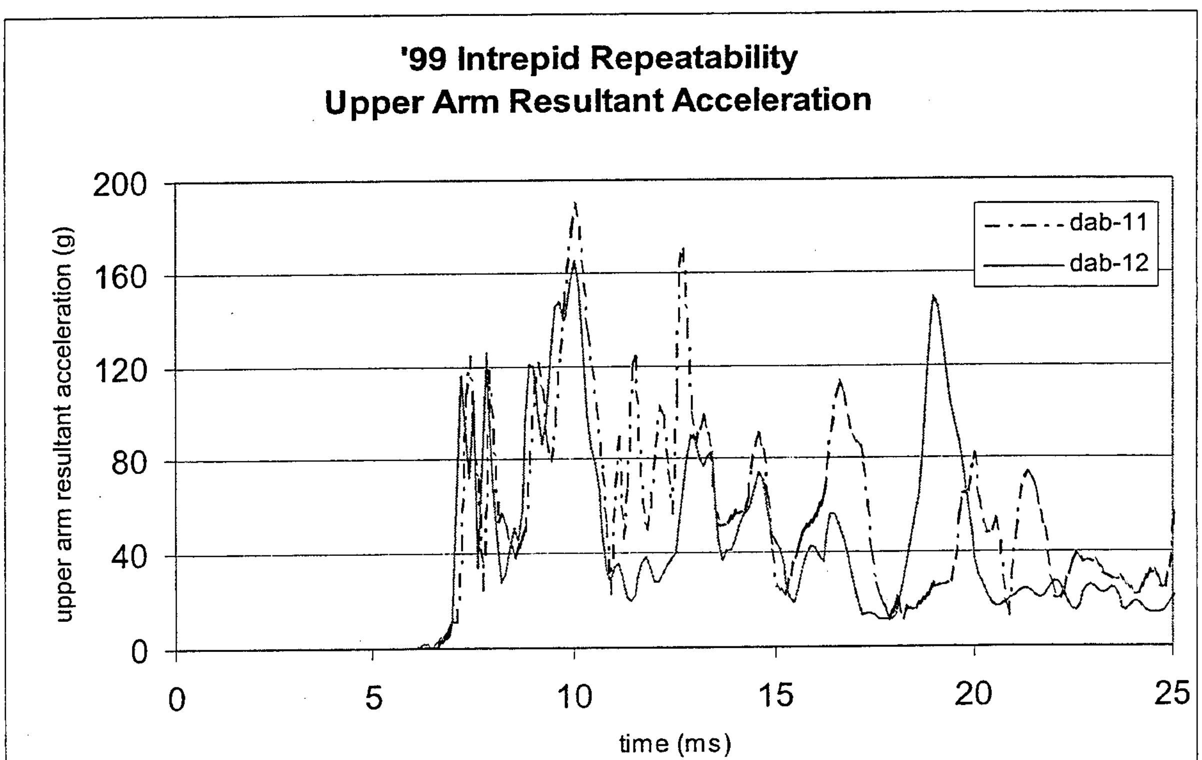

Fig. D.6. '99 Intrepid Repeatability - Upper Arm Resultant Acceleration

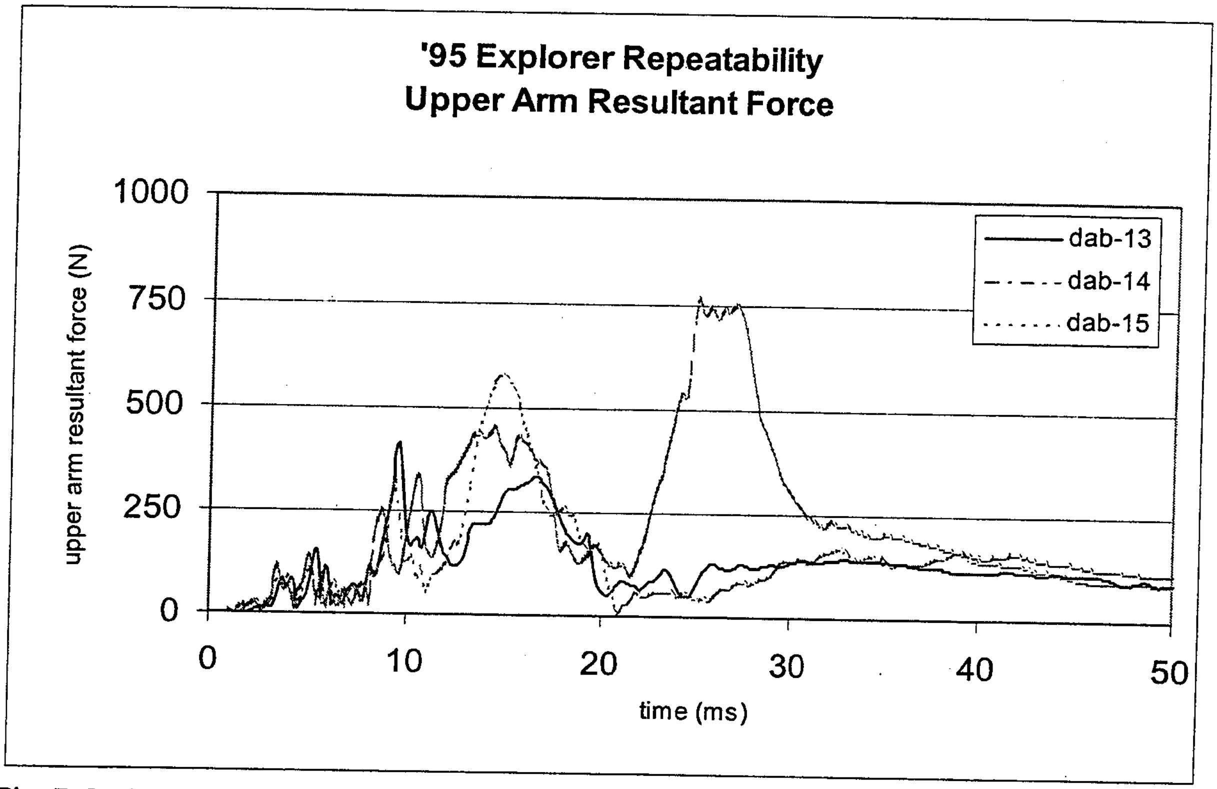

Fig. D.7. '95 Explorer Repeatability - Upper Arm Resultant Force

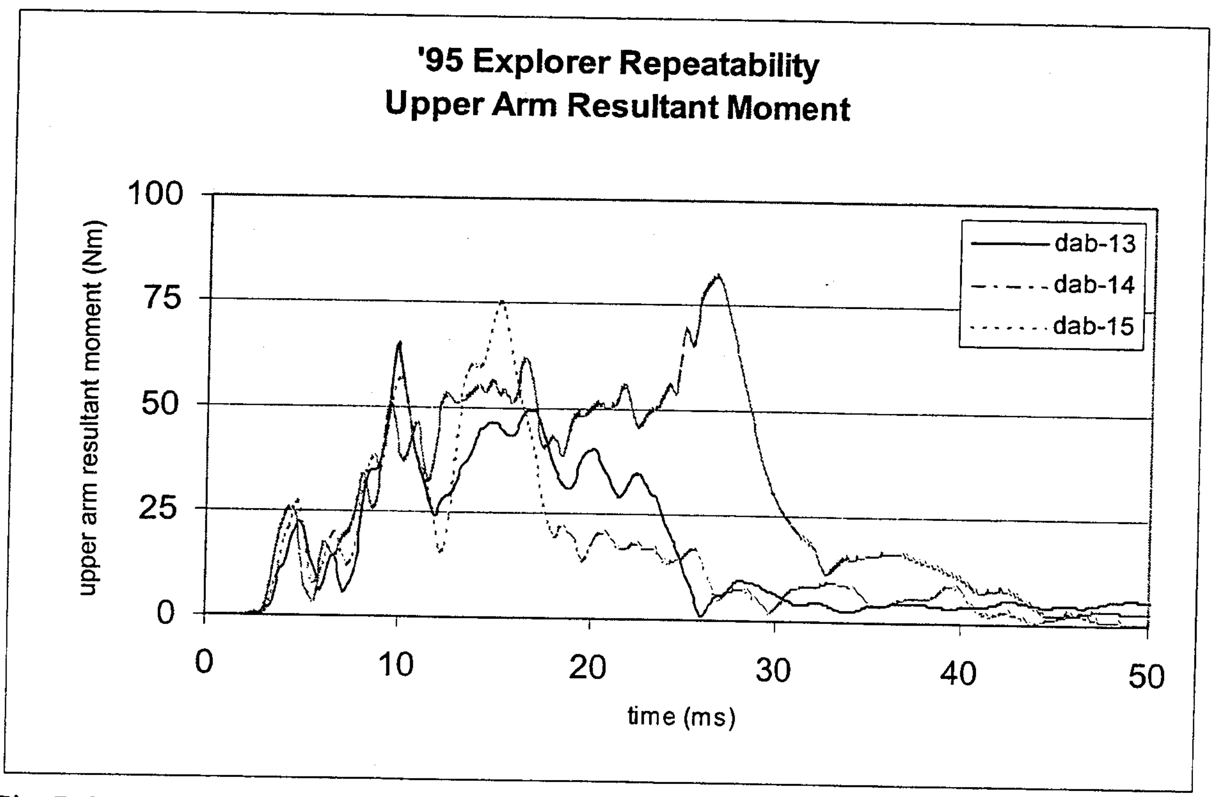

Fig. D.8. '95 Explorer Repeatability - Upper Arm Resultant Moment

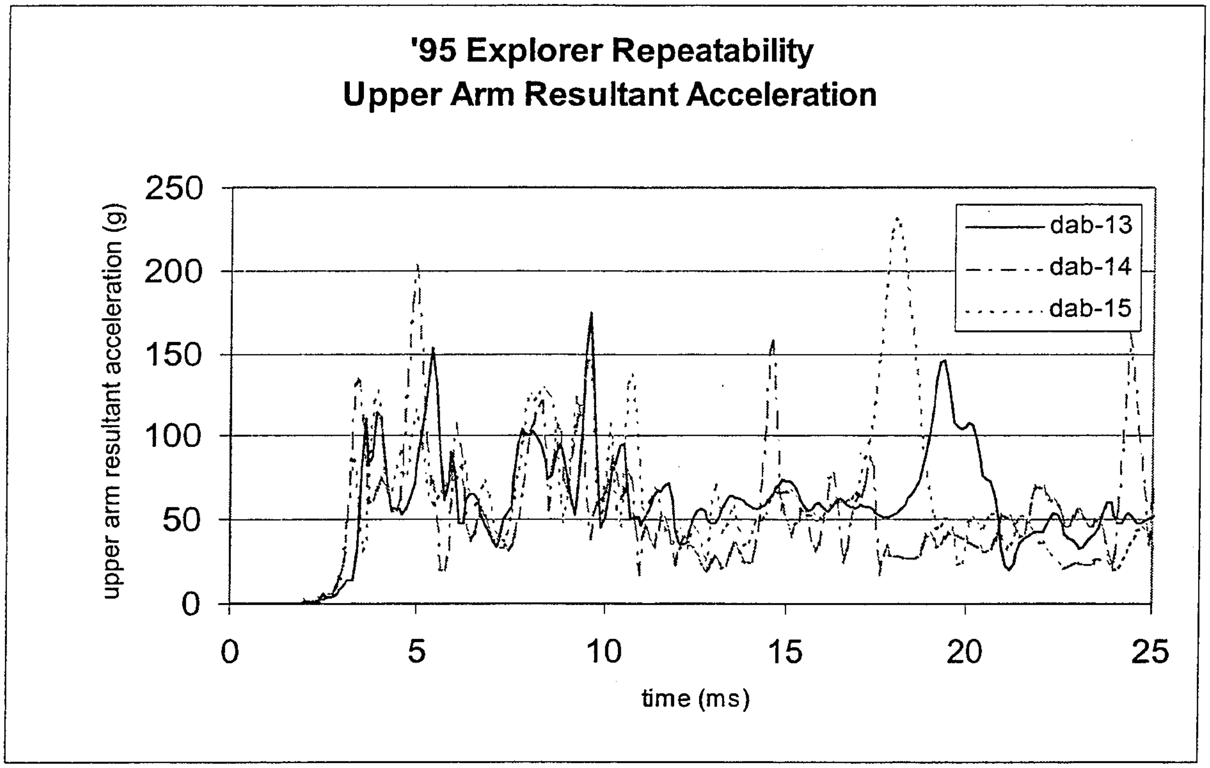

Fig. D.9. '95 Explorer Repeatability - Upper Arm Resultant Acceleration

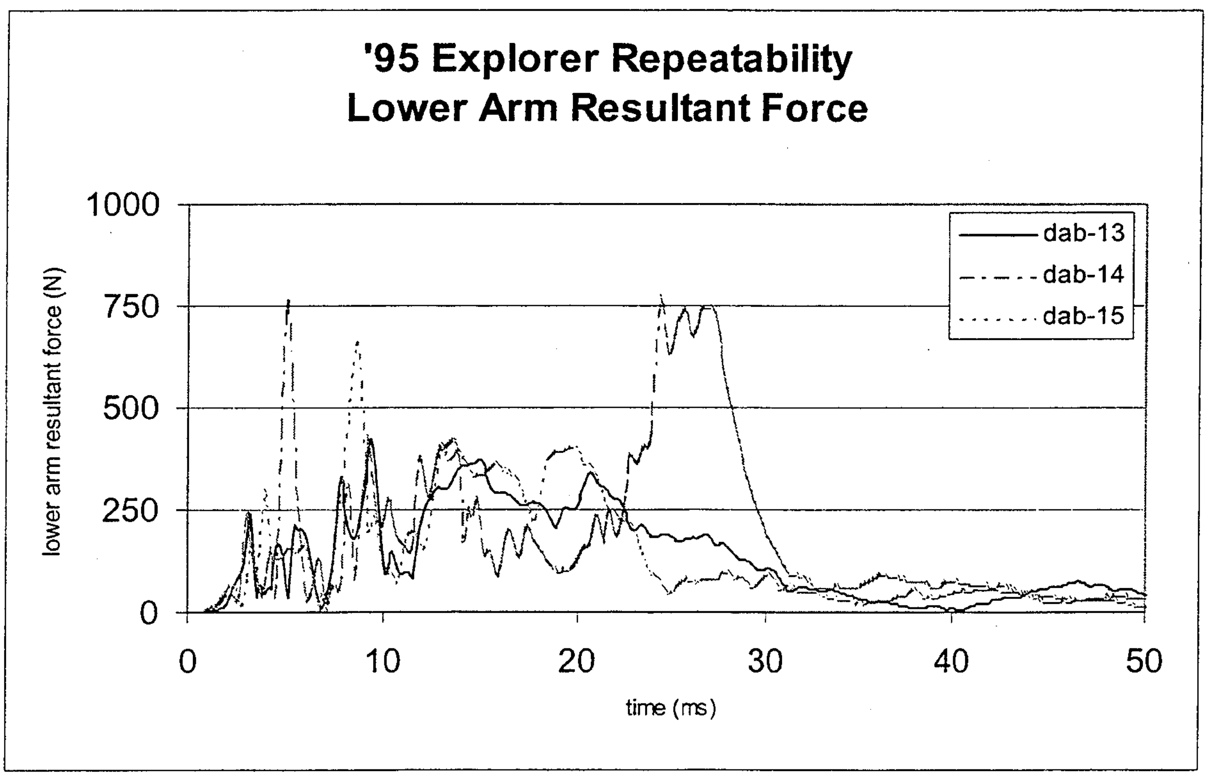

Fig. D.10. '95 Explorer Repeatability - Lower Arm Resultant Force

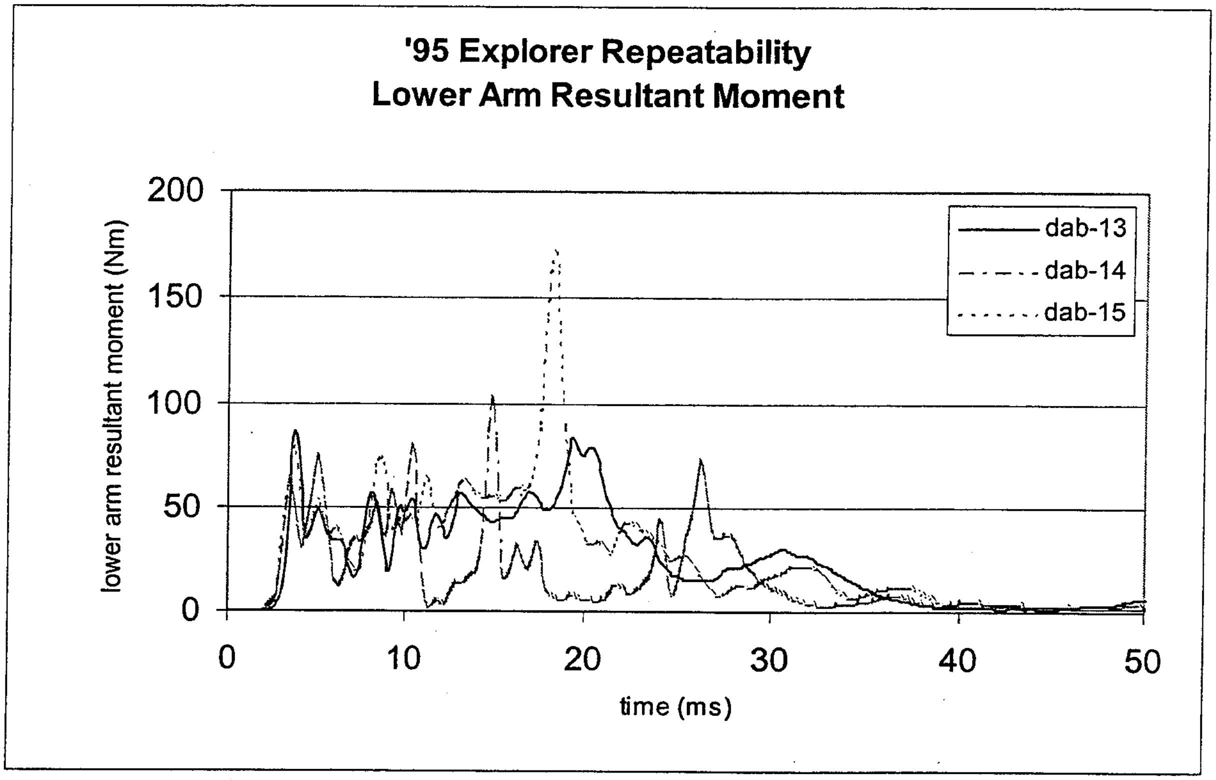

Fig. D.11. ‘95 Explorer Repeatability - Lower Arm Resultant Moment

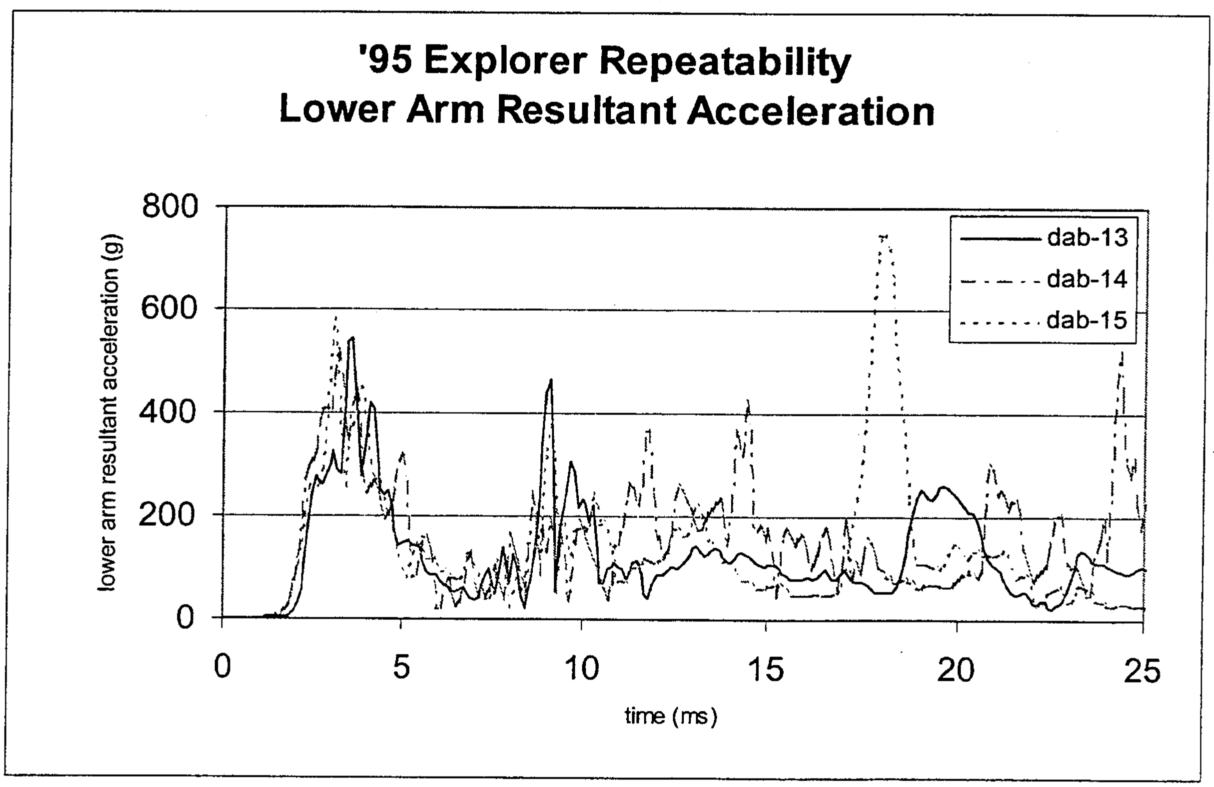

Fig. D.12. ‘95 Explorer Repeatability - Lower Arm Resultant Acceleration

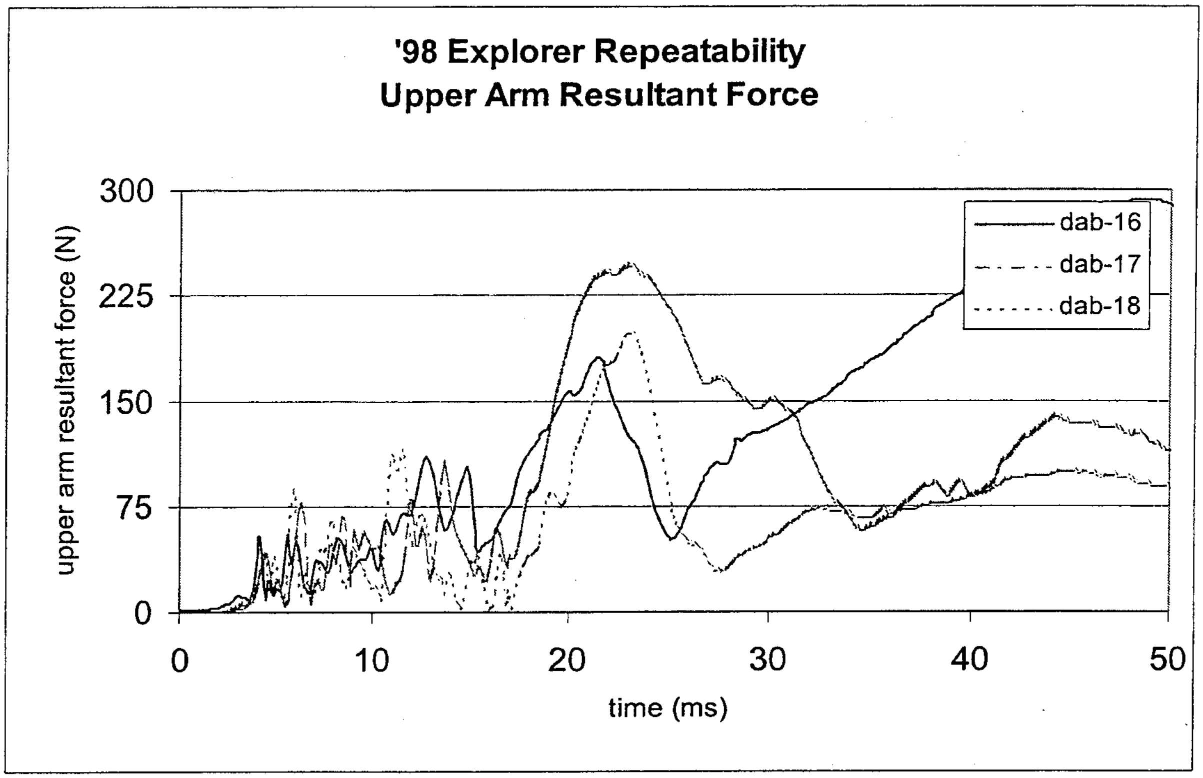

Fig. D.13. '98 Explorer Repeatability - Upper Arm Resultant Force

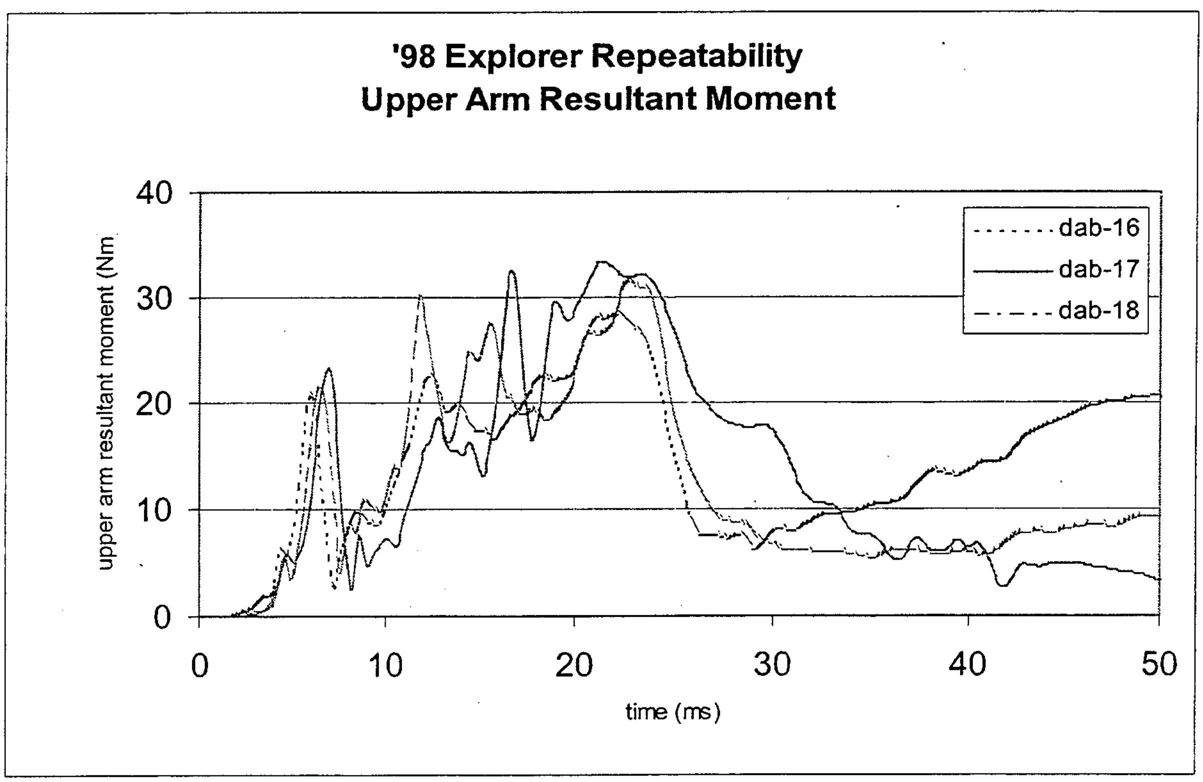

Fig. D.14. '98 Explorer Repeatability - Upper Arm Resultant Moment

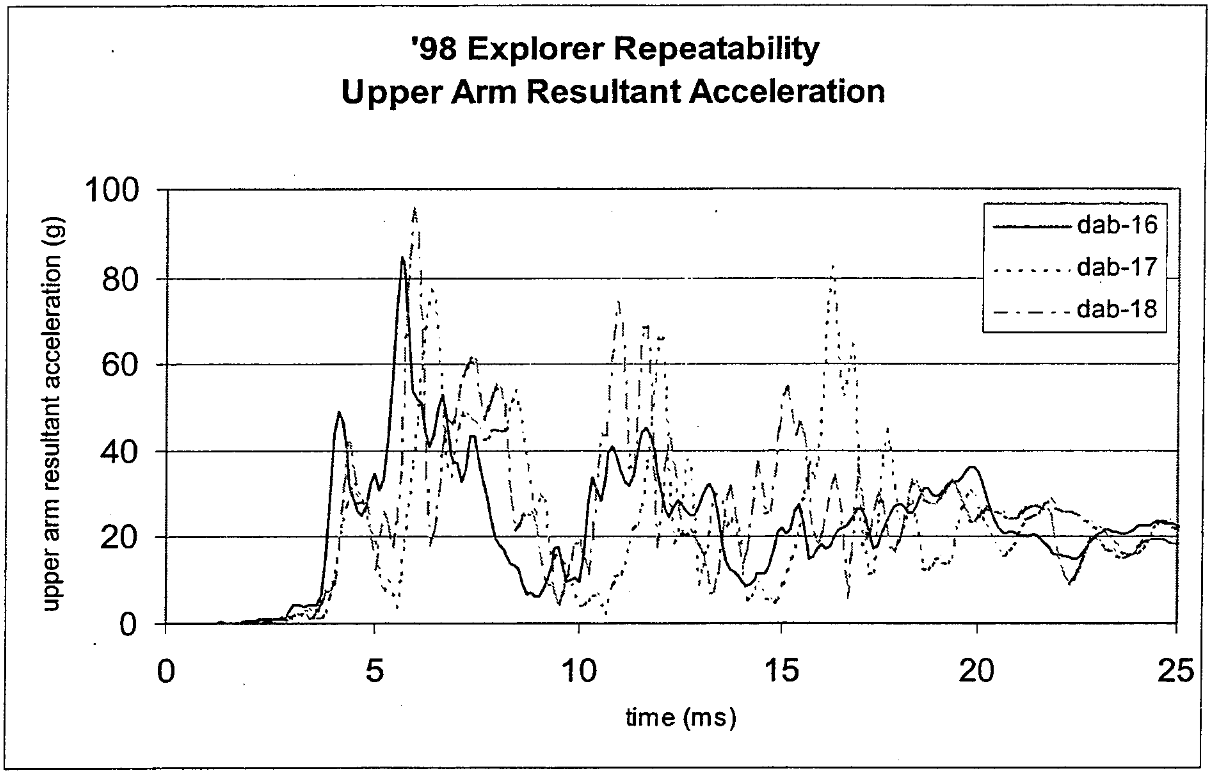

Fig. D.15. '98 Explorer Repeatability - Upper Arm Resultant Acceleration

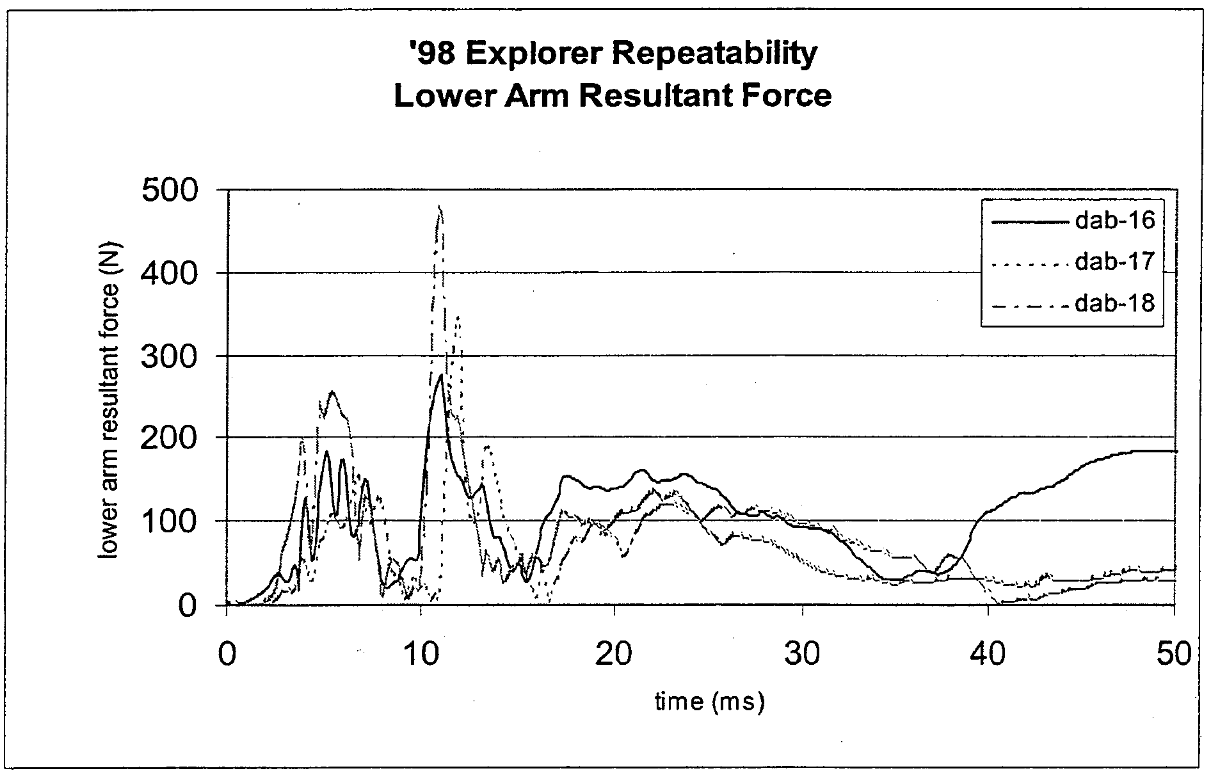

'Fig. D.16. '98 Explorer Repeatability - Lower Arm Resultant Force

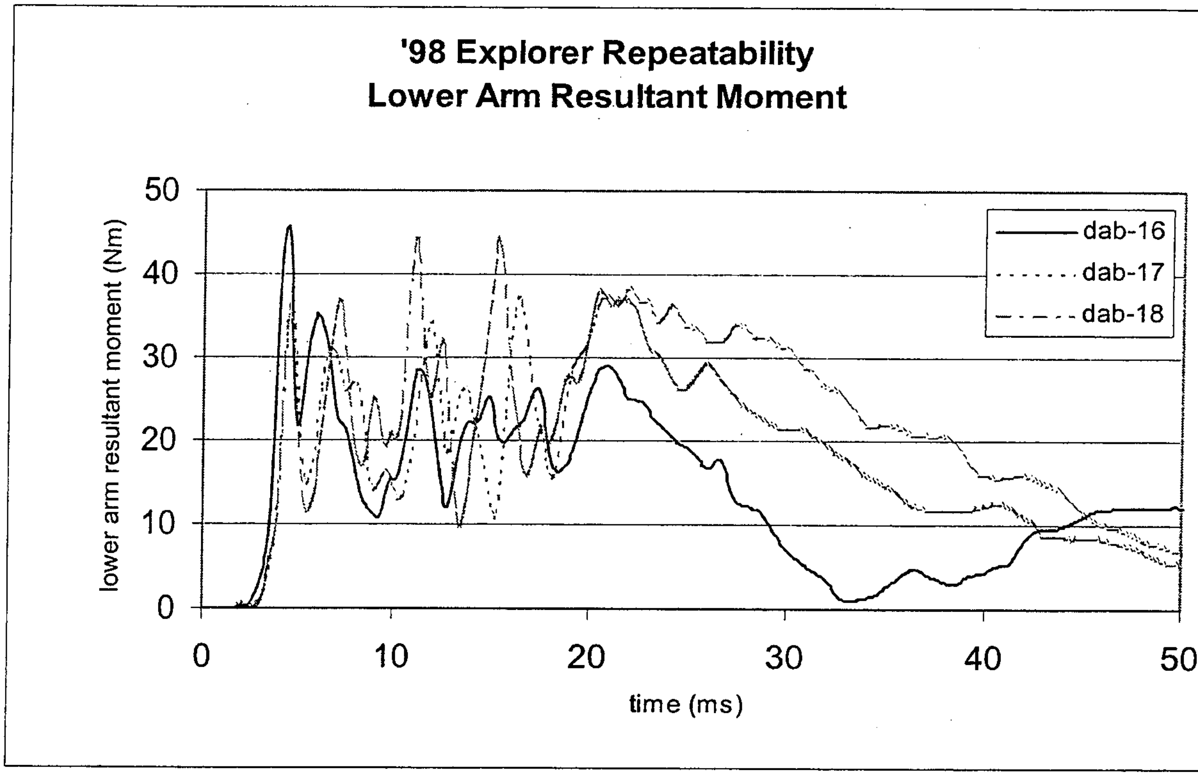

Fig. D.17. '98 Explorer Repeatability - Lower Arm Resultant Moment

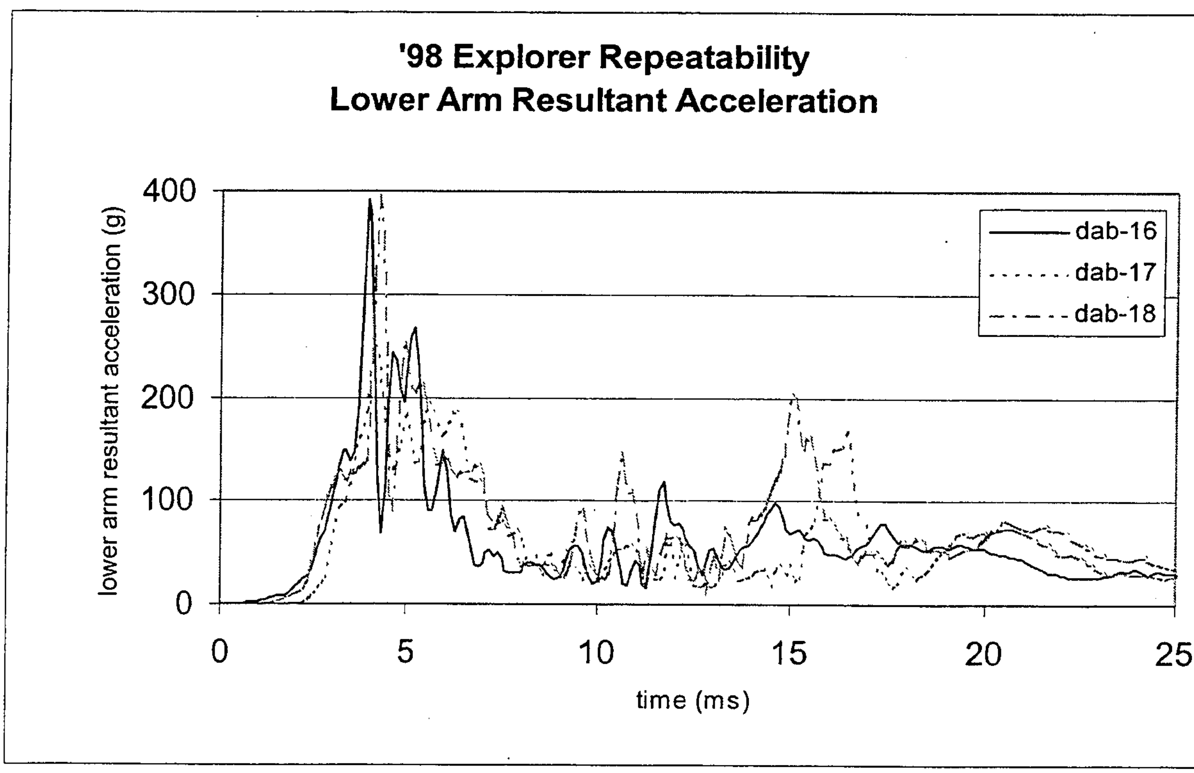

Fig. D.18. '98 Explorer Repeatability - Lower Arm Resultant Acceleration

Appendix E

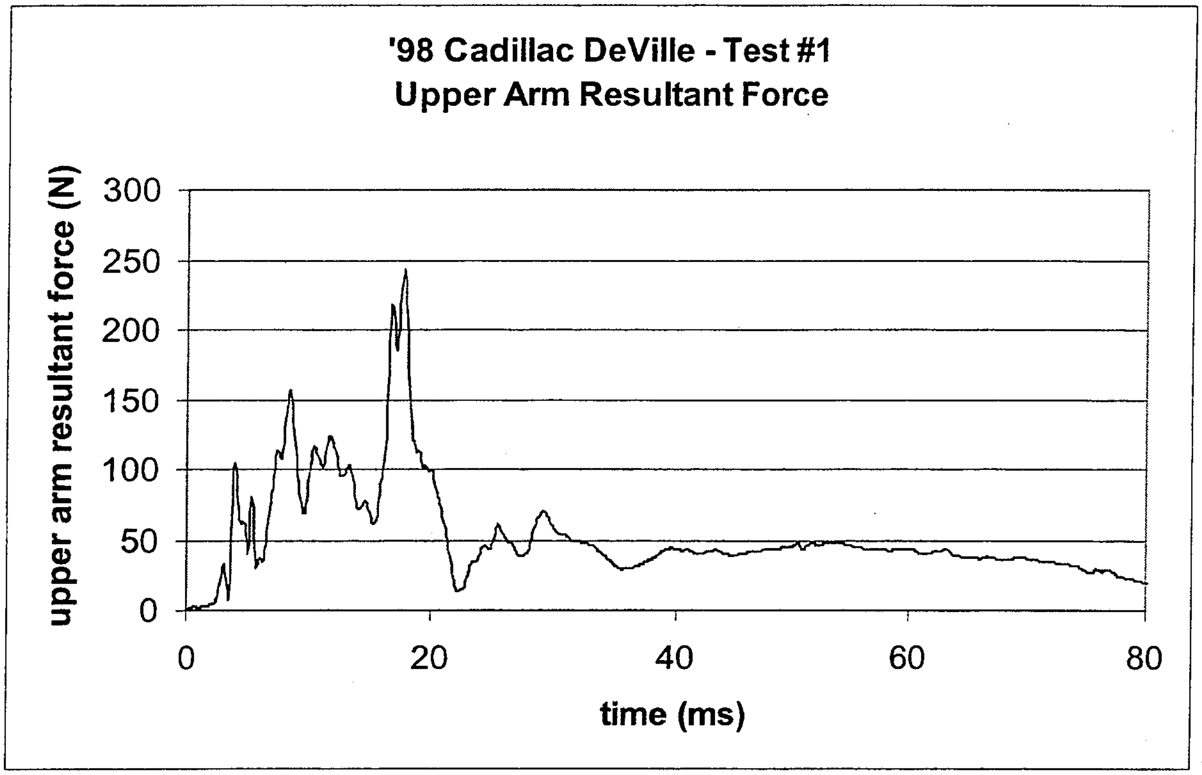

Fig. E.1. '98 Cadillac - Test 1. Upper Arm Resultant Force.

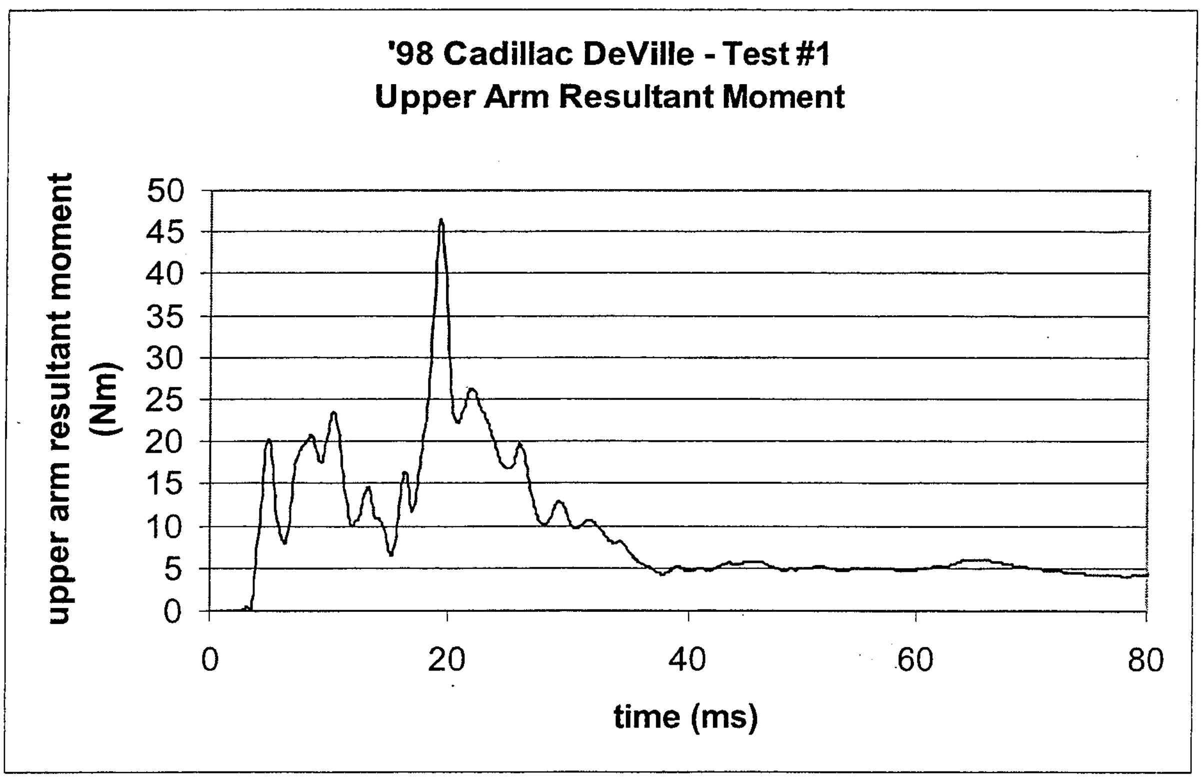

Fig. E.2. '98 Cadillac - Test 1. Upper Arm Resultant Moment.

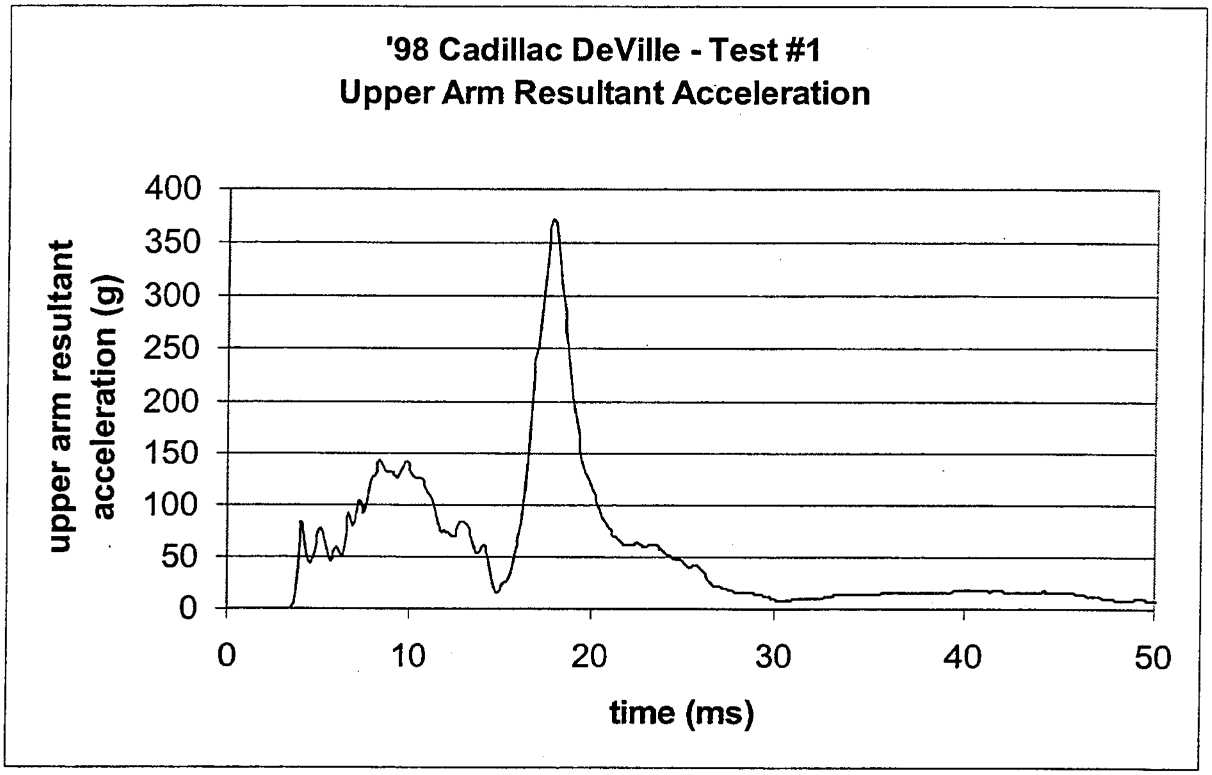

Fig. E.3. '98 Cadillac - Test 1. Upper Arm Resultant Acceleration.

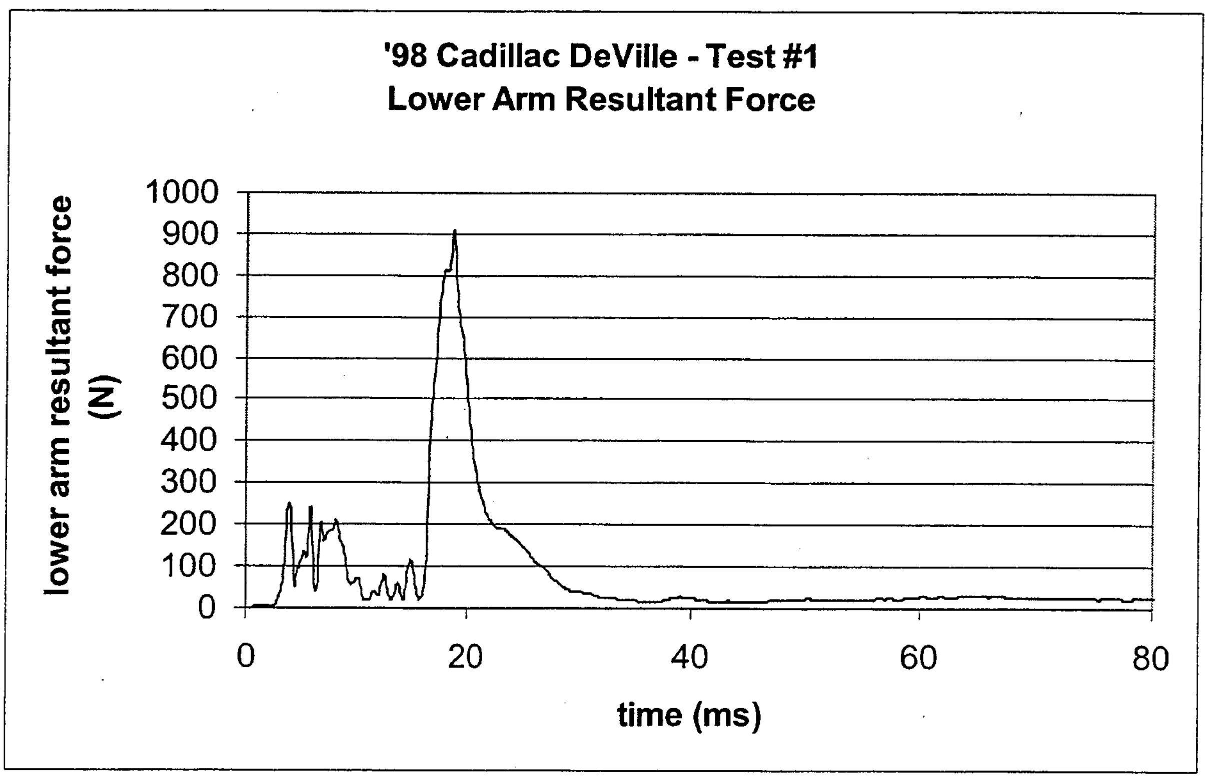

Fig. E.4. '98 Cadillac - Test 1. Lower Arm Resultant Force.

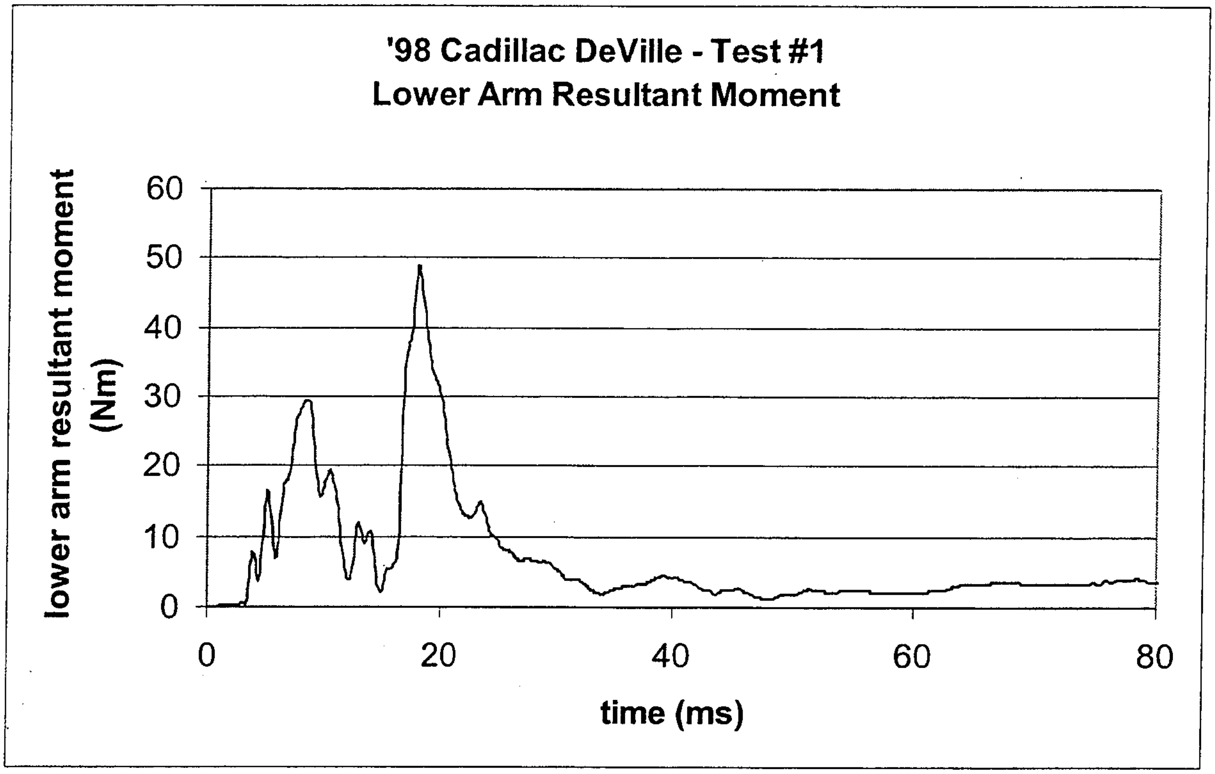

Fig. E.5. '98 Cadillac - Test 1. Lower Arm Resultant Moment

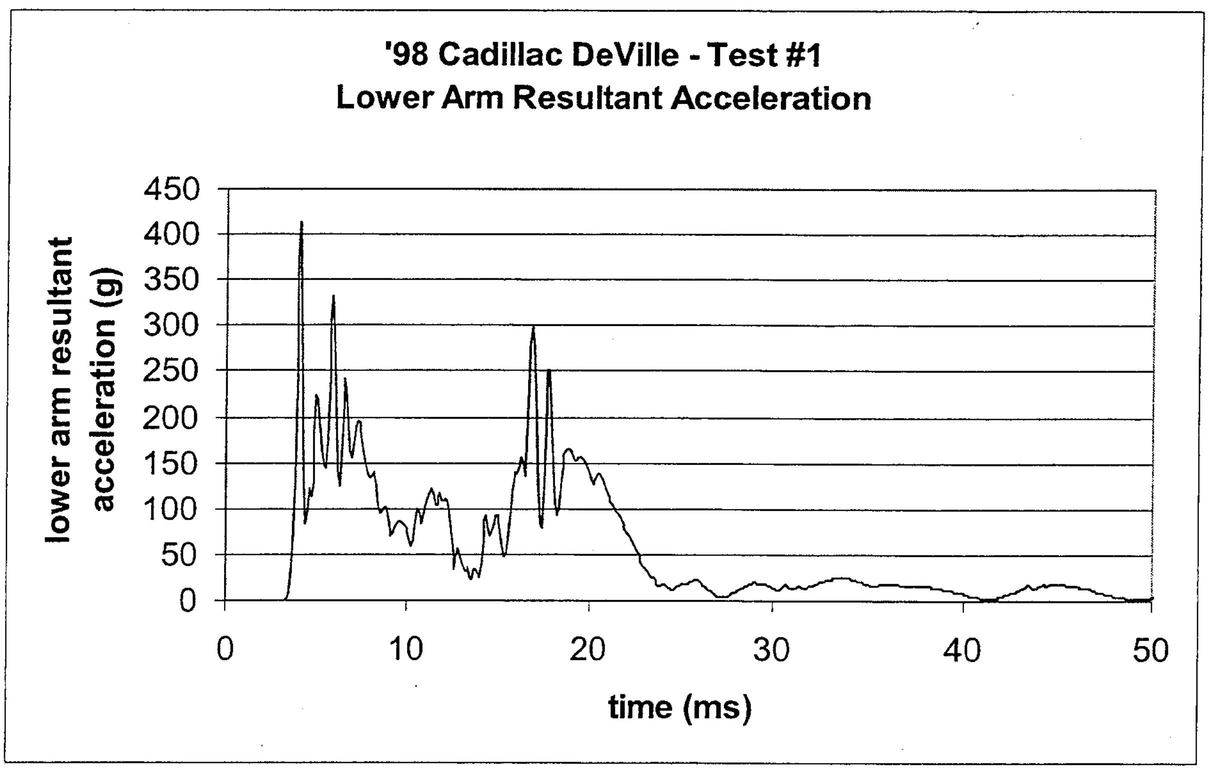

Fig. E.6. '98 Cadillac - Test 1. Lower Arm Resultant Acceleration.

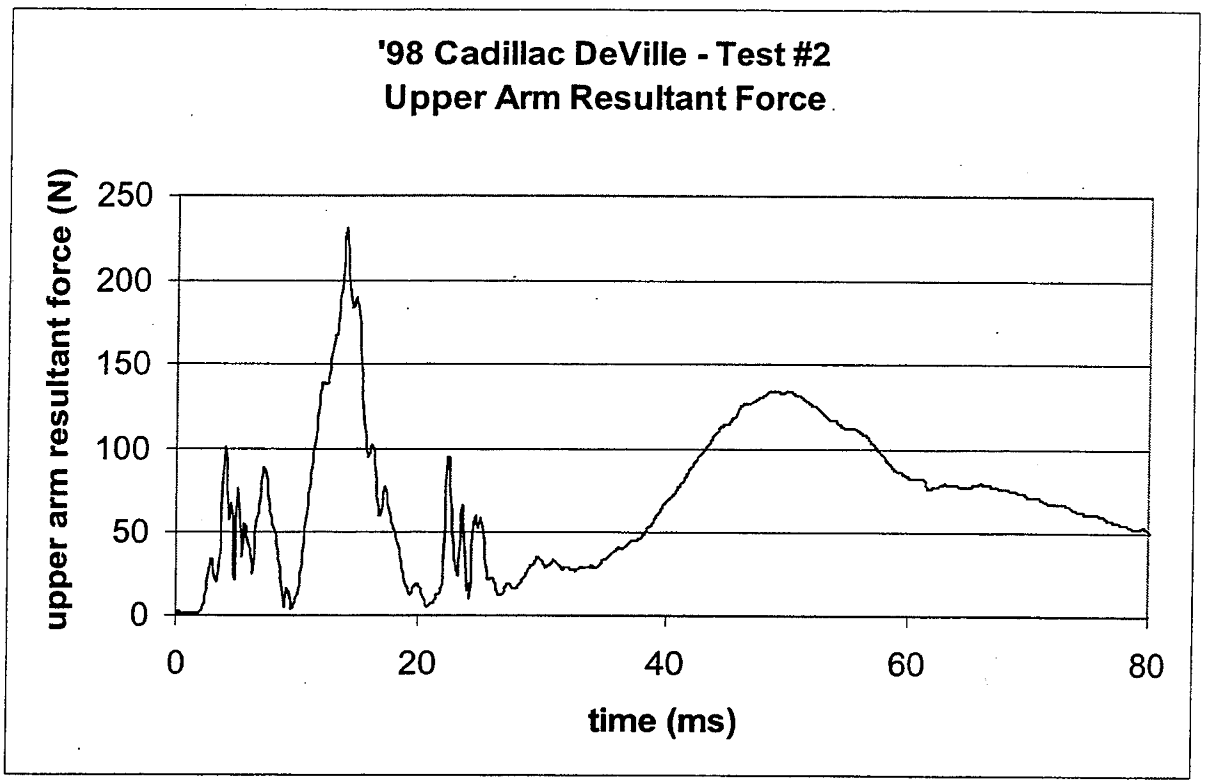

Fig. E.7. '98 Cadillac - Test 2. Upper Arm Resultant Force.

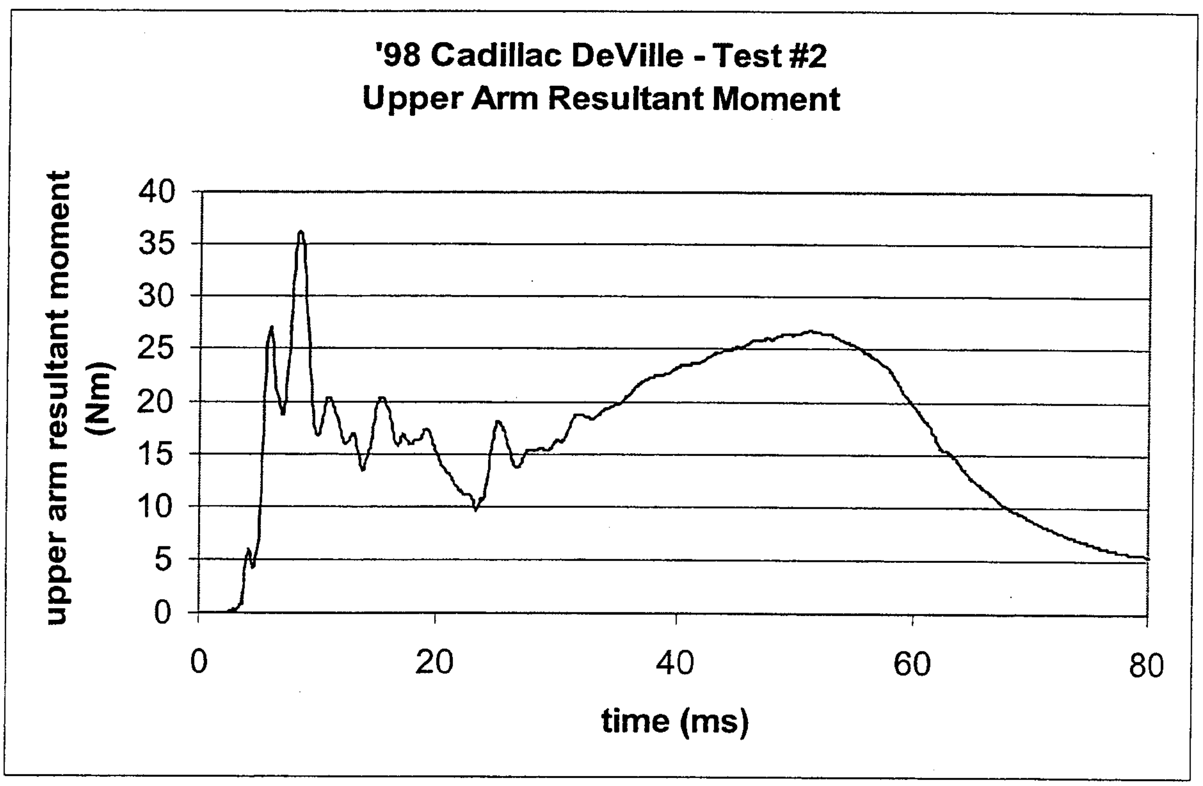

Fig. E.8. '98 Cadillac - Test 2. Upper Arm Resultant Moment.

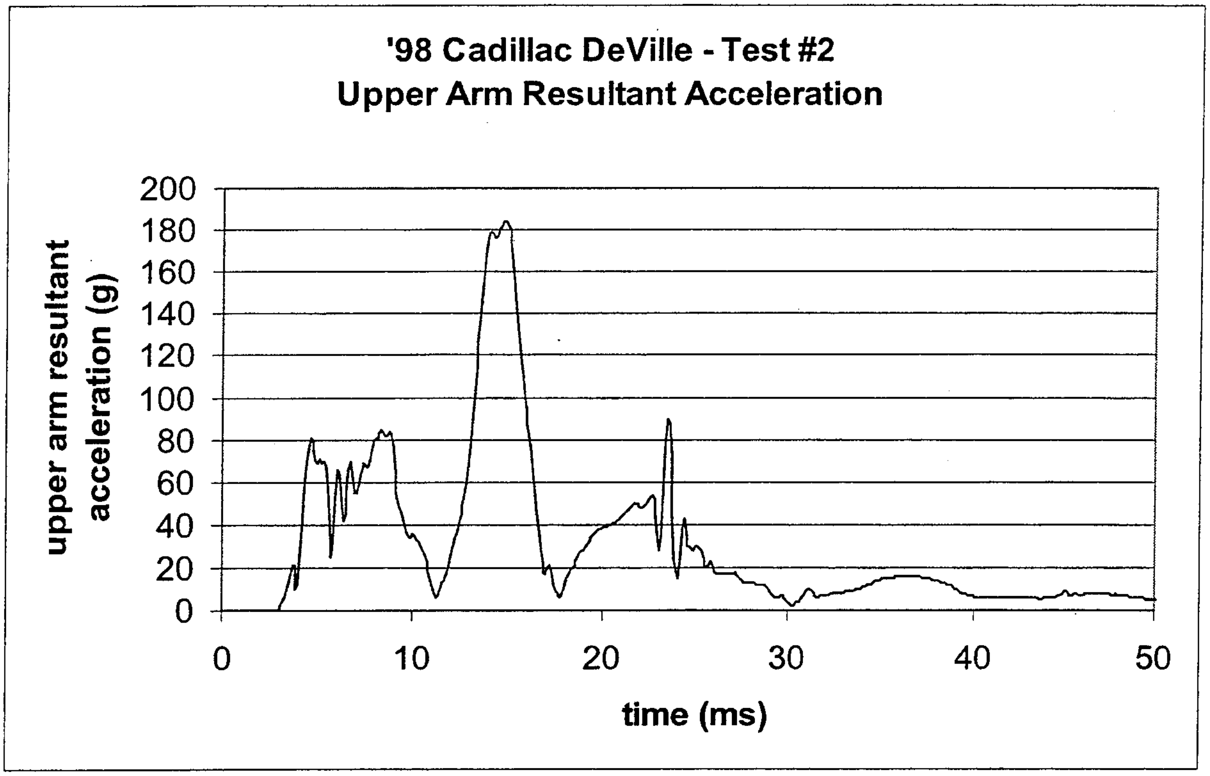

Fig. E.9. '98 Cadillac - Test 2. Upper Arm Resultant Acceleration.

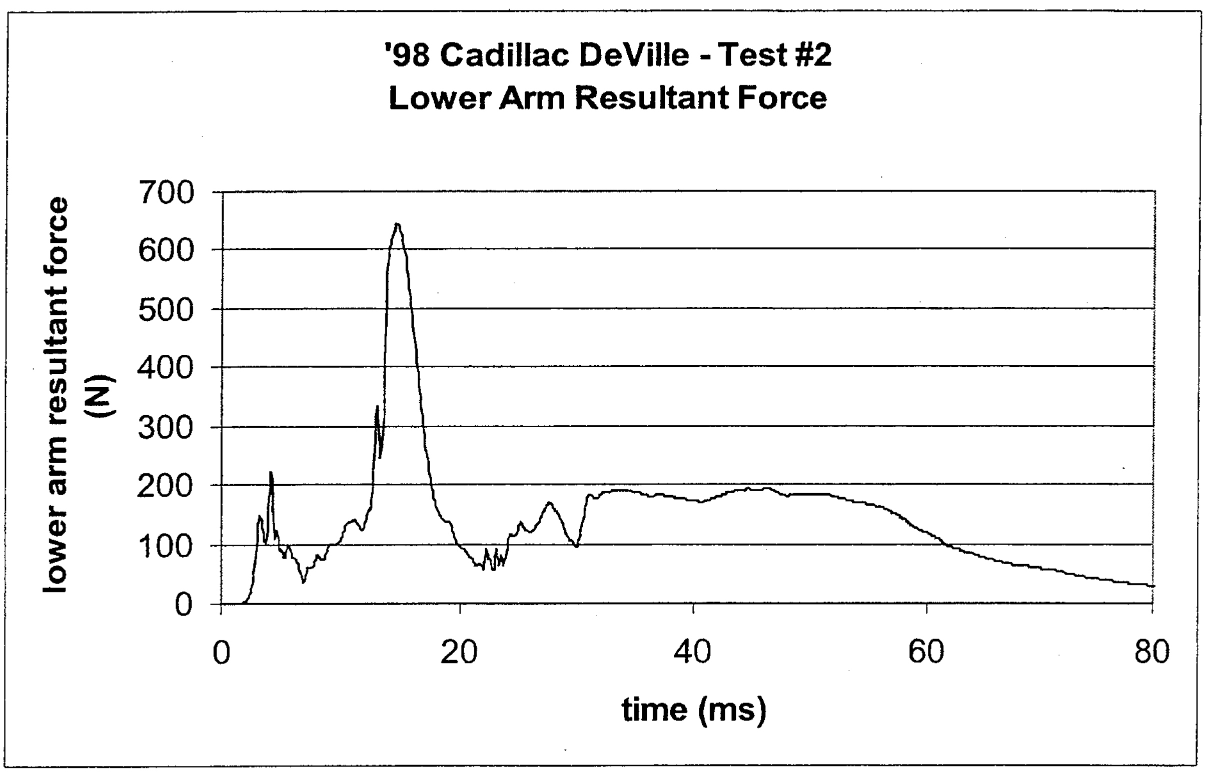

Fig. E.10. '98 Cadillac - Test 2. Lower Arm Resultant Force.

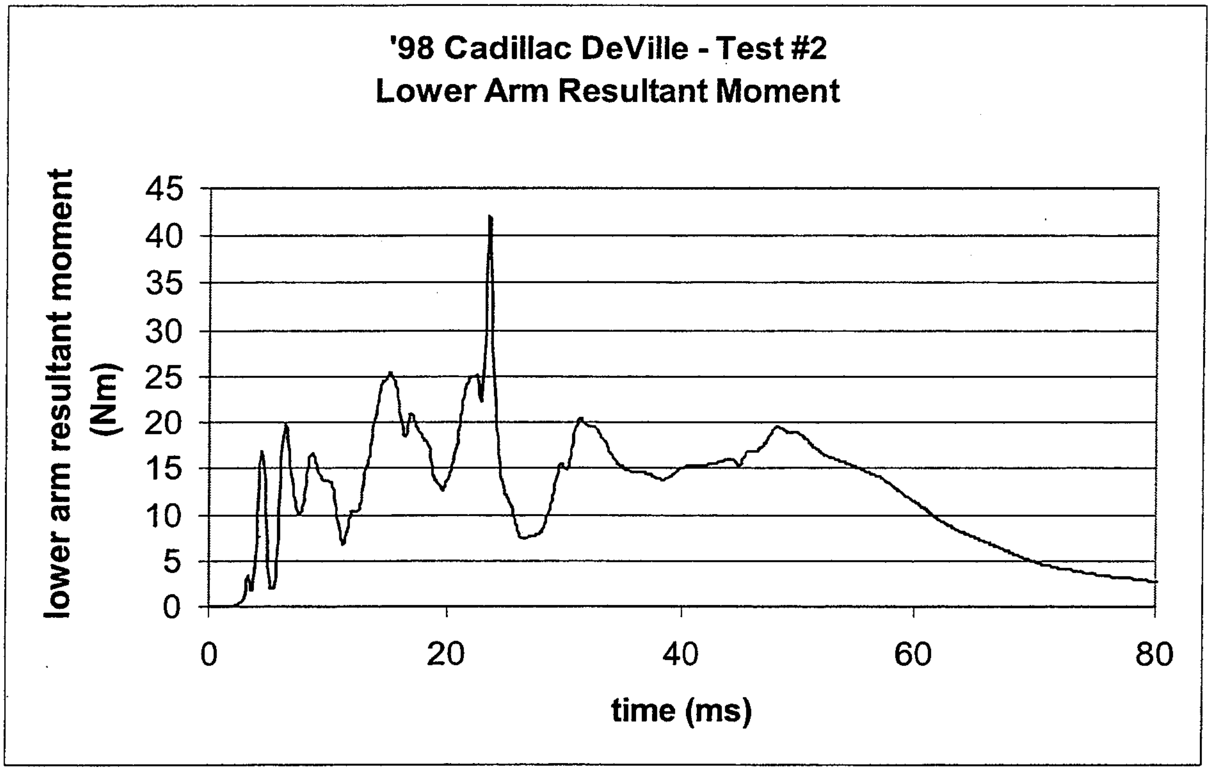

Fig. E.11. '98 Cadillac - Test 2. Lower Arm Resultant Moment.

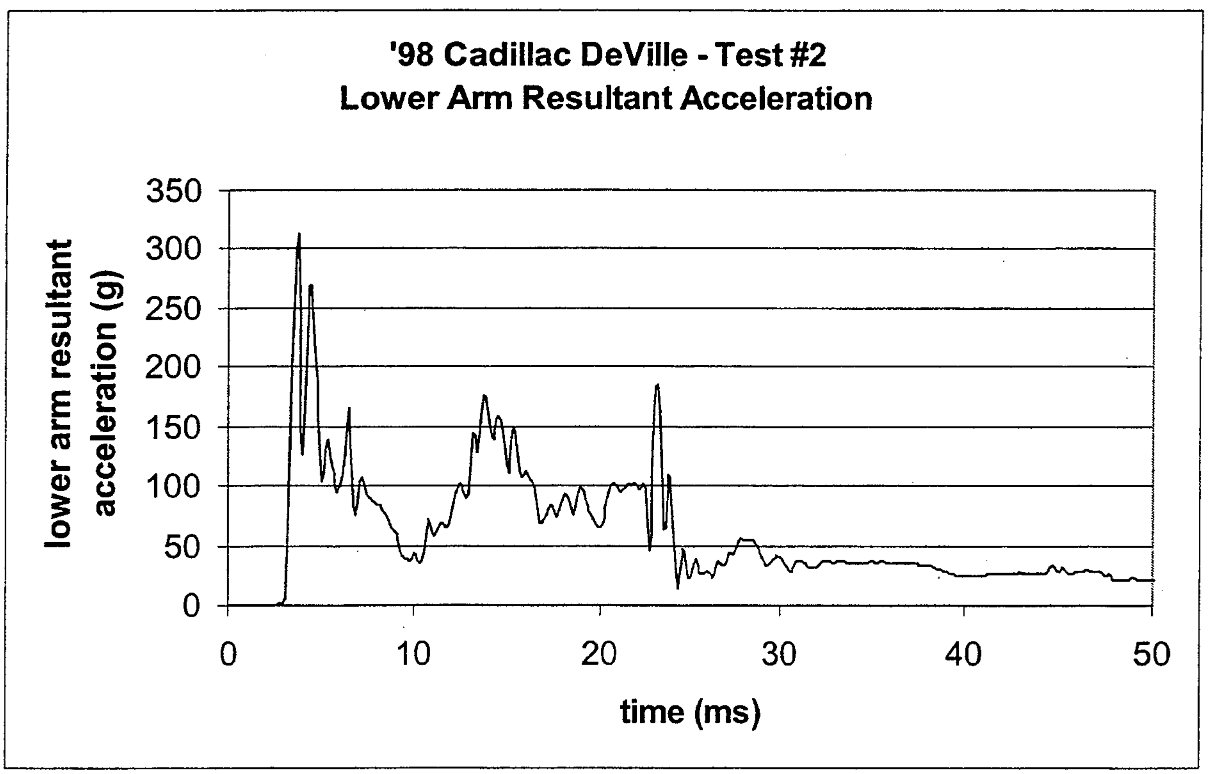

Fig. E.12. '98 Cadillac - Test 2. Lower Arm Resultant Acceleration.

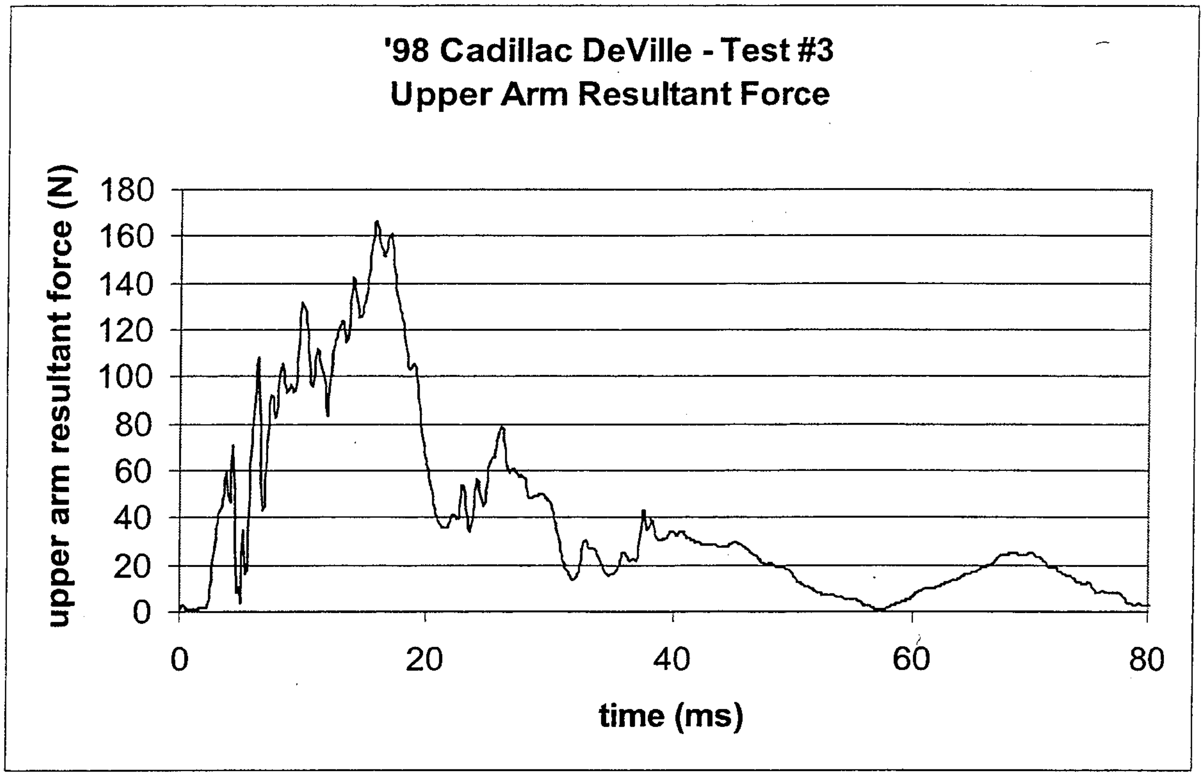

Fig. E.13. '98 Cadillac - Test 3. Upper Arm Resultant Force.

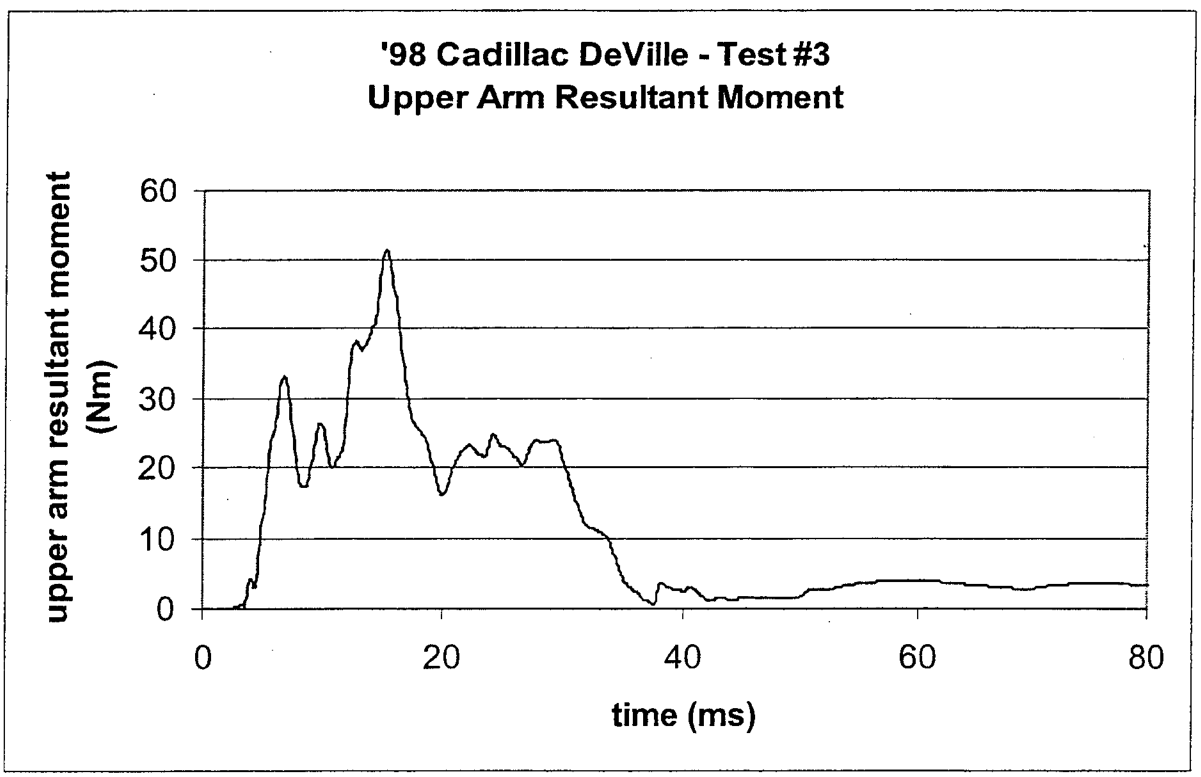

Fig. E.14. '98 Cadillac - Test 3. Upper Arm Resultant Moment.

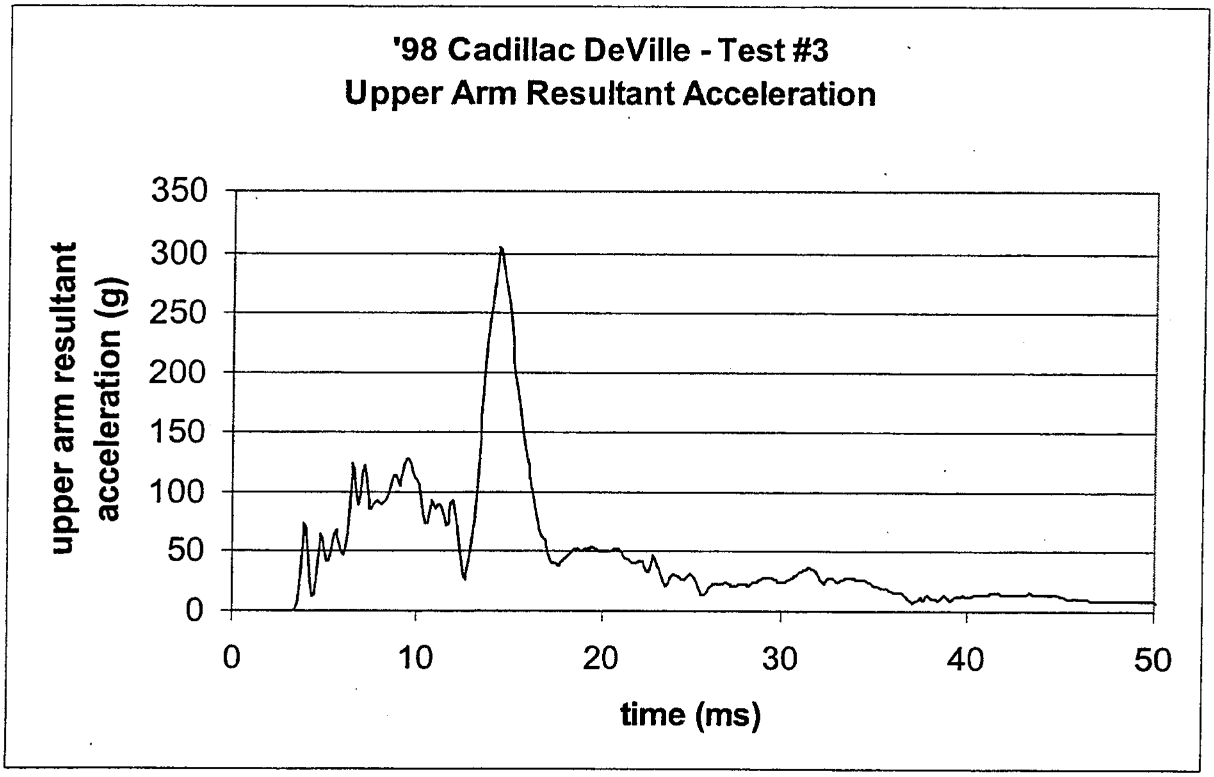

Fig. E.15. '98 Cadillac - Test 3. Upper Arm Resultant Acceleration.

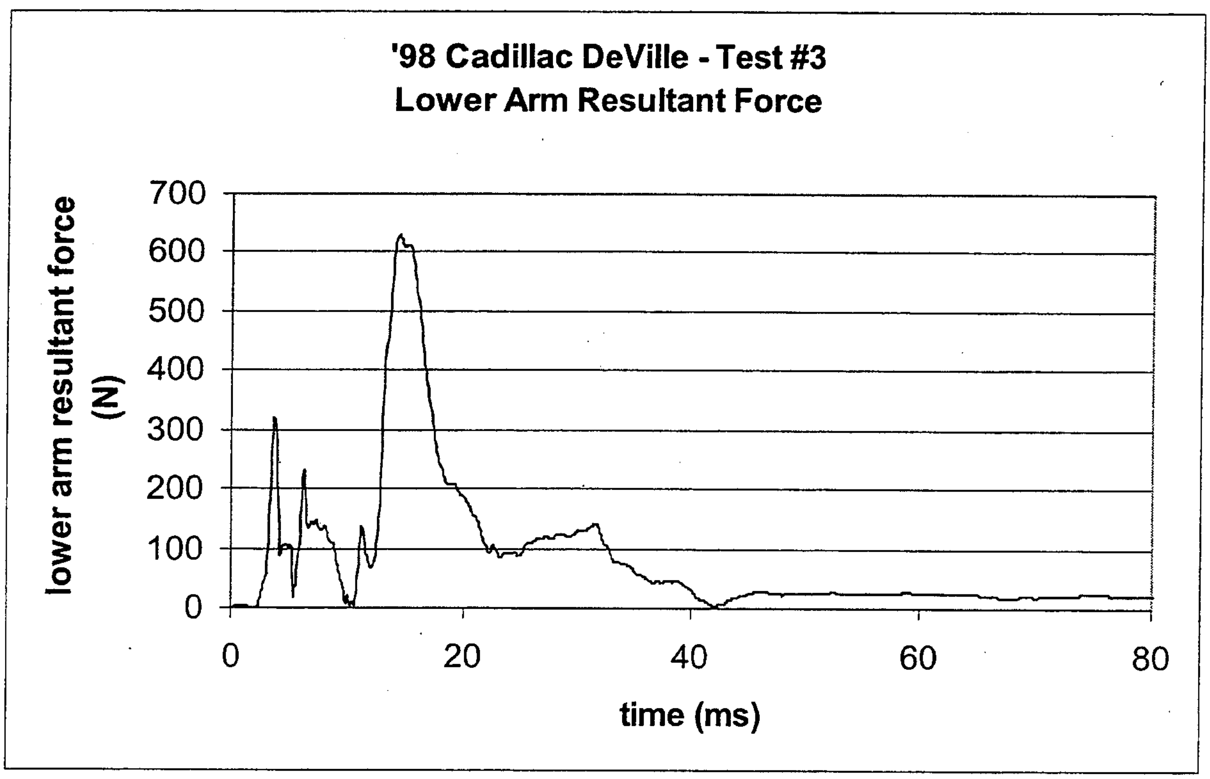

Fig. E.16. '98 Cadillac - Test 3. Lower Arm Resultant Force.

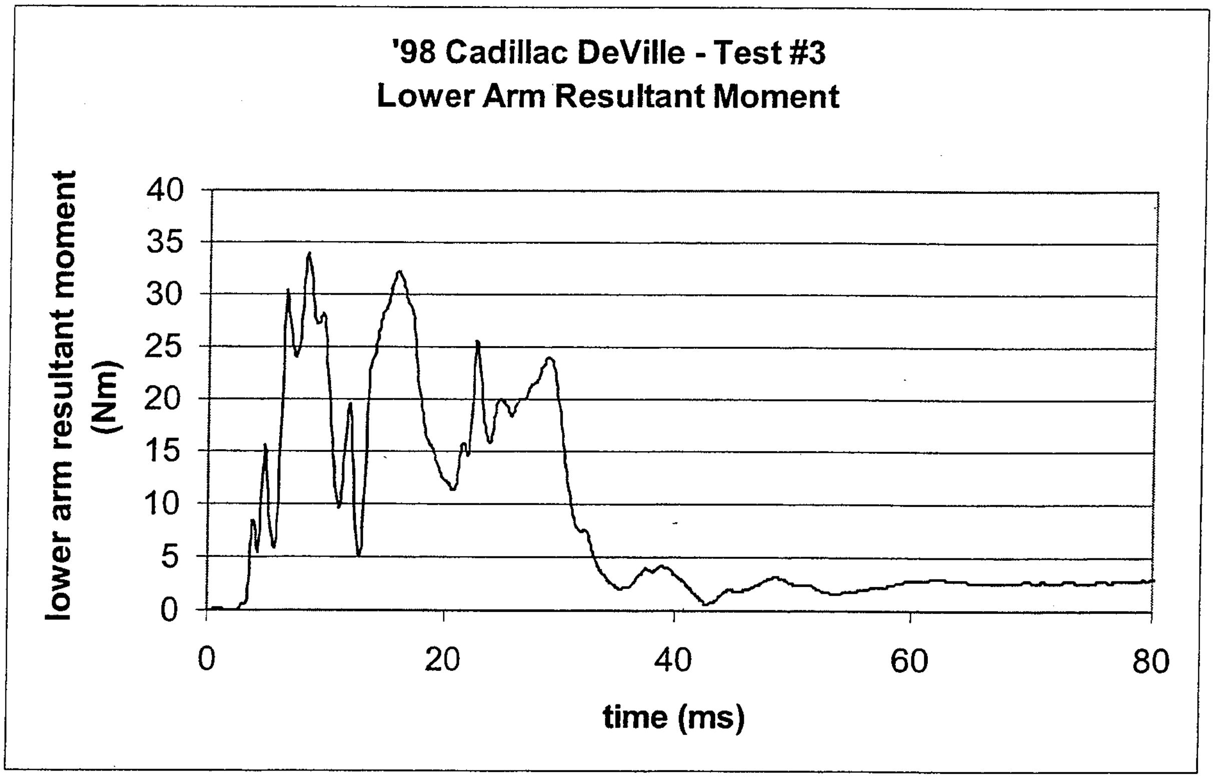

Fig. E.17. '98 Cadillac - Test 3. Lower Arm Resultant Moment.

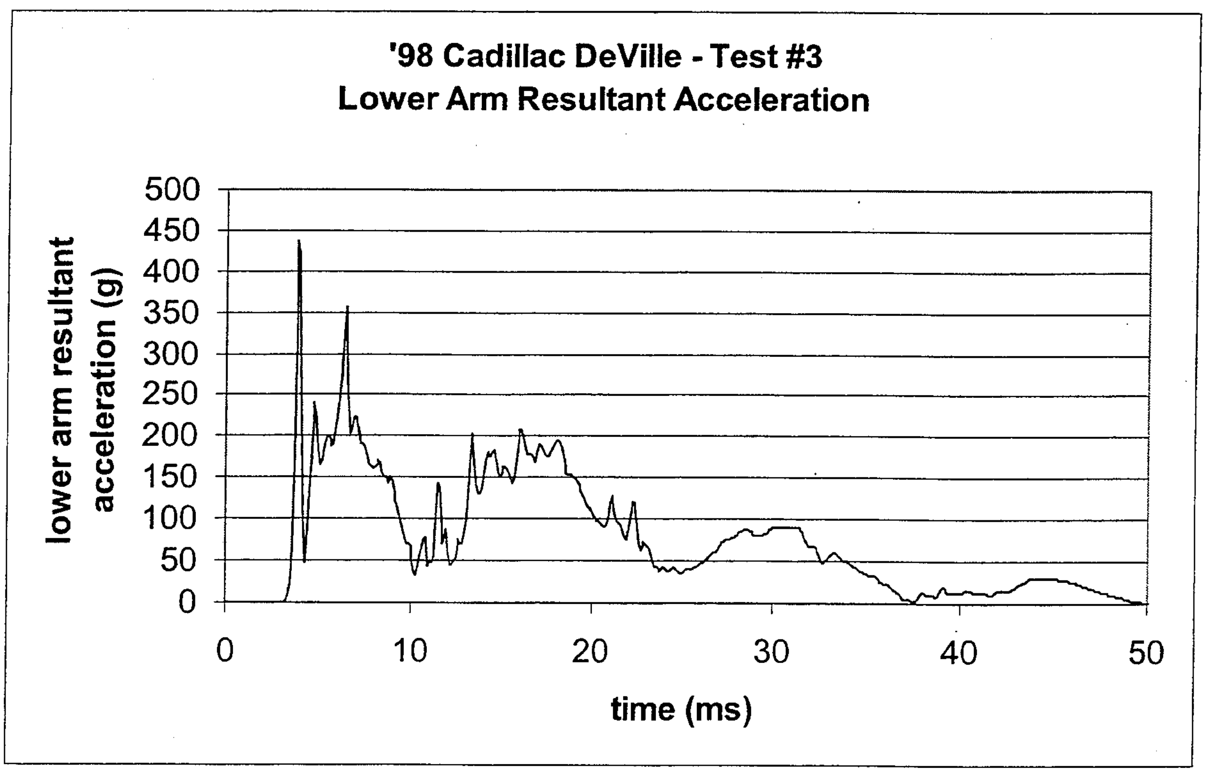

Fig. E.18. '98 Cadillac - Test 3. Lower Arm Resultant Acceleration.

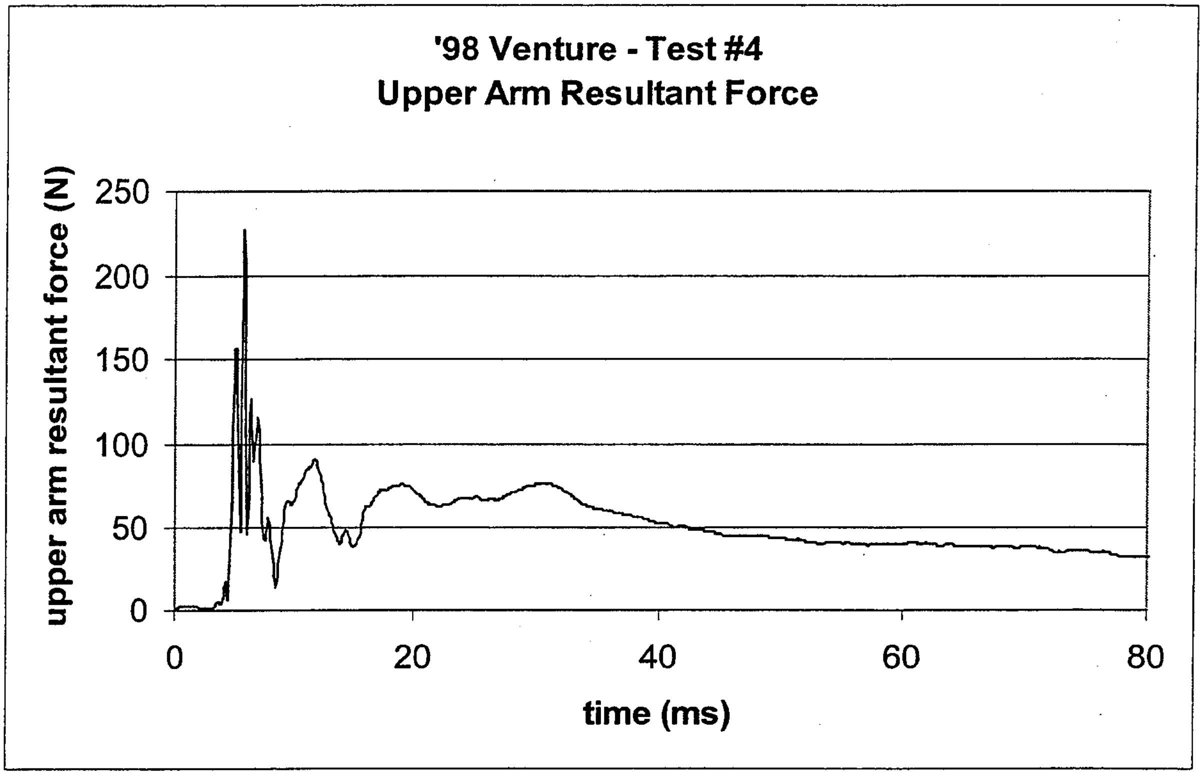

Fig. E.19. '98 Venture - Test 4. Upper Arm Resultant Force.

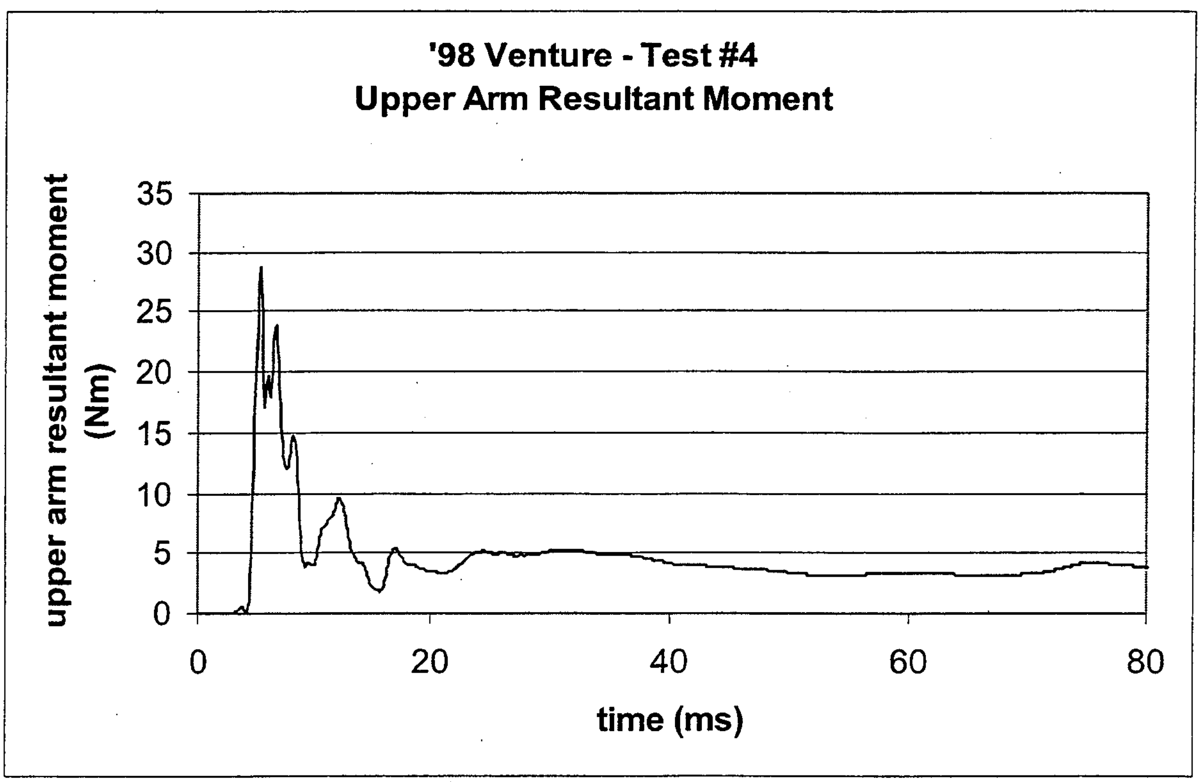

Fig. E.20. '98 Venture - Test 4. Upper Arm Resultant Moment.

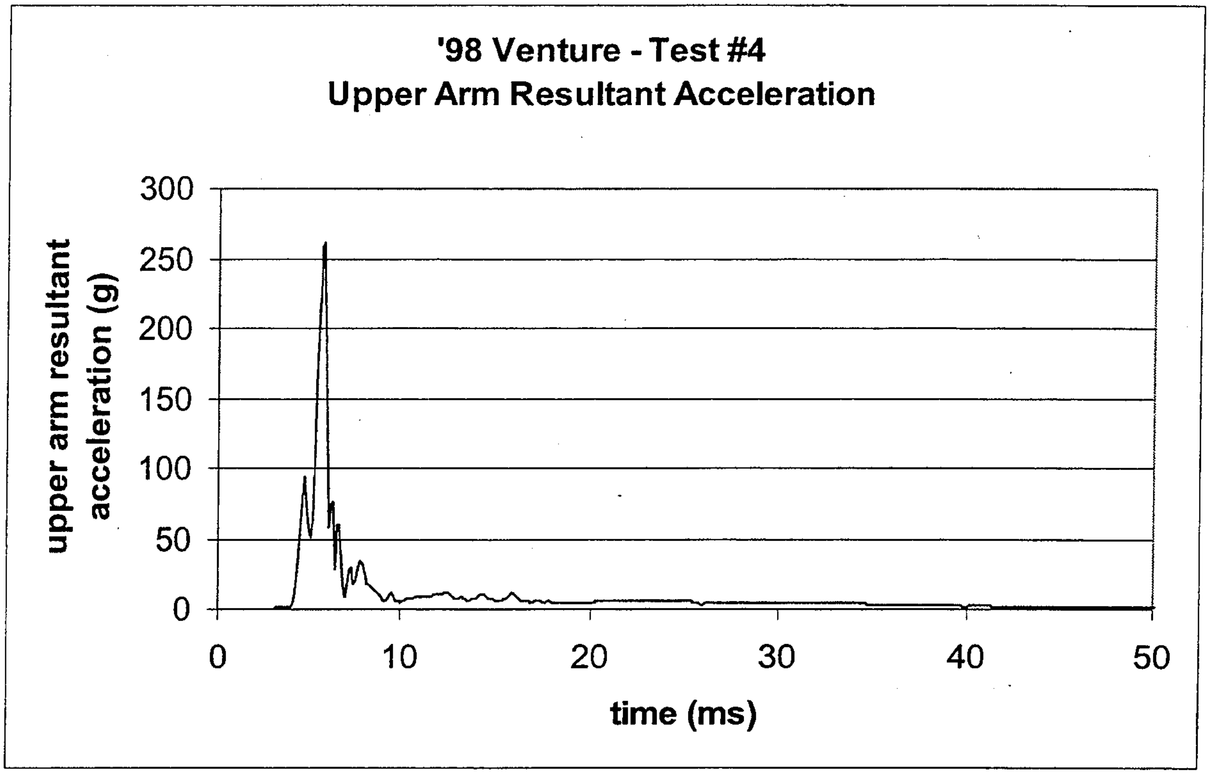

Fig. E.21. '98 Venture - Test 4. Upper Arm Resultant Acceleration.

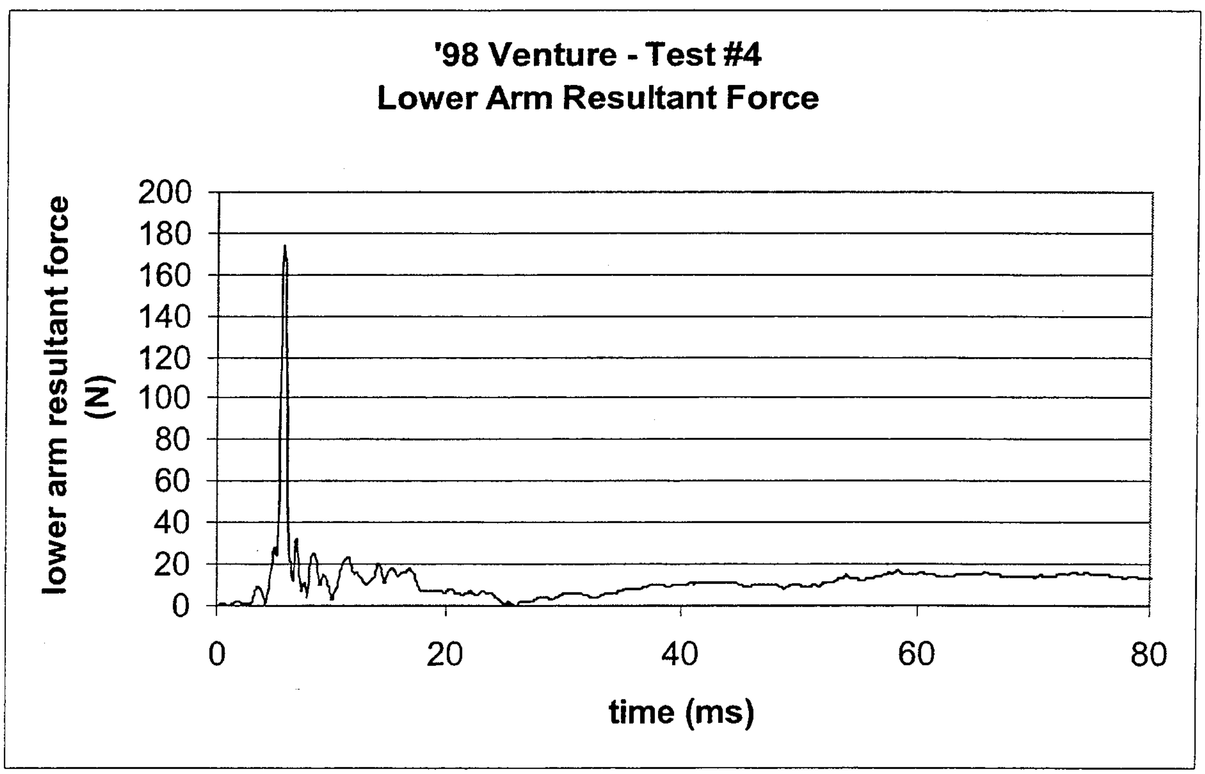

Fig. E.22. '98 Venture - Test 4. Lower Arm Resultant Force.

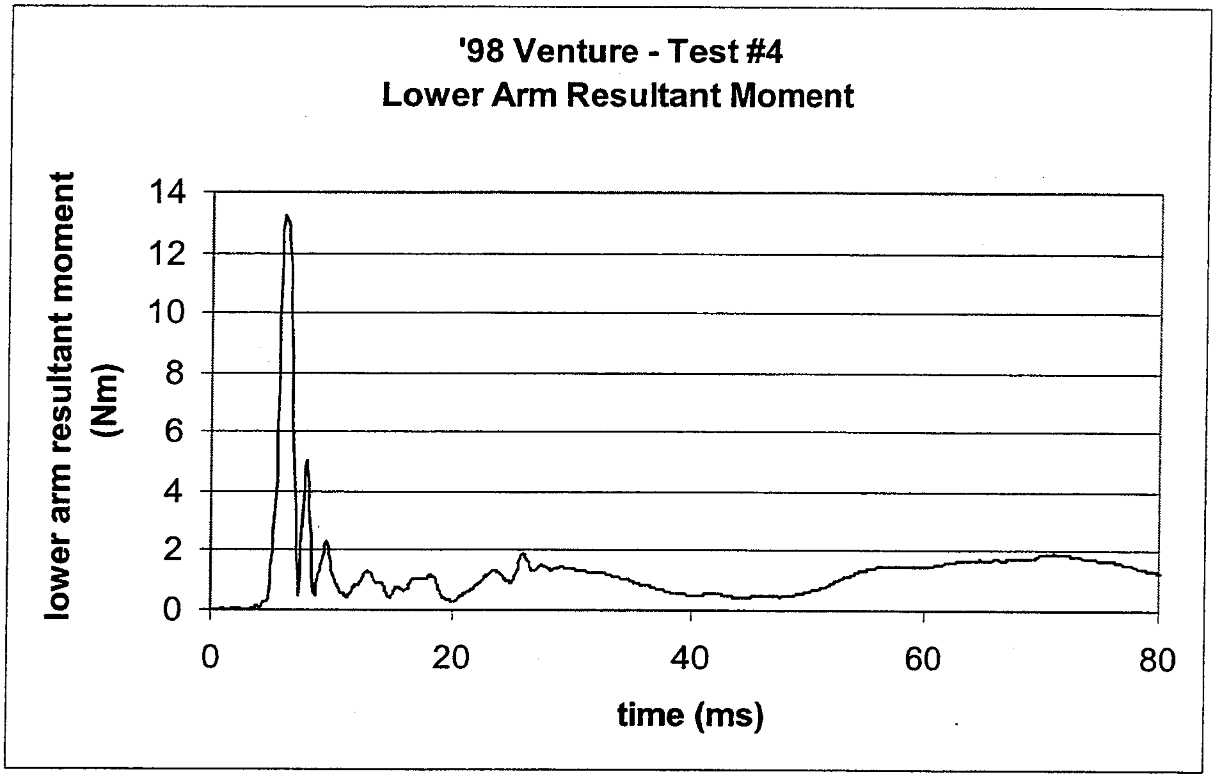

Fig. E.23. '98 Venture - Test 4. Lower Arm Resultant Moment.

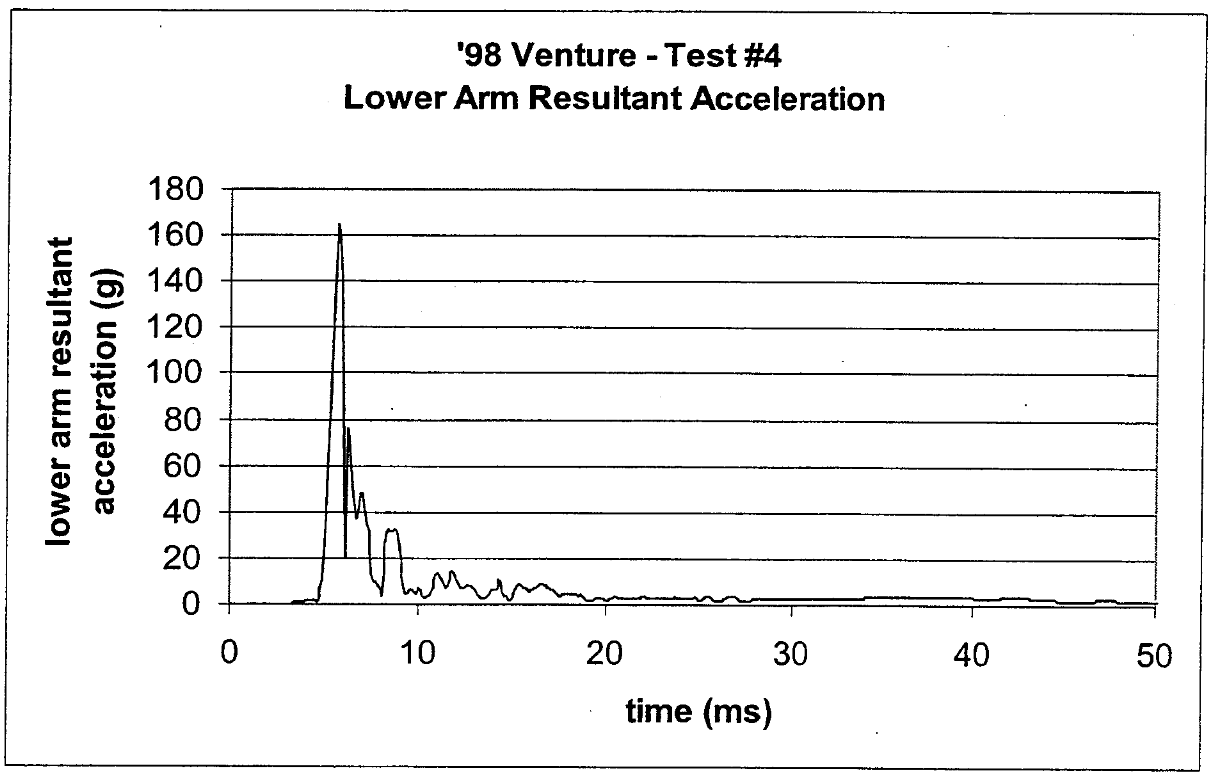

Fig. E.24. '98 Venture - Test 4. Lower Arm Resultant Acceleration.

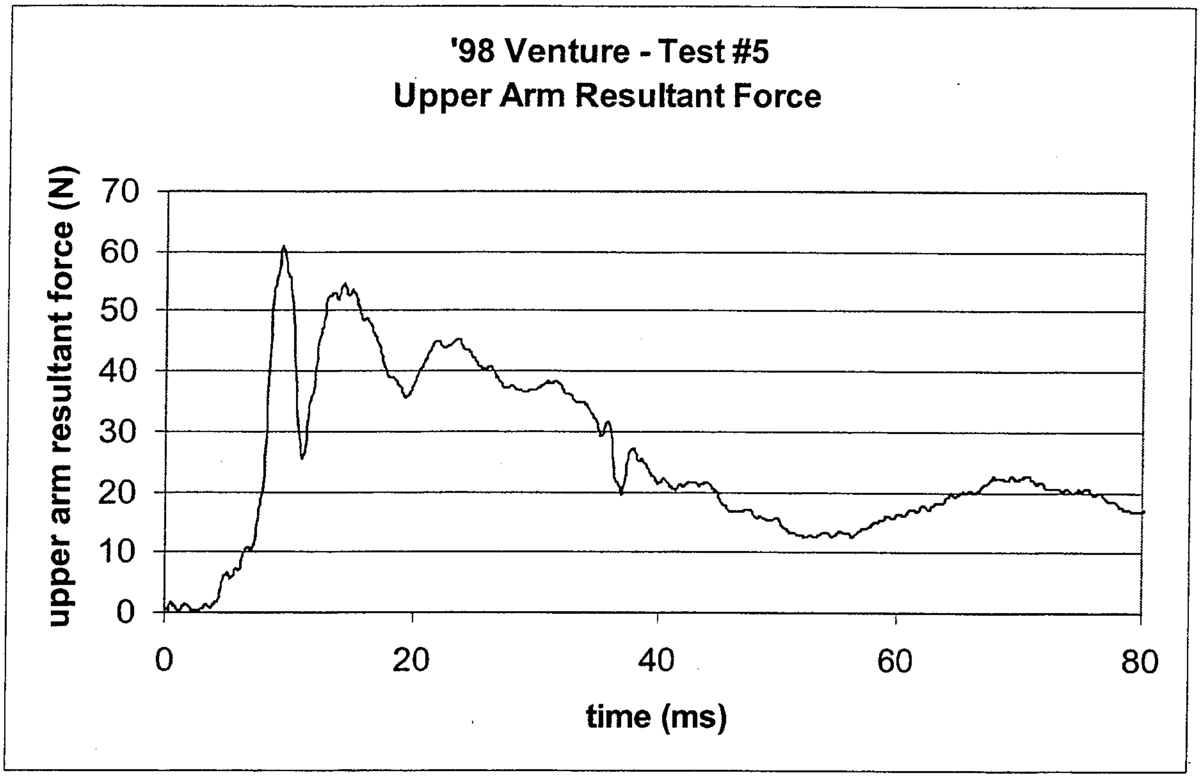

Fig. E.25. '98 Venture - Test 5. Upper Arm Resultant Force.

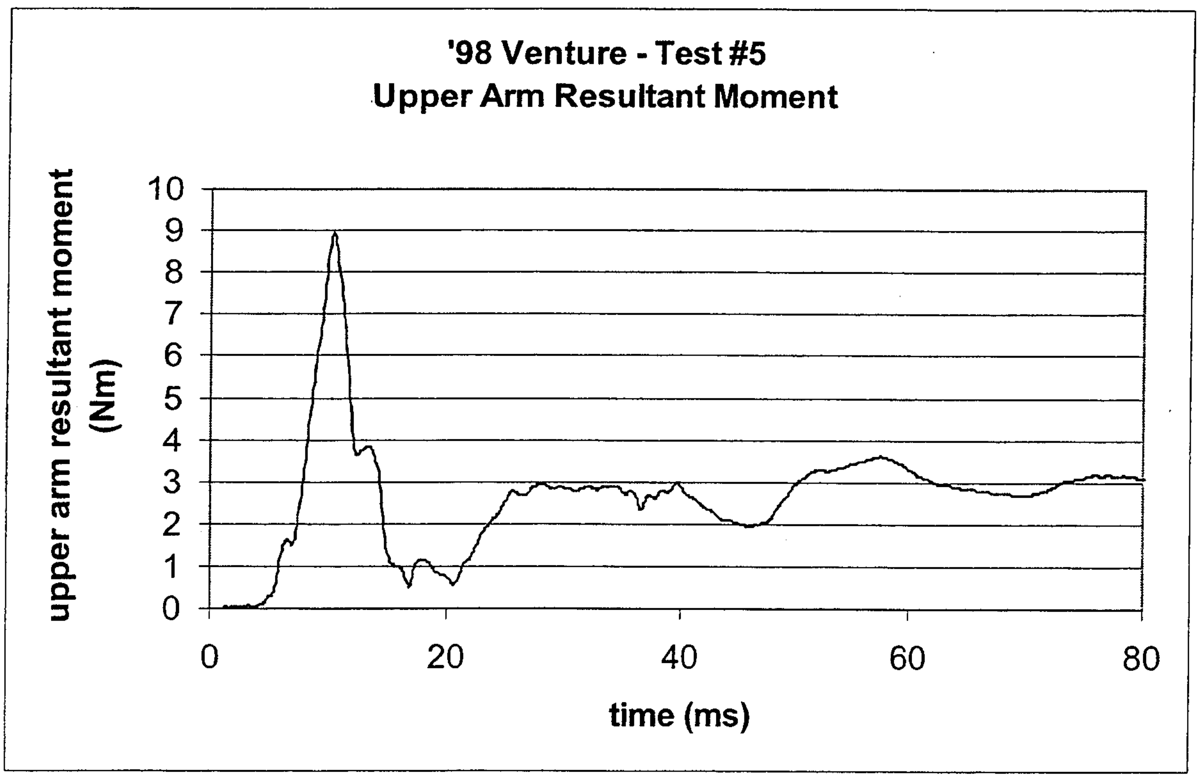

Fig. E.26. '98 Venture - Test 5. Upper Arm Resultant Moment.

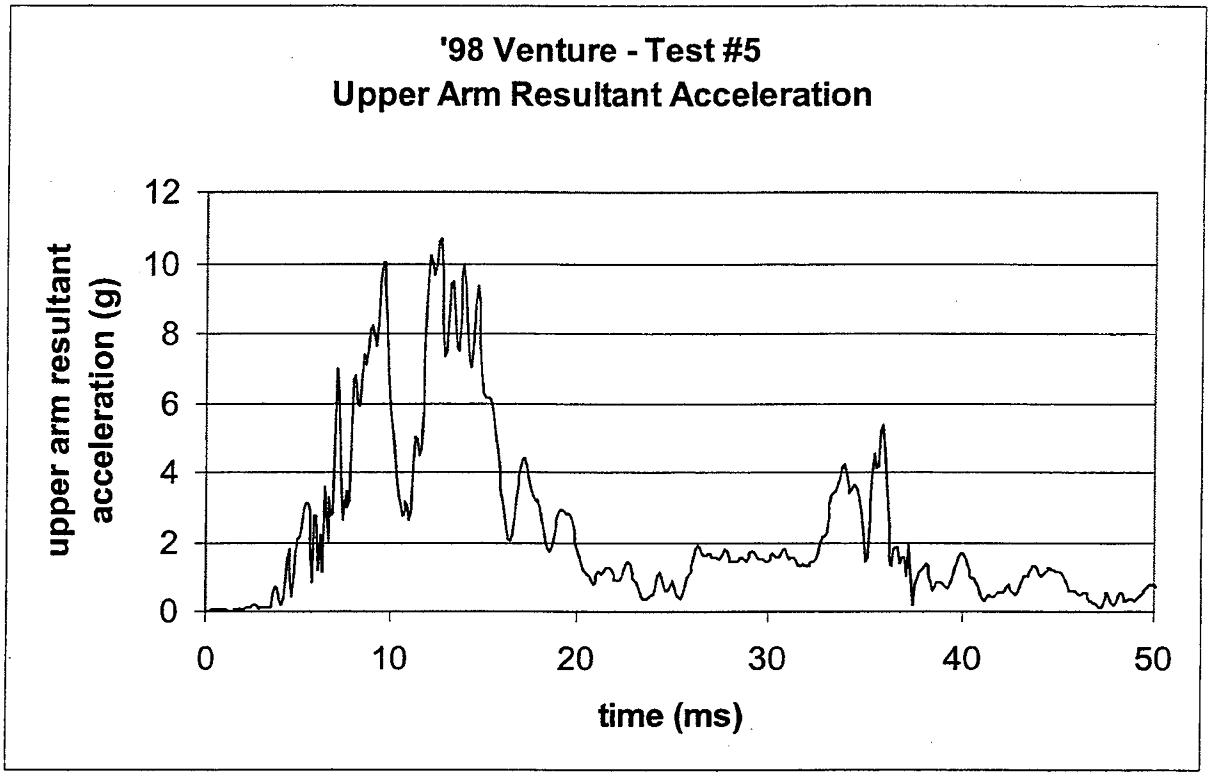

Fig. E.27. '98 Venture - Test 5. Upper Arm Resultant Acceleration.

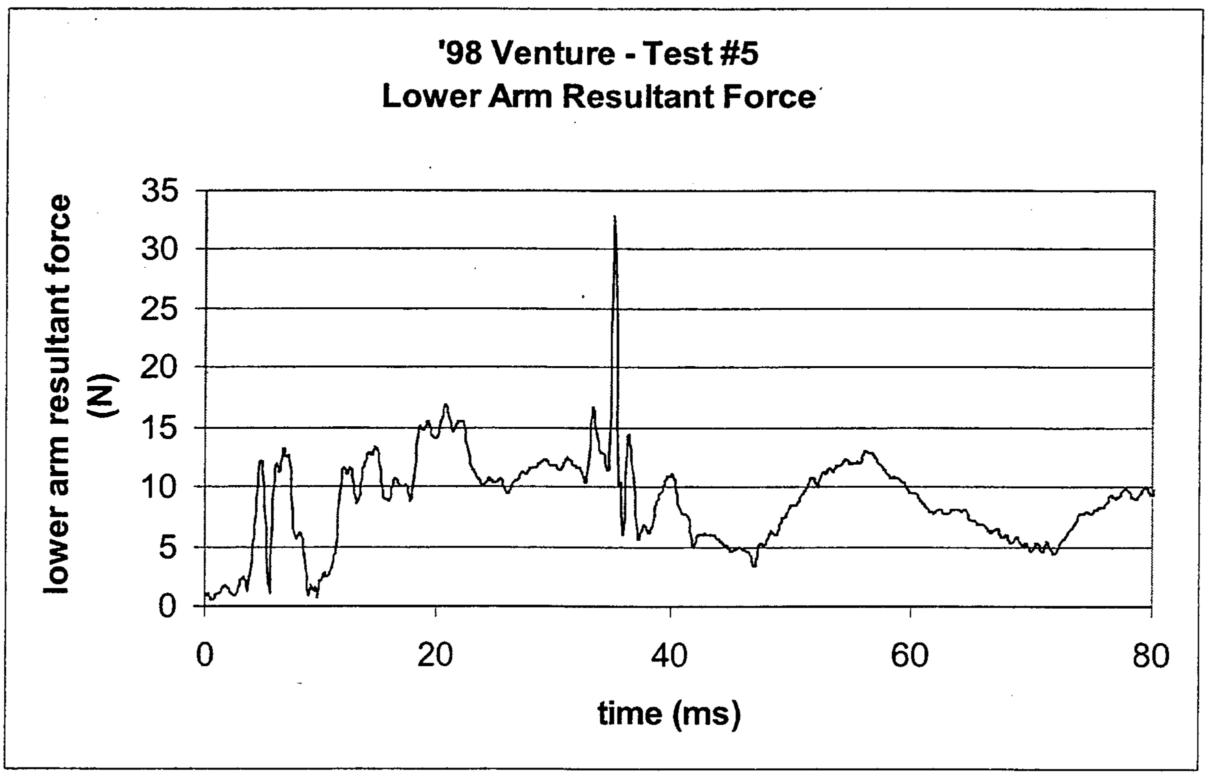

Fig. E.28. '98 Venture - Test 5. Lower Arm Resultant Force.

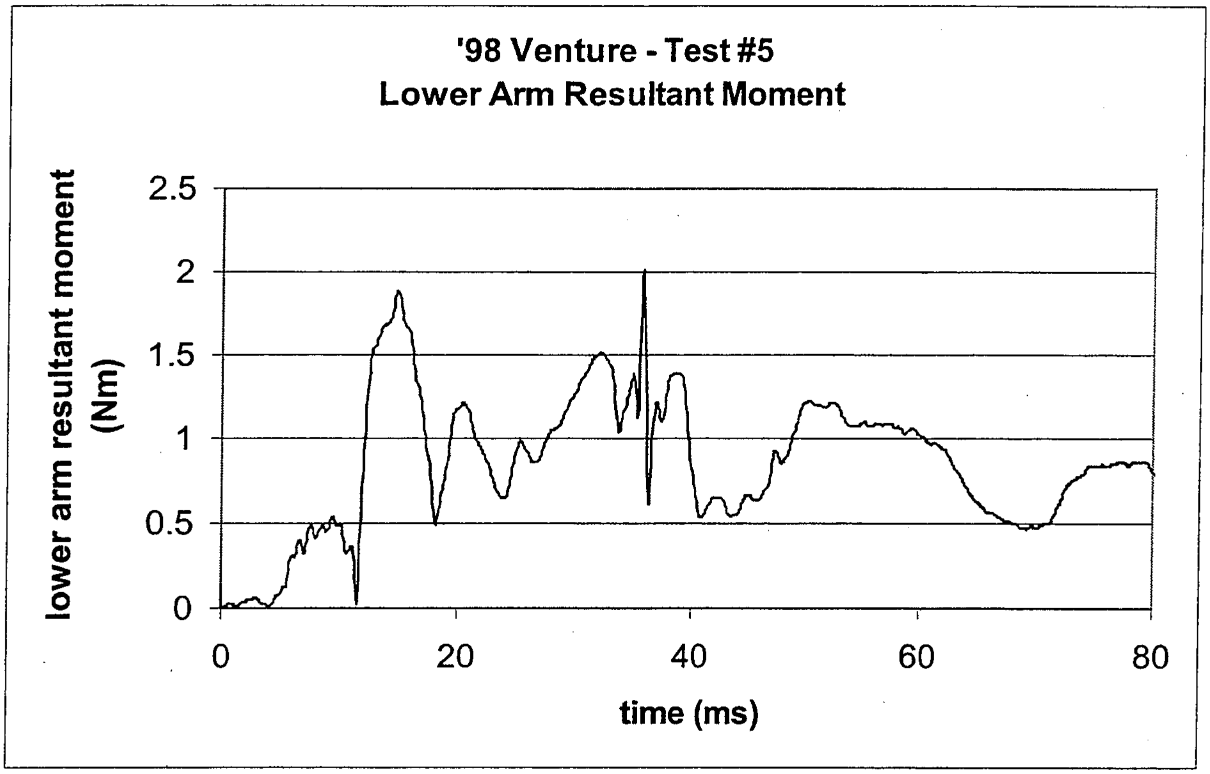

Fig. E.29. '98 Venture - Test 5. Lower Arm Resultant Moment.

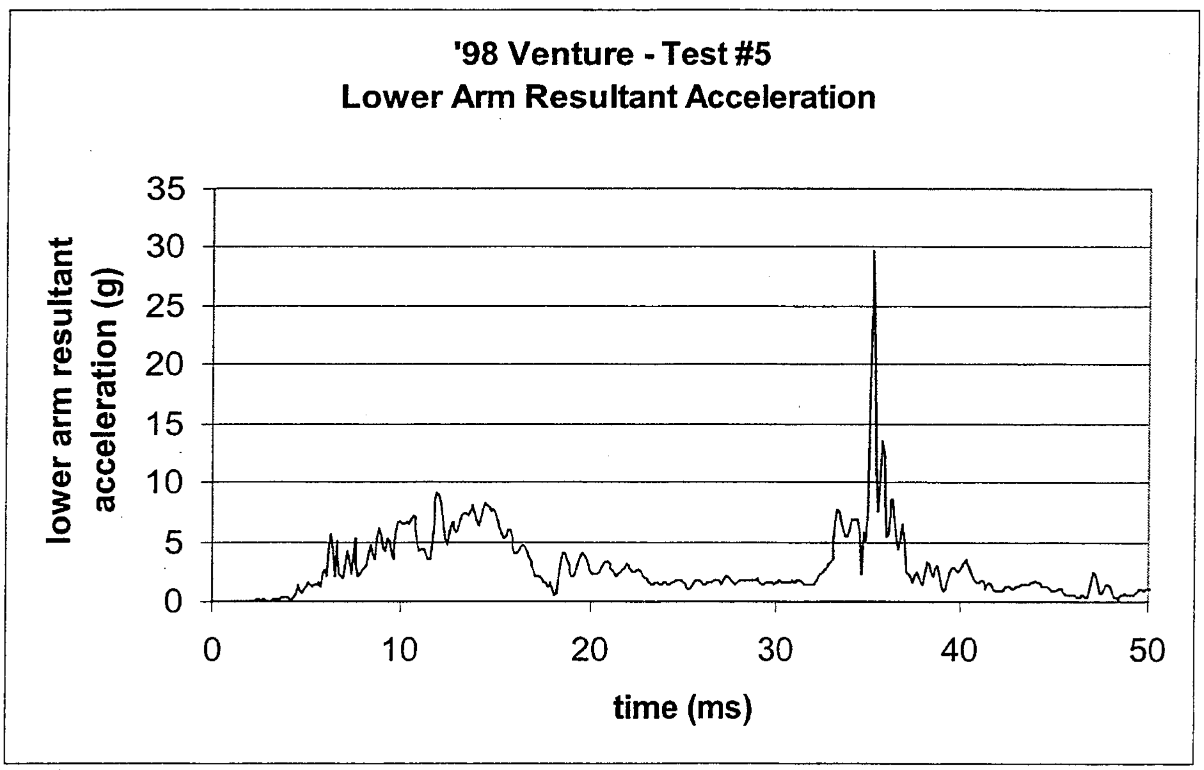

Fig. E.30. '98 Venture - Test 5. Lower Arm Resultant Acceleration.

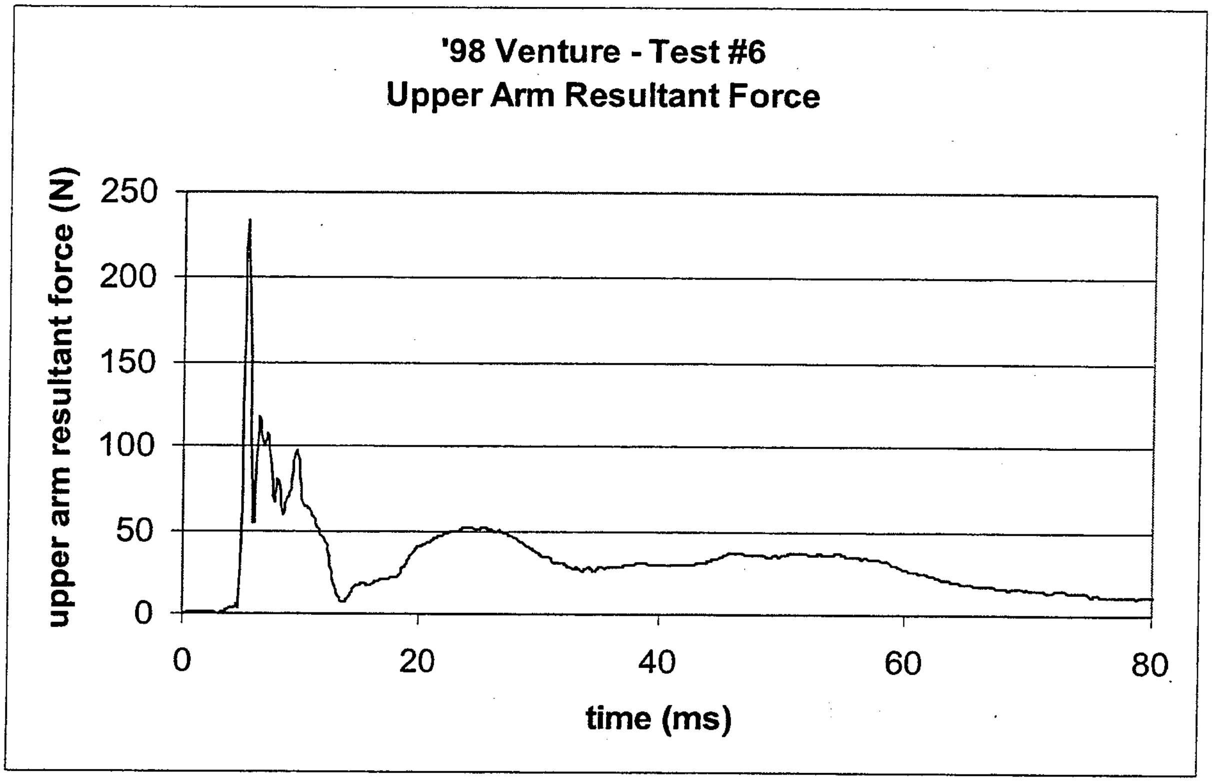

Fig. E.31. '98 Venture - Test 6. Upper Arm Resultant Force.

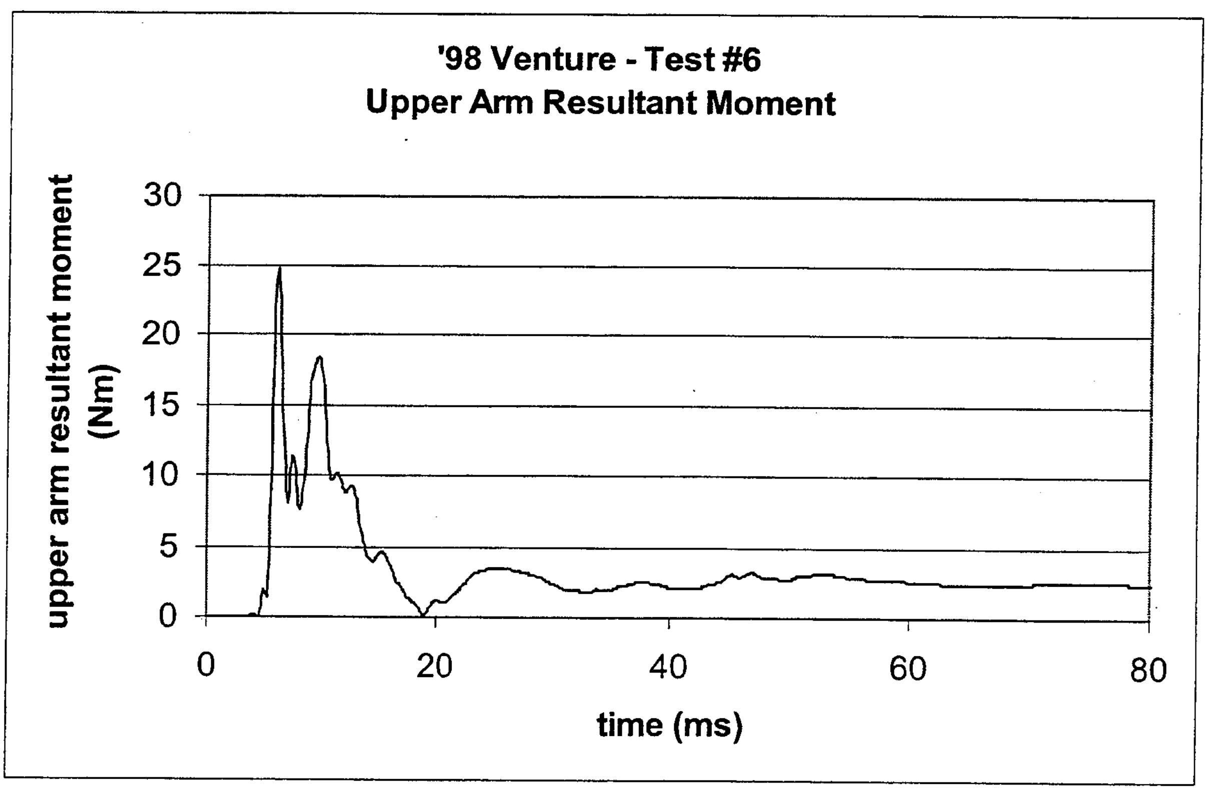

Fig. E.32. '98 Venture - Test 6. Upper Arm Resultant Moment.

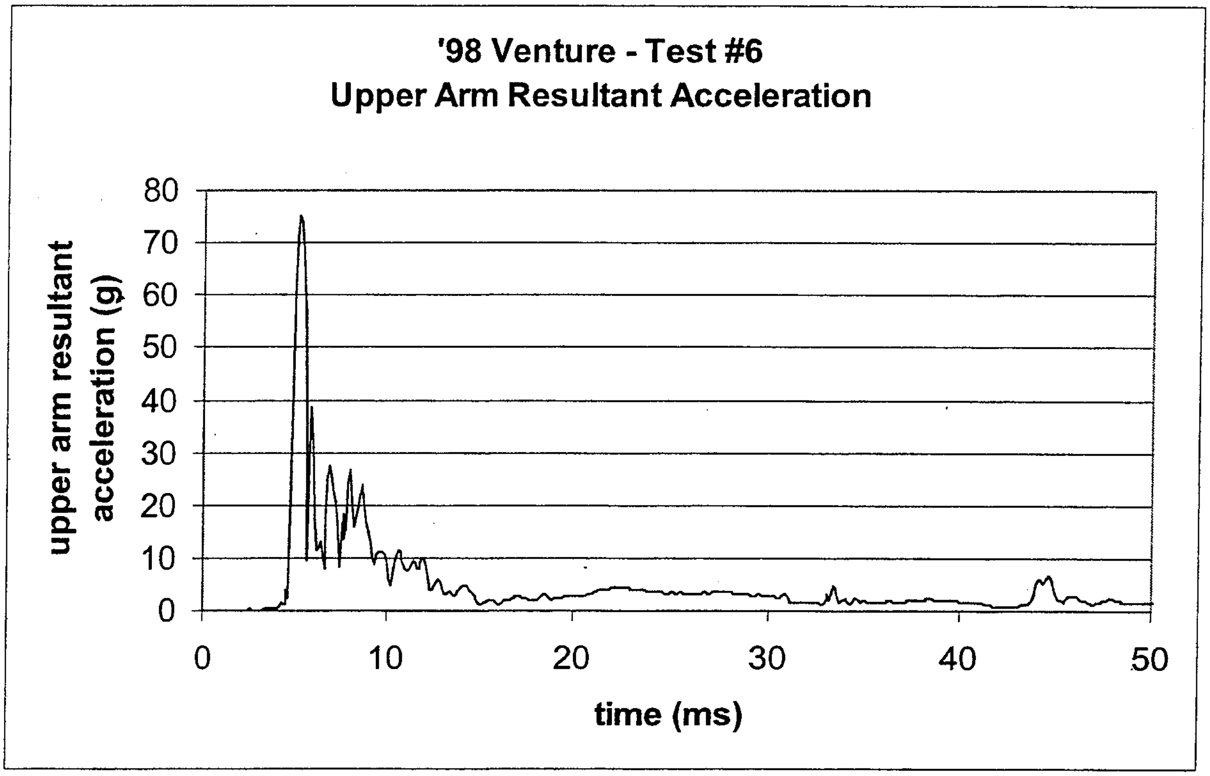

Fig. E.33. ‘98 Venture - Test 6. Upper Arm Resultant Acceleration.

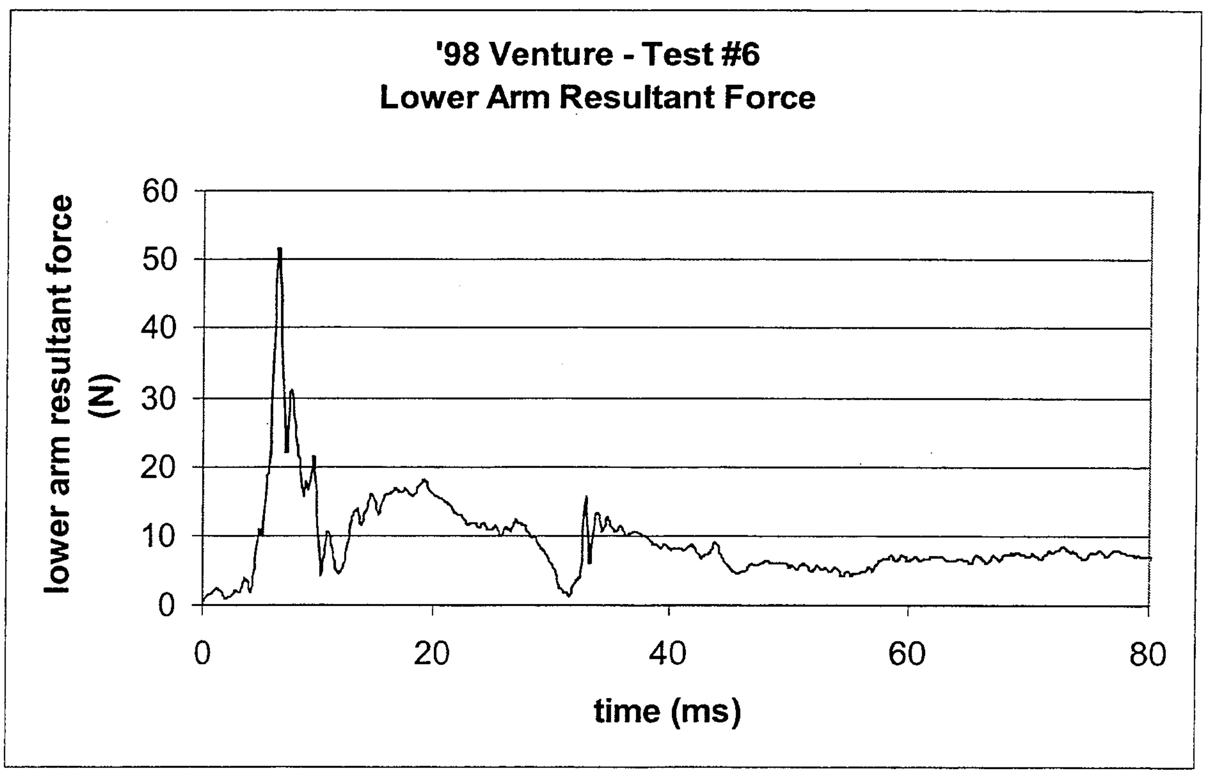

Fig. E.34. ‘98 Venture - Test 6. Lower Arm Resultant Force.

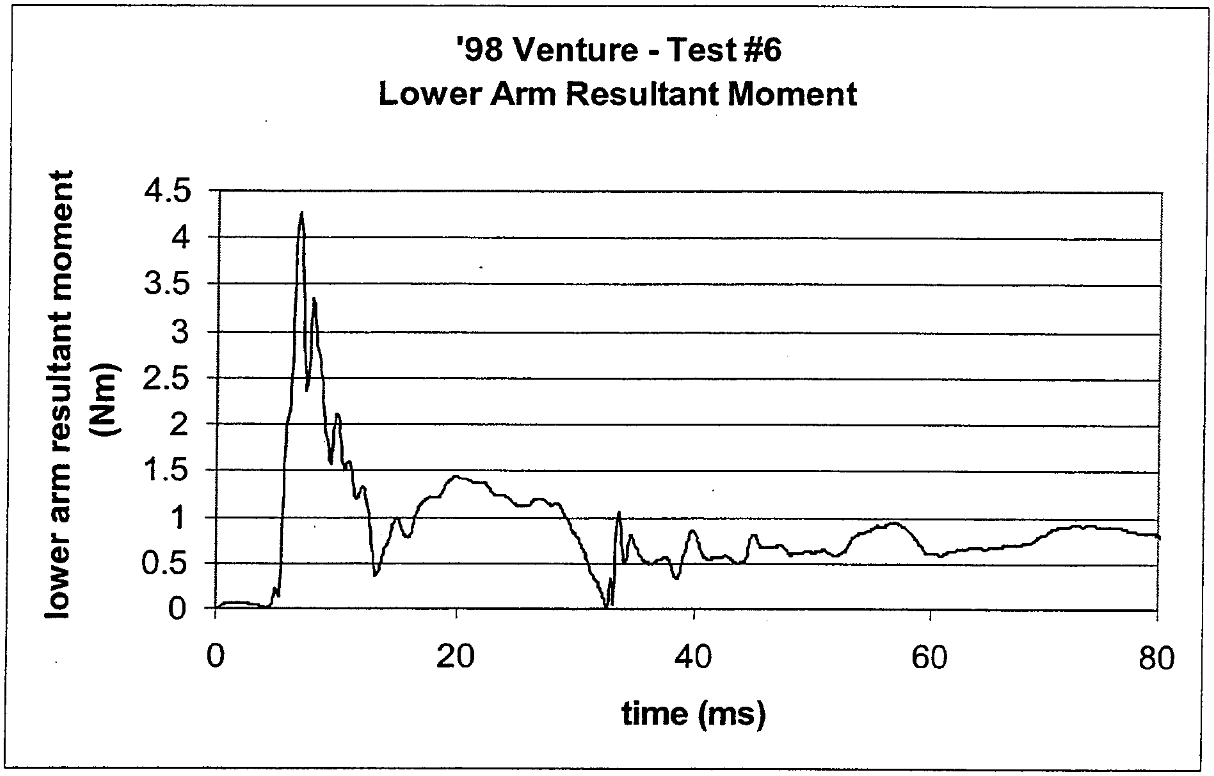

Fig. E.35. '98 Venture - Test 6. Lower Arm Resultant Moment.

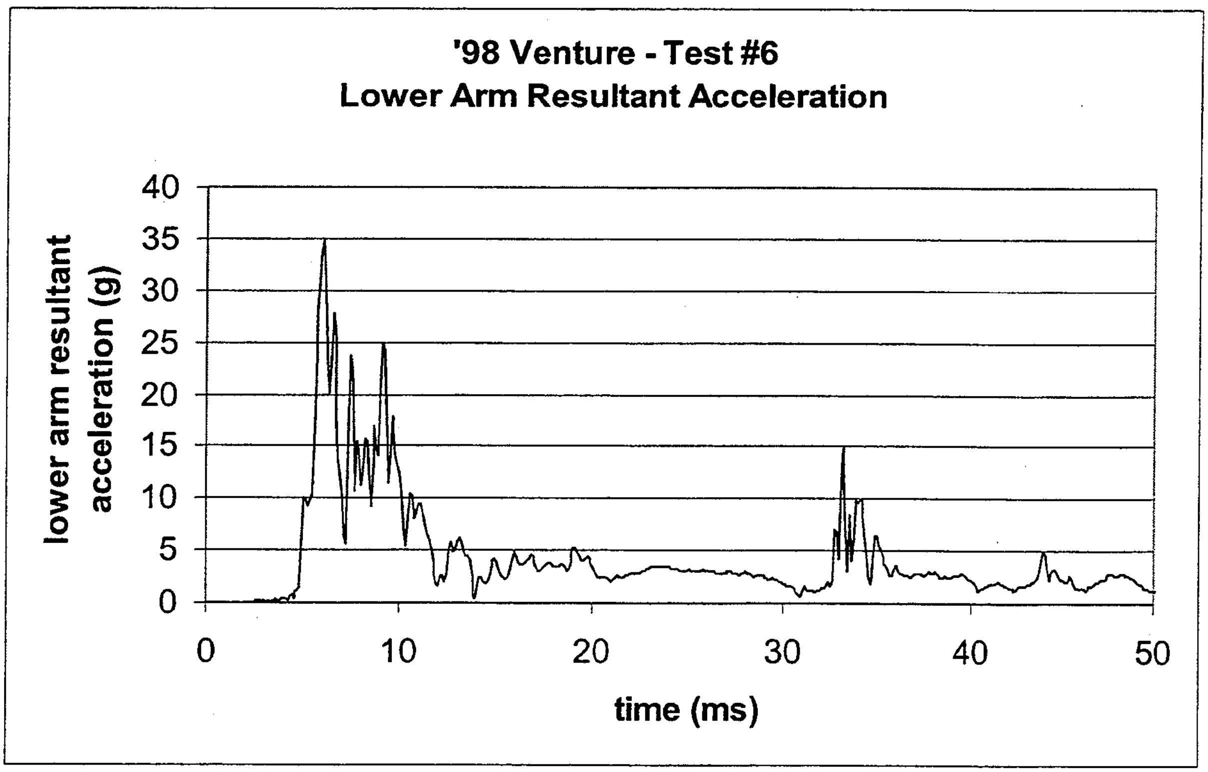

Fig. E.36. '98 Venture - Test 6. Lower Arm Resultant Acceleration.